Quantifying Technology Infusion and Policy Impact on Low Earth Orbit Communication Satellite Constellations

by

Darren Datong Chang

Submitted to the Department of Aeronautics and Astronautics
and
the Engineering Systems Division
in partial fulfillment of the requirements for the degree of
Dual-Master of Science in Aeronautics and Astronautics and
Technology and Policy
At the
MASSACHUSETTS INSTITUTE OF TECHNOLOGY
June 2004

Author . . . . . .
Department of Aeronautics and Astronautics
and
Technology and Policy Program, Engineering Systems Division
May 12, 2004

Certified by . . . . . .
Olivier L. de Weck
Robert N. Noyce Assistant Professor of Aeronautics and Astronautics
and Engineering Systems
Thesis Supervisor

Accepted by. . . . . .
Dava J. Newman
Associate Professor of Aeronautics and Astronautics
and Engineering Systems
Director, Technology and Policy Program

Accepted by . . . . . .
Edward M. Greitzer
H.N. Slater Professor of Aeronautics and Astronautics
Chair, Committee on Graduate Students

Quantifying Technology Infusion and Policy Impact on Low Earth Orbit Communication Satellite Constellations

by

Darren Datong Chang

Submitted to the Department of Aeronautics and Astronautics
and
Engineering Systems Division
on May, 2004, in partial fulfillment of the
requirements for the degrees of
Dual-Master of Science in Aeronautics and Astronautics and Technology and Policy Program

Abstract

Technology infusion and policy implementation bring impacts to the trade space of complex engineering systems. This work describes in detail the frameworks for quantitative analyses on these impacts, demonstrates their use on the sample system, and presents the analysis results. The low earth orbit (LEO) communication satellite constellation system serves as the platform for carrying out the system trade space analysis. The system is re-produced in computer environment in the form of a multiple-input-output MATLAB model. The model contains multiple modules that incorporate the physics, economy, and policies of the real-world system. The inputs to the model are system design variables and the outputs are system performance, capacity, and cost. The Pareto optimal solution set of the baseline trade space is generated by the model using a full-factorial run that covers the entire design space.

To simulate technology infusion, technical and cost attributes of four new technologies are quantified and infused into the system model. The infusion of technologies and combinations of technologies into the system is simulated. Policy implementation is simulated by changing the policy constraints in the model. The technology-infused trade space and policy-implemented trade space have new sets of Pareto optimal solutions. By comparing these solution sets with the baseline optimal solution set in the objective space, we can quantify the impact of technology infusion and policy impact. In conclusion, the methodologies of quantifying the impact of technology infusion and policy implementation on complex engineering systems is repeatable and has been tested against real-world systems. The information generated demonstrates their usefulness to technology selection and policy decision-making processes.

Thesis Supervisor: Olivier L. de Weck
Title: Robert N. Noyce Assistant Professor of Aeronautics and Astronautics and

Engineering Systems

Acknowledgments

The first person I would like to thank is Professor Olivier de Weck, without whose guidance and support this work would not have been possible. The others that I must thank are my father, Zhang Jie, whose love and support has been vital all these years, and my mother, Liu Haiyan, who although not able to see this result with her own eyes, but the memory of whom has been an important source of power for me all these years. I would also like to express my gratitude to my colleagues in Japan, whose help and friendship are important in making this work a reality. They are, among others, Suzuki Ryutaro, Kadowaki Naoto, Koyama Yoshisada, Orikasa Teruaki, Kimura Shinichi, and Homma Masanori. Back home, I owe my gratitude to these members of the MIT community for their help and suggestions: Prof. Joel Schindall, Phil Springmann, Deb Howell, and Kalina Galabova, among others. Members of the scientific community at large, such as Thomas Lang, should also be thanked.

This research has been supported by the Alfred P. Sloan Fundation under grant number 2000-10-20 with Dr. Gail Pesyna serving as the program monitor, Prof. Richard de Neufville and Dr. Joel Cutcher-Gershenfeld serving as project managers and Mrs. Ann Tremelling of the Engineering Systems Division (ESD) as the fiscal officer.

Contents

List of Figures

List of Tables

Nomenclature

Abbreviations

FCC	Federal Communications Commission
GEO	Geosynchronous Equatorial Orbit
ITU	International Telecommunication Union
LCC	Life Cycle Cost
LEO	Low Earth Orbit
MF-CDMA	Multiple Frequency - Code Division Multiple Access
MF-TDMA	Multiple Frequency - Time Division Multiple Access
MSDO	Multidisciplinary System Design Optimization
PII	Policy Infusion Interface
TII	Technology Infusion Interface

Symbols

Design variables

1. c	constellation type
2. h	altitude
3. ε	minimum elevation
4. di	diversity
5. P_t	satellite transmit power
6. $G_{t\ dB}$	satellite antenna edge cell spot beam gain
7. ISL	inter-satellite link
8. MAS	multiple access scheme
9. T_{sat}	satellite lifetime

Constants

1. AKM apogee kick motor type
2. $AKMI_{sp}$ apogee kick motor specific impulse
3. $StationI_{sp}$ station keeping specific impulse
4. MS modulation scheme
5. ROF Nyquist filter roll-off factor
6. CS cluster size
7. $NUIF$ neighboring user interference factor
8. R_c convolutional coding code rate
9. K convolutional coding constraint length
10. R_{ISL} inter sat link data rate
11. $G_{e\ dB}$ gain of user terminal antenna
12. P_e user terminal power
13. IDT initial development time

Policy constraints

1. FB_{up} uplink frequency bandwidth
2. FB_{down} Downlink frequency bandwidth
3. FLV Foreign launch vehicle

Objectives

1. $R_{lifetime}$ total lifetime data flow
2. N_{users} number of simultaneous users
3. LCC life-cycle cost
4. N_{year} average annual subscribers
5. T_{total} total airtime
6. CPF cost per function

Benchmarking metrics

1. N_{sat} number of satellites
2. N_{users} number of simultaneous users
3. LCC life-cycle cost
4. M_{sat} satellite mass
5. N_{cell} number of cells
6. T_{orbit} orbital period
7. $EIRP$ satellite transmit average EIRP
8. $N_{gateway}$ number of gateways

Requirements

1. BER bit error rate
2. R_{user} user data rate
3. $Margin$ link margin

Key Definitions

Low Earth Orbit	If the objective $\mathbf{J}*$ of a design vector $\mathbf{x}*$ is non-dominated by any other objective in the objective space, then $\mathbf{x}*$ represents a Pareto optimal design.
MF-CDMA	Multiple Frequency - Code Division Multiple Access. Using a unique pseudorandom noise (PN) code, code division multiple access (CDMA) transmitting station spreads the signal in a bandwidth wider than actually needed. Each authorized receiving station must have the identical PN code to retrieve the information. Other channels can operate simultaneously within the same frequency spectrum as long as different, orthogonal codes are used. In MF-CDMA, multiple CDMA carriers at different frequencies are used to increase the number of channels.
MF-TDMA	Multiple Frequency - Time Division Multiple Access. In MF-TDMA, a communication channel simultaneously occupies a specific time slot in the time domain and a specific frequency carrier in the frequency domain. Thus the total number of channels is the product of the number of time slots and the number of frequency channels. Both the time domain and frequency domain are used efficiently.
Pareto optimality	If the objective $\mathbf{J}*$ of a design vector $\mathbf{x}*$ is non-dominated by any other objective in the objective space, then $\mathbf{x}*$ represents a Pareto optimal design.
Policy implementation	System designs are typically limited by related policies, for example, car engine design is constrained by emission requirement, or architectural design is limited by zoning law. The change of these policies will have an effect on the design of the system. The imposition of the policies on the system is called policy implementation in this thesis.
Technology infusion	The use of technology in a system on the sub-system level. The system will be affected by the physical and cost attributes of the technology. For example, the use of jet engine in airplane system, or the use of nuclear weapon in the international political system.

Trade space	The trade space includes the design space and objective space. The "design space" refers to the x-space, i.e. the domain of design variables where designers have design freedom. The term "objective space" refers exclusively to the J-space, i.e. the space of system attributes, behaviors or objectives that are used by decision makers. The "trade space" is the umbrella that encompasses both the design space and the objective space.

Chapter 1

Introduction

1.1 Overview of the Study

This thesis addresses two fundamental aspects of the design problem of complex systems. One aspect is on the impact brought by the infusion of new technologies into the system. New technology will typically change the physical character of the system and therefore alter its behavior. System merits such as performance-versus-cost will be affected by the new technology as a result of the physical change. Understanding the relation between new technology and the system character is important in selecting the new technologies to be infused into a system. The other aspect of the system design problem is the impact brought by policy implementation. If new technologies tend to bring more freedom to the design, then policy implementation typically imposes more constraints. For example, in the design of an automobile system, the environmental policy forces engine design to satisfy the emission issue while the gasoline price, which is related to the foreign policy, influences the efficiency requirement of the propulsion. Therefore the policy impact is another piece of vital knowledge that the system design should have.

The study analyzes the above-mentioned issues by a comparison of the trade space between a baseline case and the technology-infused and the policy-implemented cases. In particular, the study will observe how the Pareto optimality of the trade space is changed from the baseline case to the technology-infused or policy-implemented case.

The platform from which the research is launched is low earth orbit (LEO) communication satellite constellation system. This system is chosen because it represents a complex engineering system: large, multidisciplinary, costly, and spanning a long lifetime.

1.2 Historical Background of the Study

1.2.1 The Need for LEO Communication Satellite System

There are two major systems in the genre of LEO communication satellite constellations - Iridium by Motorola and Globalstar by Loral. The conceptual design of both systems started in late 1980s. Iridium filed for its construction permit and frequency allocation in 1990 from Federal Communication Commission (FCC) and Globalstar followed suit in 1991. In the following paragraphs, we will briefly review the background of the telecommunication industry in late 1980s and early 1990s.

At that time, many of the telecom applications that we are familiar today had not become available yet. Both Internet and terrestrial-based cellular phone systems were technological wonders yet to be invented, or at least, to mature as a consumer-oriented technologies. Therefore, most information was transmitted by voice signals via public switched telephone network (PSTN). But PSTN was limited to developed areas and unavailable in under-developed areas and the wildness. The only way to provide global communication was via geostationary earth orbit (GEO) satellites. A constellation formed by three GEO satellites 120^o apart (measured from the center of the Earth) can provide communication coverage to anywhere on the earth below $\pm 70^o$ latitude. GEO systems, however, have the distance disadvantage: because GEO systems orbit the earth at an altitude of 36,000 km, the time delay for one-way transmission between the satellite and ground is approximately 120 ms, which is undesirable for voice communication. The loss along the path of 36,000 km is also high. High power and large antennae are required for the user terminal on the ground to overcome the loss. This made portable carriage of the terminal impractical. With

bulky and expensive terminals, GEO systems could only win over a small group of users typically consisting of mariners, field workers, and military personnel. They were unable to generate a customer base large enough to lower the cost of service.

Practical personal satellite communication could not be possible without overcoming the distance factor. Innovations in this area led to the development of Low Earth Orbit (LEO) communication satellite system, a constellation to provide global and zonal coverage.

1.2.2 Iridium System

As an international consortium of telecommunication companies, including Motorola, Raytheon, Siemens, Telesat and Bechtel, Iridium supports global voice, messaging, and paging service for mobile users. The main components of the Iridium system are satellites, gateways, and user handsets. Regional gateways handle call setup procedures and interface Iridium with the existing PSTN. A dual mode handset allows users to access either a compatible cellular telephone net work or Iridium satellites. Iridium is intended to provide cellular like service in situations where terrestrial cellular service is unavailable or areas where the PSTN is not well developed.[Fos98]

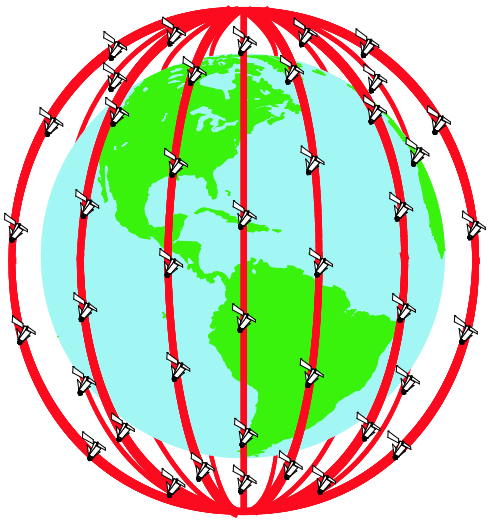

Figure 1-1: Iridium constellation (Copyright: Dr. Ray Leopold. With permission.)

Iridium History

Table 1.1 shows the critical cornerstones in the history of Iridium.[LWJ00]

Dec. 1990:	FCC filing for construction permit and frequency allocation
1991:	Founding of Iridium LLC
Jan. 1995:	FCC license received
May 1997:	First satellite launch (5 satellites by Delta II)
May 1998:	Full satellite constellation in orbit
Nov. 1998:	Start of operation (telephony, paging, and messaging)
End of 1998:	Problem with 23 satellites of the constellation
Aug. 1999:	Having a debt level in excess of $4 billion, Iridium files for Chapter 11 bankruptcy protection
Dec. 1999:	Iridium has 50,000 subscribers
Dec. 2000:	Iridium Satellite LLC acquired Iridium LLC. The Pentagon signed a $72 million, two-year contract with Iridium.

Table 1.1: Cornerstones in the history of the Iridium system

Iridium Financial Data

Because the financial aspect of the system played a significant role in the bankruptcy of the system, the related data for Iridium are listed in Table 1.2

Total system cost:	$5.7 billion
Annual operational cost:	$1 billion (including satellite replenishment and interest payments)
Financed amount:	$4.4 billion
Handheld terminal price:	$3,000 (before June 1999), $1,500 (after June 1999)
Airtime charge:	$2-7 per minute (before June 1999), $1.5-3 per minute (after June 1999)

Table 1.2: Iridium financial data

Iridium Technical Data

Key technical data of Iridium are listed in Table 1.3[LWJ00, Fos98]. These data give an overview of the key parameters of the system, shows the system's complexity, and

will serve as a basis for the benchmarking of the system model against Iridium in Chapter 2.

Iridium Follow-up Story

In December 2000, Iridium Satellite LLC acquired Iridium LLC at a price of $25 million. In the same month, Iridium signed a contract with the U.S. Defense Department. The two-year contract includes options to extend the deal until 2007. In 2001, Gino Picasso, the CEO of Iridium Satellite LLC, said he hopes to generate $90 to $100 million in annual revenue by the end of 2002, enough to cover operating expenses. (Note: the actual operational cost in 2002 is lower than the estimated cost listed in Table 1.2 because there are many fewer subscribers to the system so the operational demand is lower, and because there is no satellite replenishment in that year.) In 2002, Picasso claimed the current fleet of satellites was performing well and expected to last until at least 2010. But as a sign of re-vitalized business, Iridium was planning replacing the current constellation with a new generation of spacecraft.[Sil02] More information on the current status of the system can be found at www.iridium.com.

1.2.3 Globalstar System

Similar as the Iridium system, the Globalstar system is designed to bring affordable cellular-type voice and data communication to its coverage area. The major architectural difference between Globalstar and Iridium are:

- Iridium uses a polar constellation while Globalstar uses a Walker constellation. Therefore Globalstar provides coverage only to regions between the 70^o latitudes.
- Iridium's modulation scheme is MF-TDMA and Globalstar's modulation scheme is MF-CDMA. This will be further explained in Chapter 2.
- Globalstar relies on ground-based gateways to relay information between satellites and to process calls. Iridium uses inter-satellite links (ISL) to relay information between satellites and has on-board processing to process calls.

Globalstar is run by a partnership of a number of companies. Loral and Qualcomm serve as general partners, and 10 other companies serve as limited partners.[LWJ00]

Globalstar History

Although trailing a few months behind Iridium, Globalstar has followed a similar cycle of boom and bust as Iridium. The cornerstones in the history of Globalstar are listed in Table 1.4.

Globalstar Financial Data

Globalstar's financial data are listed in Table 1.5.

Globalstar Technical Data

Key technical data of Globalstar are listed in Table 1.6.[LWJ00] Besides giving an overview of the key parameters and showing the system's complexity, these data will serve as a basis for the benchmarking of the system model against Globalstar in Chapter 2.

Globalstar Follow-up Story

In early 1999, Globalstar expected a subscriber base of around 500,000 by the end of 2000 and an ultimate subscriber base of 7.5 million. After it filed for chapter 11 bankruptcy protection in mid-February 2002, Globalstar has undergone restructuring and is still in business today. For the current status of the company, please visit www.globalstar.com.

1.3 Literature Search and Open Questions

1.3.1 Kelic, Shaw and Hastings' "Cost per Function" Metric

In their work five proposed constellations are compared based on a "cost per T1 minute" metric that takes into account the lifecycle cost of a satellite-based T1 in-

ternet link at a data rate of 1.544 Mbps.[KSH98] The cost in that paper, however, is not the cost to the operator, but rather the price of a T1-minute to the customer that will ensure a 30% internal rate of return. This contribution builds upon earlier work by Hastings, Gumbert[Gum95] and Violet.[Vio95]

1.3.2 Shaw's Generalized Information Network Analysis (GINA) Methodology

Shaw enabled the modelling of most distributed satellite systems (DSS) as information processing networks. This methodology is called the Generalized Information Network Analysis (GINA) methodology.[Sha99] GINA allows the adoption of the mathematics for information network flow to quantitative system analysis. The analysis specifies measurable, unambiguous metrics for the cost, capability, performance and adaptability. Detailed trade space analyses for a distributed space-based radar have been made to demonstrate the effectiveness of the GINA methodology.

1.3.3 Jilla and Miller's Inclusion of Multi-Disciplinary Optimization (MDO)

Jilla and Miller developed a multi-objective, multi-disciplinary design optimization methodology for mathematically modelling the distributed satellite system (DSS) conceptual design problem as an optimization problem.[JM02] The seven-step methodology enables an efficient search of the trade space that is too large to enumerate, analyze, and compare all possible architectures. Design architectures are mapped into the trade space using a GINA model of the space system, then multi-disciplinary optimization algorithms including simulated annealing (SA) are applied to the trade space to identify the Pareto optimal designs. Sensitivity analyses are performed to identify the most important high fidelity models and the most influential design variables. Iterations are executed to improve both the fidelity of the GINA model and the optimization algorithms.

1.3.4 Suzuki and Coworkers' New Technologies for LEO Communication Satellites

Suzuki and coworkers described a set of key technologies that are under development as enablers of a next-generation global multimedia mobile satellite communications system in low earth orbit in Japan.[SSI+00, SNM+02] These technologies include optical inter-satellite link system, on-board ATM switch and modulation methods, digital beam forming satellite antenna, and on-board switching system.

1.3.5 Previous Studies Related to Technology Infusion

Historically, technology assessment has been the focus of the Management of Technology (MOT) community. Utterback has observed the evolution of technologies over time and derived a model of the dynamics of technological and industrial evolution from it [Utt94]. Tschirky discusses technology assessment as an integral function of technology and general management [Tsc91] and describes it as the "systematic identification and estimation of present and future impact of technology application in all areas of society." Technology classification has been proposed by van Wyk [vW88]. Gordon and Stower make an explicit connection between technology forecasting and complex system simulation [GS78]. One way to distinguish between incremental, architectural, modular and radical innovation has been proposed by Henderson and Clark [HC90]. While architectural innovation changes only the linkages between core concepts and components but keeps the technologies the same, modular innovation keeps the linkages the same, but substitutes new technologies within the architecture. Radical innovation overturns both the architecture and technologies at the same time. The approach presented in this thesis is most applicable to *modular innovation*.

More recently a systematic approach to technology selection for infusion in complex systems has been proposed by Mavris, DeLaurentis and co-workers [URDM02]. This approach is called "Technology Identification, Evaluation and Selection" (TIES) and is useful for sorting through a large set of candidate technologies to be infused in aircraft systems. The technology selection problem is treated as a bi-level op-

timization problem. It considers the compatibility and dependence relations between the new technologies. Messac and Mattson developed the s-Pareto Frontier approach.[MM02] Within region of interests, a conglomeration of the Pareto fronts of all candidate technologies is considered. This conglomeration is called the s-Pareto Frontier.

One crucial aspect in determining the predictive accuracy of technology assessment is the stage of maturity of technologies under consideration. We refer to NASA's technology readiness level (TRL) scale [LW92] to estimate the uncertainty in these predictions in future work. Technology uncertainty itself is not explicitly considered in this thesis, but is recommended for future work in Chapter 5.

1.3.6 Weigel's Inclusion of Policy into Space Systems Conceptual Design

In her Ph.D. thesis, Weigel proposed qualitative and quantitative analysis methods to enable the creation of policy robust system architecture and design. Space systems form the application domain considered. According to Weigel, policy should be made an active consideration in the engineering architecture and design process as early as during the conceptualization phase. A seven-step process checklist is proposed to understand and analyze the policies impacts. Weigel's thesis contributes to the analysis of the interactions between policy and politico-technical system architecture and design.

1.4 Motivation for Current Study

1.4.1 To Fill the Gap

Use of the GINA methodology and architectural trade space analysis have not been applied to LEO communication satellite constellation systems. A trade space analysis of LEO systems may help us decipher the reasons for the financial failure of the Iridium and Globalstar systems from a system architectural perspective. With the

current discretization of the design variables, the size of the trade space is manageable even with a full-factorial run of all possible designs. Therefore the multi-disciplinary optimization algorithms used by Jilla and Miller are not necessary in identifying the Pareto optimal solutions of the trade space. In the future, with finer discretization of the design variables, the optimization algorithms should be applied in search of optimal solutions, as will be suggested in Chapter 5.

The present study uses the impact of technologies on the Pareto front as a measurement of technology effectiveness. This differs from previous work in the sense that there is no attempt to develop a single scalar metric of technology effectiveness. It will become clear that there are subtleties in technology infusion that are lost by converting to a single measure of effectiveness. The treatment of the Pareto frontiers represents the tradeoff between system performance and capacity versus cost brought by the infusion of technology. We can be particularly interested in the tradeoff at certain points fixed by external conditions such as market demand or budget constraints.

Policy implementation may cause change in Pareto frontiers of the trade space similar as technology infusion. The impact of policy implementation on the system can be understood by analyzing this change. No previous research effort has been made in this direction.

1.4.2 Impact on the Current State of Knowledge

This research represents a new effort in quantifying the impact of technology infusion and policy implementation on complex systems. It is the first time that the impact of technology choice and policy decision on the Pareto front in the objective space is conducted. This approach will demonstrate the complexity and subtlety involved in judging the influence of new technologies and policies. Furthermore, the methodology used in this research has a general applicability to technology infusion and policy implementation problems for other engineering systems.

It should be noticed that technology infusion and policy implementation impact the system model in fundamentally different ways: while technology infusion must be

modelled in detail "inside" the system - by interacting with the existing physics of the system and changing internally dependent system technical parameters and cost factors, policy acts mainly from the "outside" by imposing constraints and changing fixed parameter assumption. This difference will be demonstrated in Chapter 3 and 4.

1.5 Thesis Preview

Here we give a brief preview of the thesis in both a graphical road-map and words.

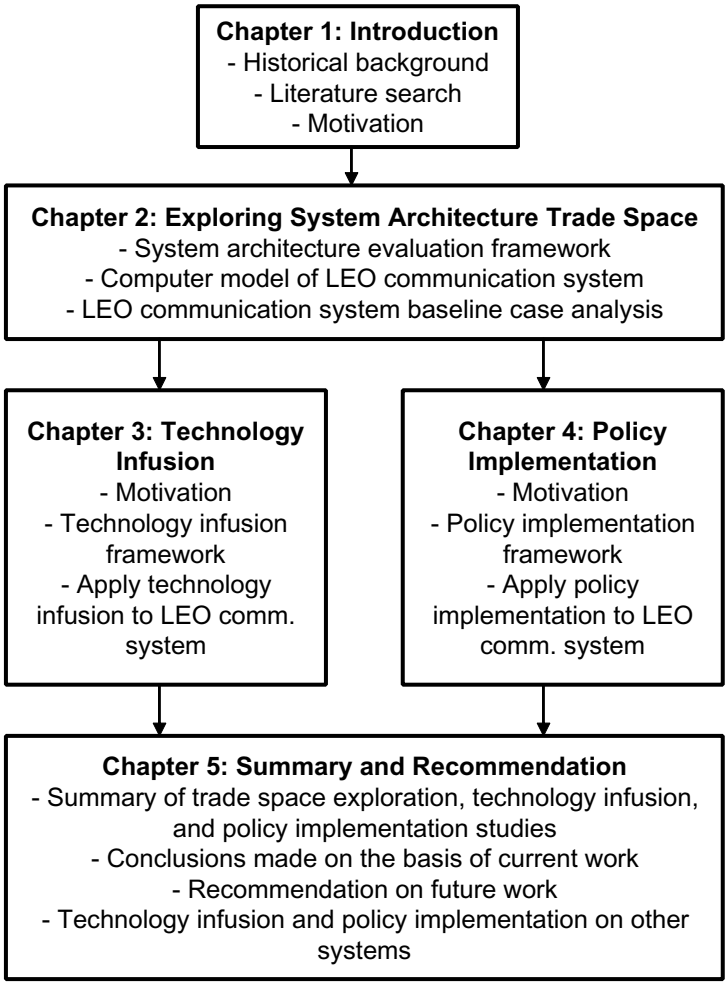

Figure 1-2: Thesis road-map

In the chapter immediately following the introduction chapter, we outline the

system architecture evaluation framework that includes six steps for building, exploring, and optimizing the system trade space. Then the framework is applied to LEO communication satellite constellation systems, starting with modelling it in computer environment and eventually finding the Pareto optimal solutions for the baseline case.

Both Chapter 3 and 4 are built upon the system model and baseline case optimal solution set developed in Chapter 2. In Chapter 3, technology infusion study is conducted. We first discuss the motivation for technology study. Then we introduce the six-step technology infusion framework. This framework is applied to evaluate the impact of infusing four new technologies into LEO satellite systems. Postprocessing and interpretation are performed on the evaluation results.

Parallel with Chapter 3, Chapter 4 performs policy implementation study. The motivations for policy implementation study are given at the beginning of the chapter. What follows is an introduction of a five-step policy implementation framework. The framework is applied on LEO satellite systems to evaluate the impact of implementing two policies. Postprocessing and results interpretation are performed at the end of the chapter.

Chapter 5 first summarizes the three major parts of the thesis: trade space analysis, technology infusion, and policy implementation. Then we draw conclusions on the basis of the current study. We also discuss the future work that can be developed based on this thesis. At the end we briefly contemplated the general notion of technology infusion and policy implementation on all systems, including engineering systems, architectures, and political systems.

1.6 Summary

We first provided an overview of the study objective and approach. Then we went through the historical background of the LEO communication satellite constellation system. We reviewed the previous works done on architectural analysis, new satellite technologies, and policy impact study. At the last we analyzed how this study will fill the gap left by existing works.

Ground segment	
- Number of gateways:	12
- Control station:	1 (plus 1 for backup)
Space segment	
- Constellation type:	Polar
- Number of satellites:	66
- Number of orbital planes:	6
- Orbital altitude:	780 km
- Inclination angle:	86.4^o
- Minimum elevation angle:	8.2^o
- Satellite in-orbit mass:	689 kg
- Radio-frequency (RF) power:	400 W
- Space lifetime:	5 years
- Launch vehicles:	Delta II(USA), Long March(China), Proton(Russia)
Communication segment	
- User uplink and downlink bandwidth:	1621.35-1626.5 MHz
- Telephony and modem data rate:	2.4 kb/s
- Satellite capacity:	1,100 duplex channels
- Constellation capacity:	49,368 duplex channels
- Link margin:	16 dB
- Number of inter-satellite links (ISL) per satellite:	4
- ISL frequency bandwidth:	23.18-23.38 GHz
- Feeder link frequency bandwidth:	29.1-29.3 GHz (uplink), 19.4-19.6 GHz (downlink)
- Onboard switching:	Yes
- Multiple access:	MF-TDMA
User terminals	
- Mass:	400 g
- Antenna length:	15 cm
- Talk time:	2 h
- Standby time:	20 h
- Peak transmit power:	7 W
- Mean transmit power:	0.6 W
- Antenna gain:	2 dBi
- G/T:	23 dB/K

Table 1.3: Iridium technical data

June 1991	FCC filing for construction permit and frequency allocation
Jan. 1995:	FCC license received
Feb. 1998:	First satellite launch (4 satellites by Delta II)
Sept. 1998:	Loss of 12 satellites during a Zenith launch failure
Oct. 1999:	Start of pre-operation with 32 satellites and 9 gateways
End of 1999:	40,000 handsets shipped to distributors
Start of 2000:	Start of commercial service with full satellite constellation and 38 gateways
August 2001:	Globalstar reduced rates to $0.17 per minute.
Feb. 2002:	Having a debt of $3.34 billion, Globalstar files for Chapter 11 bankruptcy protection[Spa02]
May 2003:	Total revenue of $11.6 million and 84,000 subscribers for the first quarter.
Dec. 2003:	Globalstar acquired by Thermo Capital Partners

Table 1.4: Cornerstones in the history of the Globalstar system

Total system cost:	$3.3 billion
Financed amount:	$3.8 billion (fully financed)
Handheld terminal price:	$1,000
Airtime charge:	$1-3 per minute

Table 1.5: Globalstar financial data

Ground segment	
- Number of gateways:	50
- Control station:	2 ground operation control centers + 2 satellite operation control centers
Space segment	
- Constellation type:	Walker
- Number of satellites:	48
- Number of orbital planes:	8
- Orbital altitude:	1414 km
- Inclination angle:	52^o
- Minimum elevation angle:	10^o
- Satellite in-orbit mass:	450 kg
- Radio-frequency (RF) power:	380 W
- Space lifetime:	7.5 years
- Launch vehicles:	Delta II(USA), Zenith-2(Russia), Soyuz(Russia)
Communication segment	
- User uplink and downlink bandwidth:	1610-1626.5 MHz (uplink), 2483.5-2500 MHz (downlink)
- Telephony and modem data rate:	2.4 kb/s
- Satellite capacity:	2,500 duplex channels
- Constellation capacity:	120,000 duplex channels
- Link margin:	6 dB
- Number of inter-satellite links (ISL) per satellite:	0
- ISL frequency bandwidth:	N/A
- Feeder link frequency bandwidth:	50.91-52.50 GHz (uplink), 68.75-70.55 GHz (downlink)
- Onboard switching:	No
- Multiple access:	MF-CDMA
User terminals	
- Mass:	370 g
- Talk time:	3.5 h
- Standby time:	9 h
- Peak transmit power:	400 mW
- Mean transmit power:	50 mW
- Antenna gain:	2.6 dBi

Table 1.6: Globalstar technical data

Chapter 2

Exploring System Architectural Trade Space

2.1 Introduction

In this chapter, we introduce the system architecture evaluation framework. We begin by explaining the purpose of the system model that we build. We also introduce the limiting assumptions taken in building the model. Then we go through the six steps of the framework in detail.

2.2 Purpose of the System Model

LEO communication satellite constellation is a complex system whose background knowledge resides in multiple fields including spacecraft design, launch vehicle, communication, cost analysis, etc. Where should we start to understand this complex system?

As system architects, the first step we take in understanding the system is to understand the functional system requirements of the system. For this study, the ultimate requirement for LEO communication satellite constellation systems is to provide good quality voice communication. Depending on the multiple access scheme and diversity of the system, technical specifications needed in order to meet the

requirement are derived, including bit error rate, data rate per user channel, and link margin. These technical specifications form the requirement vector $\mathbf{r}$.

We then need to look at the design space of the system, which is filled by all possible architectures of system design that differ from each other by a vector of design variables $\mathbf{x}$. A design variable represents an important attribute of the system whose alternation will significantly change the system performance, capacity, and cost. For example, orbital altitude and transmitter power are design variables for a LEO communication satellite system. An exhaustive combinations of all possible design variable values form the design space.

The different architectures of the design share a vector of constants $\mathbf{c}$. The values of these constants are the same for all architectures because they all use the same sub-technologies. For example, the apogee kick motors of all architectures are assumed to have the same specific impulse. The radio transmissions are assumed to use the same modulation scheme. Therefore, across the entire design space, the values of these constants do not change.

Besides design variables and constants, there are a vector of policy constraints $\mathbf{p}$ imposed by bureaucratic installations like the FCC. An example of this is the radio transmission bandwidth assigned to the system. Both the policy constraints and design requirements are shared by all architectures across the design space.

Together, the design requirements $\mathbf{r}$, the design variables $\mathbf{x}$, constants $\mathbf{c}$, and policy constraints $\mathbf{p}$ form the known metrics of the system. For a complex system, how can the designers predict quickly how well the design will achieve the final objectives $\mathbf{J}$ based on the known metrics? This rapid performance prediction capability that maps from the design space to objective space is necessary to understand the entirety of the trade space. To achieve such prediction capability, a computer-based model that reproduces the real-world designs in a computer environment must be developed first. Thus the simulation performs a mapping from decision space to objective space:

$$\mathbf{J} = f(\mathbf{x}, \mathbf{c}, \mathbf{p}, \mathbf{r}) \tag{2.1}$$

To benchmark the fidelity of the model, a vector of benchmarking metrics **B** is also generated by the simulation for comparison with real systems. These comparisons will give us an idea on how well the simulation reproduces the reality.

2.3 Limiting Assumptions of the System Model

The model is designed to simulate LEO communication satellite constellations and no other satellite systems, and this basic assumption is reflected in some limiting factors as listed:

- Circular orbits are assumed.
- LEO is between the altitudes of 500 and 1,500 km. The launch vehicles modelled cover an altitude up to 2,000 km. To run the simulation for orbits higher than 2,000 km, the launch vehicles capacity database needs to be enlarged.
- The typical elevation angle for LEO communication is under 30^o. The constellation geometry calculation might be invalid if the elevation angle approaches 90^o. The normal elevation range from 0^o to 40^o can be perfectly simulated although some large elevation angles may return no solution.
- If the satellite mass is too large to be carried up by any available launch vehicle, the simulation will return no solution. The user should exercise his or her common sense when designing the system.
- The maximum diversity, i.e., the number of satellites visible to a ground user simultaneously, of the simulated system is 4. All LEO constellation systems designed at present have a diversity at or below 4.
- Multiple access scheme is the method by which multiple channels can be connected with a single satellite. The most popular two multiple access schemes are modelled: multiple frequency-time division multiple access (MF-TDMA) and multiple frequency-code division multiple access (MF-CDMA). No other multiple access scheme is modelled.

The model represents the typical LEO satellite communication constellation systems despite these limiting assumptions. But the user of the model should be aware of the limitations when testing systems beyond the usual design range.

2.4 System Architecture Evaluation Framework

With the system model in place, the problem of architectural trade space exploration becomes relatively straightforward. The following six steps are inspired by Jilla and Miller[JM02] and modified here to suit this research.

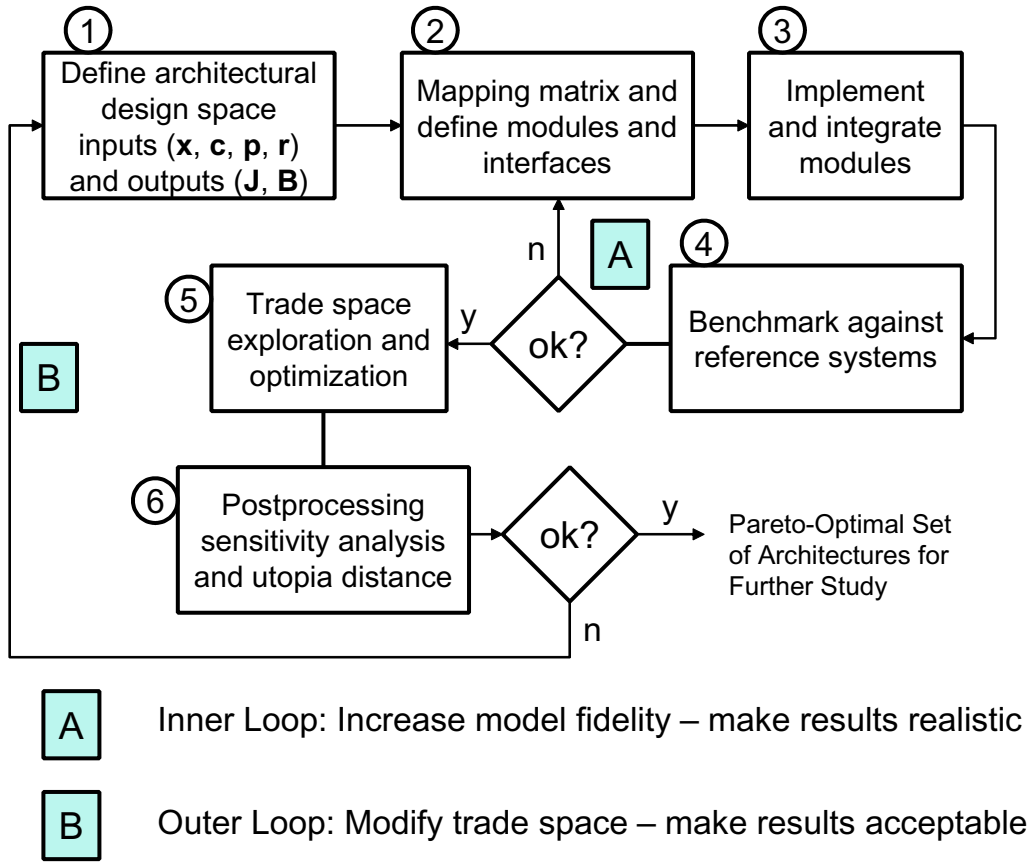

Figure 2-1: Architectural trade space exploration methodology

1. Choose the elements of the architectural design vector **x**, constant vector **c**, policy vector **p**, requirement vector **r**, objective vector **J**, and benchmarking vector **B**. Also define the bounds of **x**.

2. Build the mapping function, subdivide the problem into modules, and define the interfaces.

3. Model technological-physical, economic and policy relationships, implement the individual modules, and test them in isolation from each other. Then integrate the modules into an overall model.

4. Benchmark the model against reference systems. Tune and refine the model as necessary (Loop A).

5. Conduct a systematic trade space exploration, using a full-factorial run.

6. Post-process the Pareto optimal set including sensitivity and uncertainty analysis. Identify the utopia point and the utopia distance of each Pareto optimal solution. If no acceptable Pareto optimal architecture is found, the trade space needs to be modified (Loop B).

Figure 2-1 shows a block diagram of the proposed architectural trade space exploration methodology.

2.5 System Model

While the proposed framework is applicable to many types of complex systems, we now turn our attention to LEO communication satellite constellations. In this section, we go through the first four steps of the methodology. This begins by clearly defining the input and output vectors of the model and ends with benchmarking the model against the two actual LEO systems Iridium and Globalstar that have been mentioned in Chapter 1.

2.5.1 Input (Design, Constant, Policy, and Requirement) Vectors and Output (Objective and Benchmarking) Vectors Definition (Step 1)

Figure 2-2 shows the vector of design variable **x**, constants **c**, policy constraints **p**, performance requirements **r**, objectives **J**, and benchmarking vector **B**.

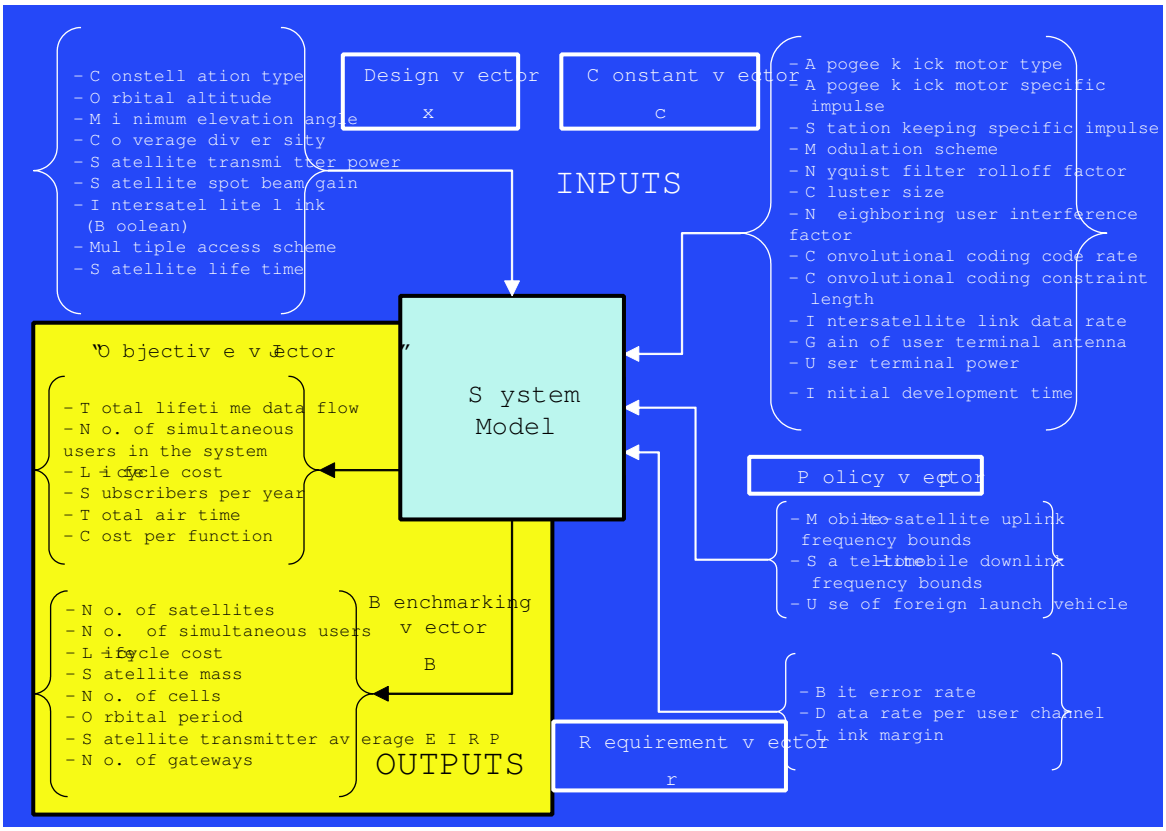

Figure 2-2: Input-output mapping of LEO communication satellite constellation model

The design vector **x** embodies the architectural design decision and is subject to the bounds shown in Table 2.1.

The constant vector **c** contains technical parameters that are assumed constant throughout the simulation. They are assumed constant either because they are determined by existing technologies, or because their variation will not affect the relative "goodness" of one design relative to another. But nevertheless, these parameters are

Symbol	Variable	x_{LB}	x_{UB}	Unit
c	constellation type	Polar	Walker	[-]
h	altitude	500	1,500	[km]
ε	min elevation	5	35	[deg]
di	diversity	1	4	[-]
P_t	sat xmit pwr	200	2,000	[W]
G_{tdB}	sat antenna edge cell spot beam gain	5	30	[dBi]
ISL	inter sat link	1	0	[-]
MAS	multiple access scheme	MF-TDMA	MF-CDMA	[-]
T_{sat}	sat lifetime	5	15	[years]

Table 2.1: Design variable definition

needed for calculations involved in the simulation. The values of the constants are listed in Table 2.2.

Symbol	Constant	Value	Unit
AKM	apogee kick motor type	2(3-axis-stabilized)	[-]
$AKMI_{sp}$	apogee kick motor specific impulse	290	[s]
$StationI_{sp}$	station keeping specific impulse	230	[s]
MS	modulation scheme	QPSK	[-]
ROF	Nyquist filter roll-off factor	0.26	[-]
CS	cluster size	12	[-]
$NUIF$	neighboring user interference factor	1.36	[-]
R_c	convolutional coding code rate	3/4	[-]
K	convolutional coding constraint length	6	[-]
R_{ISL}	inter sat link data rate	12.5	[MB/s]
$G_{e\ dB}$	gain of user terminal antenna	0	[dBi]
P_e	user terminal power	0.57	[W]
IDT	initial development time	5	[years]

Table 2.2: Constants definition

The policy vector **p** contains the bounds of the frequency bands assigned by FCC. Their values for Iridium and Globalstar are listed in Table 2.3 and 2.4. For the full-factorial case where combinations of different design variable values are run, we assume the frequency bands are same as those for Iridium. Another policy constraint is a Boolean variable representing whether to use foreign launch vehicle. It is usually turned on unless we want to test the effect of banning foreign launch vehicle in the policy impact chapter.

For this study, the requirement for LEO communication satellite constellations is

Symbol	Policy constraints	p_{LB}	p_{UB}	Unit
FB_{up}	Uplink frequency bandwidth	1621.35	1626.50	[MHZ]
FB_{down}	Downlink frequency bandwidth	1621.35	1626.50	[MHZ]
FLV	Foreign launch vehicle	1	1	[-]

Table 2.3: Iridium and full-factorial runs policy constraints definition

Symbol	Policy constraints	p_{LB}	p_{UB}	Unit
FB_{up}	Uplink frequency bandwidth	1610.00	1626.50	[MHZ]
FB_{down}	Downlink frequency bandwidth	2483.50	2500.00	[MHZ]
FLV	Foreign launch vehicle	1	1	[-]

Table 2.4: Globalstar policy constraints definition

defined as providing satisfying voice communication. Although the services provided by Iridium and Globalstar include telephony, facsimile, modem, and paging, the voice telephony is the major service and proven to be the one that is most difficult to satisfy with low link margin. So providing a reasonable voice communication is the dominant requirement. As proven by the Iridium and Globalstar cases, in order to provide the minimum acceptable voice quality, the requirement vector **r** that includes bit error rate (BER), data rate per user channel (R_{user}), and link margin ($Margin$) is dependent upon the design variables multiple access scheme (MAS) and diversity (div) as shown in Table 2.5.

Multiple access scheme	Diversity	Bit error rate (BER) [-]	Data rate per user channel (R_{user}) [kbps]	Link margin ($Margin$) [dB]
MF-TDMA	$1 \rightarrow 2$	1e-3	4.6	16
	$2 \rightarrow 3$	1e-3	4.6	10
	$3 \rightarrow 4$	1e-3	4.6	4
MF-CDMA	$1 \rightarrow 2$	1e-2	2.4	12
	$2 \rightarrow 3$	1e-2	2.4	6
	$3 \rightarrow 4$	1e-2	2.4	3

Table 2.5: Requirements definition

The objective vector **J** captures all the metrics by which the "goodness" of a particular architecture can be evaluated. The objective vector contains the total lifetime data flow that represents the total communication traffic throughout the lifetime of the system, number of simultaneous users the system can support, life-

cycle cost of the system, number of subscribers per year, total air time, and cost per function. Cost per function is the life-cycle cost divided by total lifetime data flow. All the objectives are defined in Table 2.6.

Symbol	Objectives	Unit
$R_{lifetime}$	total lifetime data flow	[GB]
N_{users}	number of simultaneous users	[-]
LCC	life-cycle cost	[B$]
N_{year}	average annual subscribers	[-]
T_{total}	total airtime	[min]
CPF	cost per function	[$/MB]

Table 2.6: Objectives definition

The benchmarking vector contains technical specifications that emerge from the design process. If the simulation uses the design vector of a real system, then comparing the benchmarking vector of the simulation with the real system will show how well the simulation reproduces the system. The closer the simulation is to the real system, the higher fidelity the model has. Table 2.7 shows the technical specifications contained in the benchmarking vector. Some of these metrics are also in the objective vector.

Symbol	Benchmarking metrics	Unit
N_{sat}	number of satellites	[-]
N_{users}	number of simultaneous users	[-]
LCC	life-cycle cost	[B$]
M_{sat}	satellite mass	[kg]
N_{cell}	number of cells	[-]
T_{orbit}	orbial period	[min]
$EIRP$	sat xmit average EIRP	[dB]
$N_{gateway}$	number of gateways	[-]

Table 2.7: Benchmarking parameters definition

2.5.2 Define, Implement and Integrate the Modules (Step 2 and 3)

Shown in the proposed framework above, after defining the input and output vectors of the architectural trade space, we will enter the inner loop A where we define, implement, integrate, and benchmark the modules. During this loop we make the necessary changes to make the model reflect reality, and consequently the simulation results converge onto the real-world systems. Here only the completed model as end-result of the iteration is presented.

In this section we focus on steps 2 and 3 of the framework which include define, implement, and integrate the modules of the model. The physical and economic laws behind the system are well-defined and reproducible in the modules. Below we will first introduce the overall structure of the model, and then define each module, and describe their implementation.

Overall Structure

The system model is module-based. To realize a modular model, the simulated system must first be divided into modules in technology and economics domains. Each module performs computation for a particular segment. The modules communicate with each other through input-output interfaces. Thus the change in one module will not require change in the other modules as long as the interface is intact. The communication between the modules reflect the physical or functional relationship between the components of the system. The model structure is shown in Figure 2-3. In the parentheses are names of the MATLAB file for the module.

The model starts with the system input file (SIF). SIF contains all the values of design vector $\mathbf{x}$, constant vector $\mathbf{c}$, and policy vector $\mathbf{p}$. SIF passes the values of the vectors to the start file (SF). Based on the design vector, SF generates the requirement vector $\mathbf{r}$. SF is like the headquarters of the model because it summons and executes each module in pre-defined order. SF is also where the input-output interaction between modules take place.

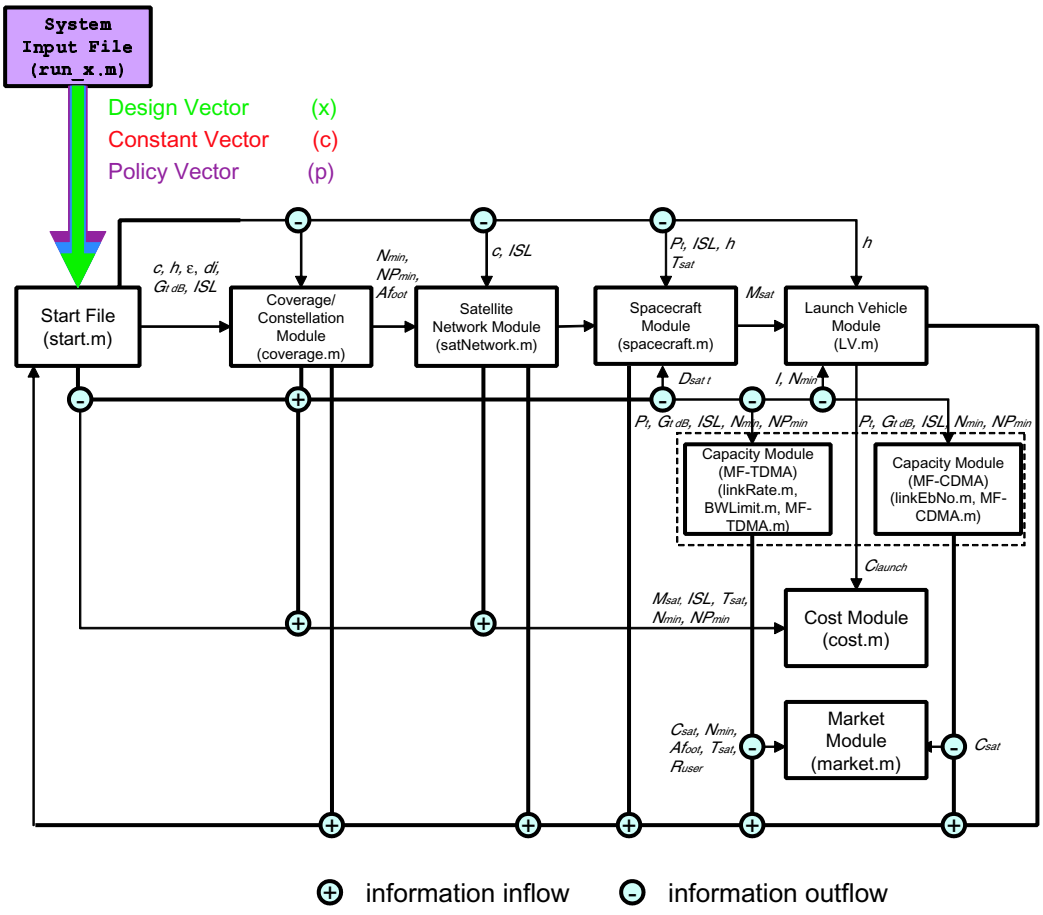

Figure 2-3: Structure of the modular model

The modules in the simulator are the following:

- Coverage/constellation module (CCM) that defines the constellation structure and coverage geometry
- Satellite network module (SNM) that scales the network
- Spacecraft module (SM) that computes the physical attributes of the spacecraft
- Launch vehicle module (LVM) that selects the capable and most economical launch vehicle
- Capacity modules (CM) that find out the satellite capacity of different multiple access schemes

- Total cost module (TCM) that computes the life-cycle cost of the system
- Market module (MM) that makes market projection and finds the amount of usage of the service

After all the modules have been summoned and executed, SF will collect results that are of interest to users of the simulator, and store them in objective vector J and benchmarking vector B.

Another way of presenting the system model structure is to use the N^2 diagram. The N^2 diagram is an N×N matrix with the MATLAB files of the model occupying the diagonal terms. The outputs of each MATLAB file are listed on the row of that file, and the inputs are listed on the column. The files are organized by modules. Some of these files are a module by itself, for example, the Coverage/constellation module. Some of the other files form a group that represents a module, for example, six files forming the Spacecraft module. The N^2 diagram shows clearly the flow of information among the files. The information passed on the upper-right corner indicates feed-forward loops, and the information on the lower-left corner indicates feed-back loops. The N^2 diagram for the system model is shown in Figure 2-4.

The detailed description of the modules is extensive and has been given in Appendices A, B, and C.

2.5.3 Benchmark against Reference Systems (Step 4)

To test the fidelity of the system model, we run the simulation using the input parameters identical to those of four real-world systems: Iridium, Globalstar, Orbcomm, and SkyBridge and compare the resulting benchmark parameters with the publicly available data. We have introduced Iridium and Globalstar in Chapter 1. Orbcomm is a global messaging LEO system that started to provide full services in 1998. Yet to be launched, SkyBridge is a much more ambitious LEO system for broadband access. The design variables, constants, and policy constraints that are collected from public resources are listed below for the four systems.

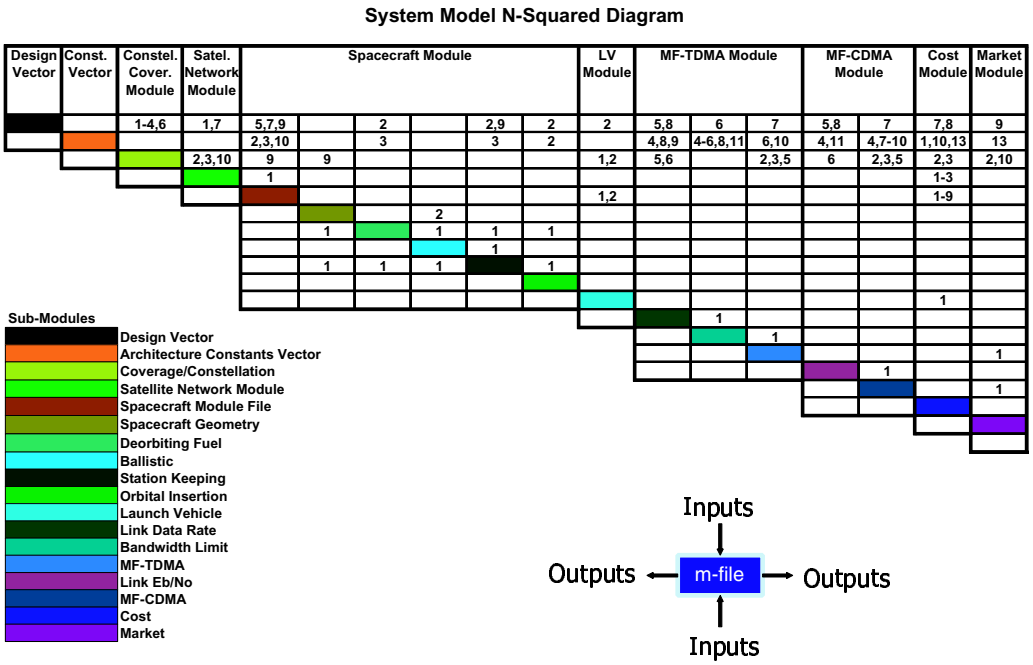

Figure 2-4: N^2 diagram for the system model

It should be noticed that the constants for the reference systems are not all same. They are customized to match the technical attributes of the real systems. But in the full-factorial run covered in the next section, the constants are the same for all the designs for a fair comparison.

After the runs are finished, the benchmarking parameters of the four cases are collected and compared side-by-side with the real-world system, as presented in the table below. The dashes in table below represent data that are not publicly available.

Figure 2-5 and 2-6 show the benchmarking results for key system attributes for Iridium and Globalstar, as well as Orbcomm and SkyBridge, respectively.

	Iridium	Globalstar	Orbcomm	SkyBridge
Constellation type	Polar	Walker	Walker	Walker
Altitude [km]	780	1414	825	1469
Min elevation [^{o}]	8.2	10	5	10
Diversity	1	2 or 3	1	4
Sat xmit pwr [W]	400	380	10	1800
Sat antenna edge cell spot beam gain [dBi]	24.3	17.0	8.0	22.8
Inter sat link	Yes	No	No	No
Multiple access scheme	MF-TDMA	MF-CDMA	MF-TDMA	MF-TDMA
Sat lifetime [year]	5	7.5	4	8

Table 2.8: Design variables of four reference systems

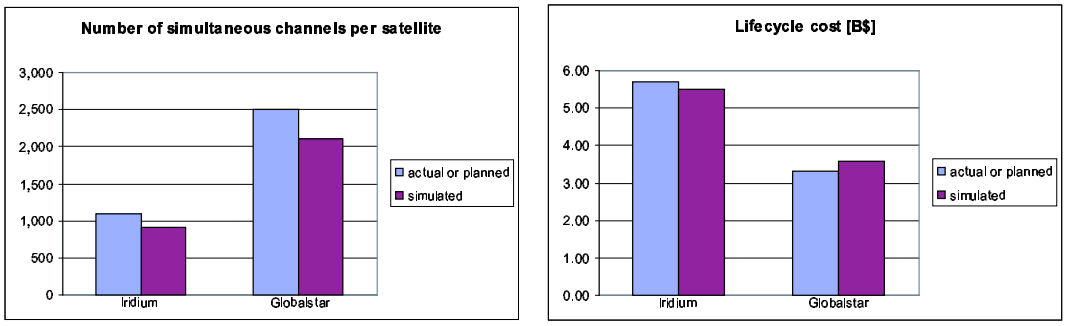

Figure 2-5: Iridium and Globalstar benchmarking results

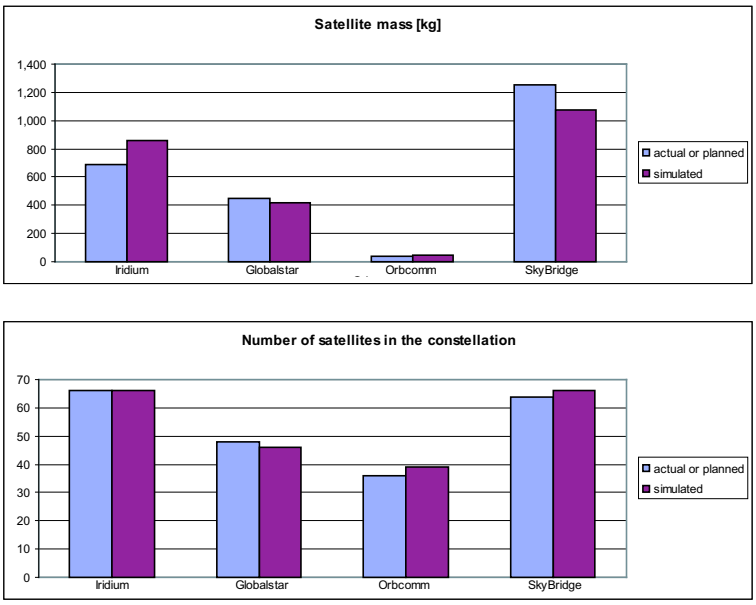

Figure 2-6: Iridium, Globalstar, Orbcomm, and SkyBridge benchmarking results

	Iridium	Globalstar	Orbcomm	SkyBridge
Apogee kick motor type	3-axis stabilized	3-axis stabilized	3-axis stabilized	3-axis stabilized
Apogee kick motor specific impulse [sec]	290	290	290	290
Station keeping specific impulse [sec]	230	230	230	230
Modulation scheme	QPSK	QPSK	QPSK	QPSK
Nyquist filter rolloff factor	0.26	0.5	0.5	0.5
Cluster size	12	1	1	1
Neighboring user interference factor	1.36	1.36	1.36	1.36
Convolutional coding code rate	3/4	1/2	1/2	1/2
Convolutional coding constraint length	6	9	9	9
Inter sat link data rate [Mbps]	12.5	0	0	0
Gain of user terminal antenna [dBi]	0	0	2	35.82
User terminal power [W]	0.57	0.5	0.5	0.5
Initial development time [year]	5	5	5	5

Table 2.9: Constants of four reference systems

	Iridium	Globalstar	Orbcomm	SkyBridge
Uplink frequency bandwidth upper bound [MHz]	1626.50	1626.50	1050.05	18100.50
Uplink frequency bandwidth lower bound [MHz]	1621.35	1610.00	1048.00	12750.00
Downlink frequency bandwidth upper bound [MHz]	1626.50	2500.00	138.00	1275.00
Downlink frequency bandwidth lower bound [MHz]	1621.35	2483.50	137.00	10700.50

Table 2.10: Policy constraints of four reference systems

	Iridium simulated	Iridium actual	Globalstar simulated	Globalstar actual
Number of satellites [MHz]	66	66	46	48
Number of [MHz] simultaneous users per satellite	905	1100	2106	2500
Life-cycle cost [billion $]	5.49	5.7	3.59	3.3
Satellite mass [kg]	856.2	689.0	416.4	450.0
Number of cells	44	48	18	16
Orbital period [min]	100.3	100.1	113.9	114
Sat xmit average EIRP [dBW]	50.32	-	42.80	-
Number of gateways	12	12	50	50

Table 2.11: Benchmarking results of Iridium and Globalstar

	Orbcomm simulated	Orbcomm actual	SkyBridge simulated	SkyBridge designed
Number of satellites [MHz]	39	36	66	64
Number of [MHz] simultaneous users per satellite	216	-	510	-
Life-cycle cost [billion $]	1.79	0.5+	8.20	6.6+
Satellite mass [kg]	45.34	41.7	1072.4	1250.0
Number of cells	1	1	30	18
Orbital period [min]	101.3	-	115.1	-
Sat xmit average EIRP [dBW]	18	-	55.4	-
Number of gateways	64	-	48	-

Table 2.12: Benchmarking results of Orbcomm and SkyBridge

For key system attributes including number of satellites, satellite mass, system capacity, and life-cycle cost, the discrepancies between the actual/planned systems and simulated systems are typically less than 20%. Although not perfect, the fidelity of the model basically satisfies the need of the system studies we will conduct using the model. Up to this point, we have completed the inner loop A shown in Figure 2-1. We are ready to explore the trade space of the LEO communication satellite system using the model.

2.6 System Design Baseline Case Analysis

2.6.1 Trade Space Exploration and Optimization (Step 5)

In this step of the optimization, we will explore the trade space with a full-factorial run. As described above, a full-factorial run is the running of exhaustive combinations of selected values of the design variables using the model. The running result will illustrate how far we can reach in the objective space in achieving the design objectives. Then we will identify the Pareto front and utopia point of the objective space. The Pareto optimal solutions are distributed along the Pareto front.

The design variable values for the full-factorial run are specified as below

i	Variable	Values	Unit
1	constellation type	Polar, Walker	[-]
2	altitude	500, 1000, 1500	[km]
3	min elevation	5, 20, 35	[deg]
4	diversity	1, 2, 3	[-]
5	sat xmit pwr	200, 1100, 2000	[W]
6	sat antenna edge cell spot beam gain	10, 20, 30	[dBi]
7	iner sat link	0, 1	[-]
8	multiple access scheme	MF-TDMA, MF-CDMA	[-]
9	sat lifetime	5, 10, 15	[years]

Table 2.13: Design variable values for the full-factorial run

In all, 5,832 designs are tested by the full-factorial run. The results are plotted in

Figure 2-7, where the x-axis represents the system capacity in terms of the number of simultaneous users the system can support, and the y-axis represents the system life-cycle cost in billion USD. Besides the full-factorial run, this plot also marks the simulated and actual Iridium and Globalstar systems.

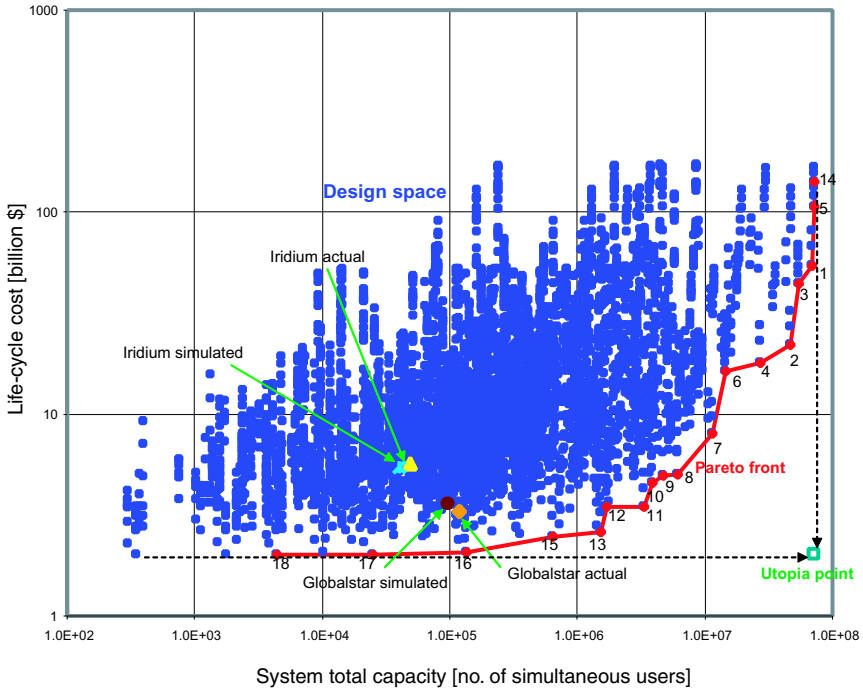

Figure 2-7: LCC vs. system capacity plot for a full-factorial run of 5,832 designs

Although this plot shows the general trend that systems with larger capacities have higher costs and systems with smaller capacities have lower costs, some designs are nevertheless clearly better than some others in both capacity and cost. For example, Globalstar has both a higher capacity and meanwhile a lower cost compared to Iridium. We say that the objective vector of the Iridium design is dominated by the objective vector of the Globalstar design. If the objective vector of a design is not dominated by the objective vectors of any other design in the design space, this design is efficient. All efficient designs together approximate the Pareto optimal designs.

Now we will look at the formal definitions of dominance and Pareto optimal solution.[dWW02b] Let $\mathbf{J^1}$, $\mathbf{J^2}$ be two objective vectors in the same objective space S. Then $\mathbf{J^1}$ dominates $\mathbf{J^2}$ if and only if (iff)

$$J_i^1 \geq J_i^2 \ \forall \ i \text{ and } J_i^1 > J_i^2 \text{ for at least one } i \tag{2.2}$$

A design $\mathbf{x}^* \in$ S is Pareto optimal iff its objective vector $\mathbf{J}(\mathbf{x}^*)$ is non-dominated by the objective vectors of all the other designs in S. In other words, design $\mathbf{x}^*$ is efficient if it is not possible to move feasibly from it to increase an objective without decreasing at least one of the other objectives. It should be noticed that $\mathbf{x}^*$ only approximates the Pareto optimal solution. The difference between Pareto optimal solutions and non-dominated solutions is that Pareto optimal solutions are always convex toward the direction of optimization, while the non-dominated solutions are not necessarily so. But for the purpose of finding the Pareto optimal solutions in our objective space, this difference can be ignored.

The front formed by the Pareto optimal solutions in the objective space is called Pareto front. In Figure 2-7, the Pareto front is plotted along the lower right boundary of the objective space. Among the 5,832 designs, 18 designs are Pareto optimal. Their design variables, total capacities and life-cycle costs are listed in Table 2.14 and 2.15. In the model, a subroutine named `ParetoFront.m` identifies the Pareto optimal solutions.

Also plotted in Figure 2-7 is the utopia point. Utopia point is a fictional design that is optimized in all objectives. The utopia point in Figure 2-7 has the highest capacity and lowest life-cycle cost of the entire objective space. A way to make comparison among the Pareto optimal designs is to compare their distances to the utopia point. This utopia distance is evaluated as what follows

$$\delta = \sqrt{\sum_{i=1}^{m} \left(\frac{J_i - J_i^{utopia}}{J_{i,worst} - J_i^{utopia}} \right)^2} \tag{2.3}$$

where J_i is the i^{th} objective of the design for which we need to find the utopia distance, and J_i^{utopia} is the i^{th} objective of the utopia point. The difference is normalized with the difference between the worst value occurring for the i^{th} objective in the entire objective space and J_i^{utopia}. In this fashion the normalized objective space

Design	Constel type	Orbital alti-tude [km]	Min. eleva-tion [^{o}]	Diversity	Sat xmit pwr [W]	Edge cell gain [dBi]	ISL	MAS	Sat life-time [year]
1	1	500	35	3	200	30	0	MF-CDMA	5
2	1	500	20	3	1100	30	0	MF-CDMA	5
3	1	500	20	3	200	30	0	MF-CDMA	5
4	1	500	35	3	1100	30	0	MF-CDMA	5
5	1	500	20	2	200	30	0	MF-CDMA	5
6	1	500	5	3	1100	30	0	MF-CDMA	5
7	1	500	35	3	2000	30	0	MF-CDMA	5
8	1	500	5	3	200	30	0	MF-CDMA	5
9	2	500	5	3	200	30	0	MF-CDMA	5
10	2	500	5	2	200	30	0	MF-CDMA	5
11	1	1000	5	3	200	30	0	MF-CDMA	5
12	2	1000	5	3	200	30	0	MF-CDMA	5
13	1	1500	5	3	200	30	0	MF-CDMA	5
14	2	1500	5	3	200	30	0	MF-CDMA	5
15	2	1500	5	2	200	30	0	MF-CDMA	5
16	2	1500	5	1	200	30	0	MF-CDMA	5
17	2	1500	5	1	200	20	0	MF-CDMA	5
18	2	1500	5	1	200	10	0	MF-CDMA	5

Table 2.14: Design variables of the Pareto optimal designs

will always fit exactly into a [0,1] hypercube. The last column in Table 2.15 lists the utopia distance values of all Pareto optimal designs. The order of the designs are listed in the order of increasing utopia distances. Utopia point related calculations are performed in a subroutine named `find_utopia.m`.

If we look at Table 2.15 more closely, a few very interesting generalizations can be made about the optimal design of LEO satellite constellations for voice communication. In general, the optimal designs are either a combination of polar constellations at low altitude and high elevation angle or a combination of Walker constellations at high altitude and low elevation angle. Multiple diversity of 3 is favored, except for a few cases at high orbital altitude. The combination of high antenna gain and low transmission power is favored over low antenna gain and high transmission power.

We can also observe that all optimal solutions do not use ISL, have MF-CDMA for multiple access scheme, and have the lowest lifetime of 5 years. These trends

Design	System total capacity	Life-cycle cost [billion $]	Utopia distance
1	69520323	54.2480	0.3095
2	54164448	44.1275	0.3542
3	47040115	22.0214	0.3709
4	72313834	106.2276	0.6117
5	27000896	17.9269	0.6348
6	14462098	16.3276	0.8051
7	72567789	142.3617	0.8238
8	11454730	7.9675	0.8429
9	6170400	5.0202	0.9151
10	4727808	4.9260	0.9350
11	3865514	4.5474	0.9469
12	3326532	3.4761	0.9542
13	1719426	3.4659	0.9763
14	1535202	2.6073	0.9789
15	641190	2.4609	0.9912
16	136532	2.0758	0.9981
17	24816	2.0210	0.9997
18	4466	1.9999	0.9999

Table 2.15: Objectives and utopia distances of the Pareto optimal designs

are consistent with reality. ISL does not help to increase the system capacity. Its advantage is to provide global communication network without reliance on ground installations, therefore avoiding the policy and security issues that might be caused by ground stations on foreign soils. (Indeed the concept of ISL was first developed for spy satellites by Motorola.) On the other hand, the development cost and the additional weight of ISL increase the system life-cycle cost. Therefore we are not surprised that no ISL design gains Pareto optimality in an objective space formed by system capacity and cost.

It is not surprising that MF-CDMA outperformed MF-TDMA throughout. CDMA can have a cluster size of 1, while TDMA has to have a higher cluster size to avoid interference between different channels. CDMA can take advantage of multi-path fading, therefore having a lower BER, data rate and link margin requirement than TDMA.

A short lifetime is preferred because a longer lifetime will require more fuel to

maintain the satellites in orbit. More fuel means higher satellite wet weight and more demanding launch capability. Therefore a system of long life is more costly than a system of short life. A longer lifetime system will gain advantage by averaging its initial deployment cost over its lifetime. But this advantage does not show in a capacity-lifecycle cost objective space. If the capacity is replaced by parameters such as total data transferred over the system lifetime, then designs of longer lifetime may emerge as Pareto optimal solutions.

To facilitate observation, the index numbers of the Pareto optimal designs in Table 2.14 and Table 2.15 marked in Figure 2-7. The general trends at the low capacity, low cost corner are Walker constellation, high orbital altitude, low elevation angle, low diversity, low power, and low edge cell gain. These trends lead to the kind of design that has sparse satellites orbiting at high altitude, supporting relatively small amount of users at low cost. The trends at the high capacity, high cost corner are polar constellation at low orbital altitude, high elevation angle, with high diversity, higher power and edge cell gain. These trends lead to the kind of design that has dense constellation orbiting at low altitude, supporting a large number of users at high cost.

So among the Pareto optimal designs, is there a optimal solution? The answer is not that straightforward. Because that along the Pareto front, in order to improve one objective, the other objective have to be sacrificed. In that sense, all solutions along the Pareto front are equal and cannot replace each other. But there are times when we want to be at a particular point on the Pareto front. For example, if we know the capacity that the market demands, we can intercept this market capacity demand (vertical line) with the Pareto front, and the intercepting point should be the design solution for this particular demand, as illustrated by point A in Figure 2-8. If we know the budget we have and we try to maximize the system capacity under the budget constraint, we can intercept this budget constraint (horizontal line) with the Pareto front and find the design solution for this particular budget constraint, as illustrated by point B in Figure 2-8.

Point A and B represent objective vectors of desired designs. In order to go from

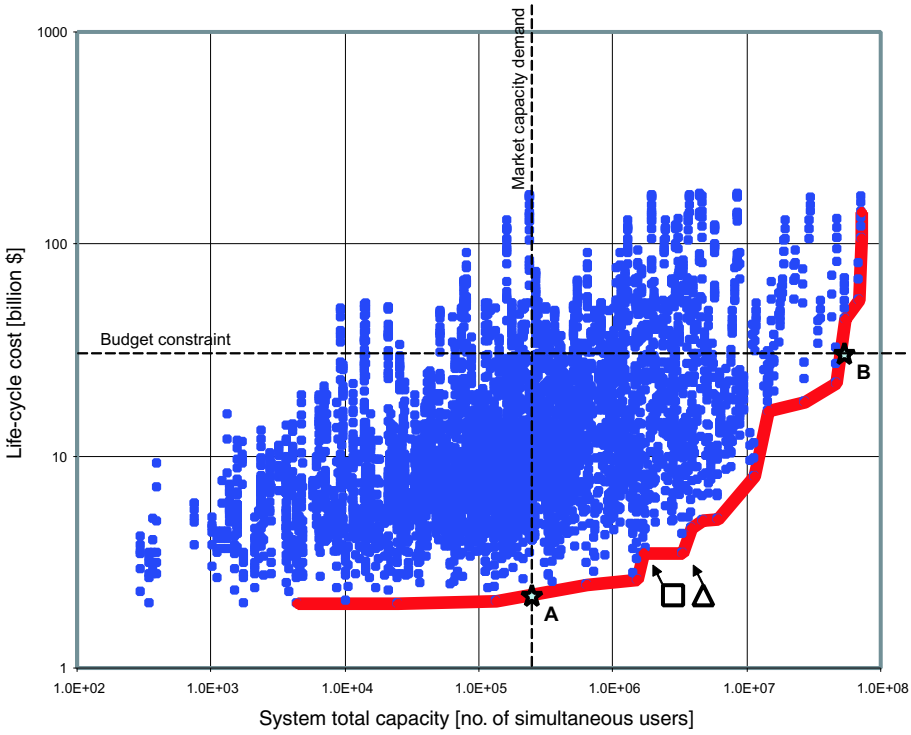

Figure 2-8: Optimal Pareto design under market capacity demand (point A) and budget constraint (point B)

the objective vectors to the desired design variables, a Pareto optimal design whose objective vector is close to the desired objective vector can be used. If the existing Pareto designs are not close enough to the desired design, full-factorial runs with more discrete values for each design variable should be performed until a fine enough design space resolution is obtained. There will be more Pareto optimal designs along the Pareto front, and we will be able to find a design that is closer to the desired objective vector.

It is also worth noticing a phenomenon where moving from one Pareto optimal design point to the other changes little in one objective but dramatically in the other objective. In the objective space illustrated by Figure 2-8, when we move from the Pareto optimal design point of (1,719,426 simultaneous users, 3.4659 B$), pointed by the arrow with a box, to the next Pareto optimal design point of (3,326,532 simultaneous users, 3.4761 B$), pointed by the arrow with a triangle, the system

capacity increases by more than 93% while the life-cycle cost increases by just about 0.3%. For the system designer, there is a good incentive to move from first point to the second point because this move is very cost-effective. Another type of move is a dramatic increase in cost but little improvement in capacity. In this situation, we want to adopt the design with lower cost.

Since we have found the Pareto optimal solutions in the objective space, we conclude Step 4 in our architectural trade space exploration. In the next section, we will perform some post-processing on the optimal solutions to better understand them.

2.6.2 Post-Processing of the Pareto Optimal Solutions (Step 6)

The process is not finished once the optimal solution set $\mathbf{x}^*$ has been found. Errors that might have occurred in the optimization process may lead the optimal solution to local optima, especially when the trade space is complex. Because we have made a full-factorial run that fully explores the design space, it is unlikely that the solution is in a local optimum. It is nevertheless interesting to understand which design variables are key drivers for the optimum solutions $\mathbf{x}^*$. This requires sensitivity analysis. Post-processing also involves uncertainty analysis. But we will focus on sensitivity analysis in our study.

The definition of sensitivity analysis is: How sensitive is the "optimal" solution set $\mathbf{J}^*$ to changes or perturbations of the design variable set $\mathbf{x}^*$. The mathematical expression of the sensitivity of a solution J to design variable x_1 is $\partial J/\partial x_1$. If the system is complex, it could be impossible to find an analytical solution for the partial derivative. In this situation, we will use finite difference approximation[dWW02a]:

$$\frac{\partial J}{\partial x_1} \approx \frac{J\left(x_1^1\right) - J\left(x_1^0\right)}{x_1^1 - x_1^0} = \frac{J\left(x_1^0 + \Delta x_1\right) - J\left(x_1^0\right)}{\Delta x_1} = \frac{\Delta J}{\Delta x_1} \tag{2.4}$$

In order to compare sensitivity from different design variables in terms of relative sensitivity, it is necessary to normalize the sensitivity calculation as

$$\frac{\Delta J}{\Delta x_i} \rightarrow \frac{\Delta J/J}{\Delta x_i/x_i} \tag{2.5}$$

We choose $\Delta x_i/x_i$ to be 10% of the original design variable value. If the design variable only allows Boolean values, then the Boolean value of the design variable is switched. Sensitivities of two Pareto optimal designs are examined. The first design is the one with smallest utopia distance. It is design #1 in Table 2.15. The normalized sensitivity values of two objectives are listed in Table 2.16 and plotted in Figure 2-9.

i	Variable	Sensitivity of system total capacity with respect to design variables	Sensitivity of life-cycle cost with respect to design variables
1	constellation type	-0.9401	-0.5634
2	altitude	-1.531	-1.4397
3	min elevation	0.6643	2.2552
4	diversity	1.1111	0.5694
5	sat xmit pwr	0.0457	0.2022
6	edge cell spot beam gain	2.3153	0.2819
7	inter sat link	-0.8748	0.4984
8	multiple access scheme	-0.9326	0
9	sat lifetime	0	0.0217

Table 2.16: Normalized sensitivity of Pareto optimal design #1

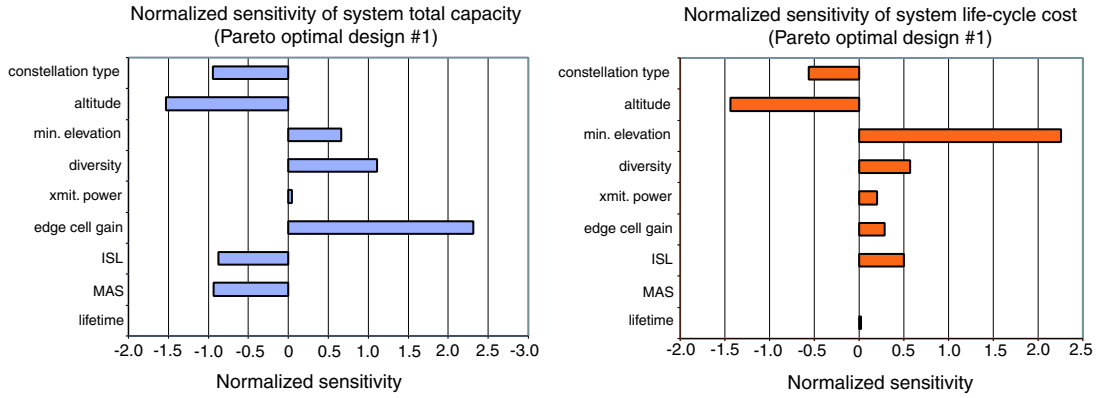

Figure 2-9: Graphical illustration of normalized sensitivity of Pareto optimal design #1

For Pareto optimal design #1, system total capacity is most sensitive to orbital

altitude and edge cell gain. Life-cycle cost is most sensitive to orbital altitude and minimum elevation angle.

If examining the sensitivity of design #1 closely, we can see that design #1, a design at the high capacity-high cost corner of the objective space, has been pushed to its limits in maximizing capacity and cost. If the constellation type becomes Walker, altitude lower, elevation angle larger, diversity higher, or edge cell gain higher, then the system capacity and life-cycle cost will both increase. But the values of the above mentioned design variables have been pushed to the limit given by the design range. It is interesting to see that changing to value of ISL from 0 to 1 will decrease the system capacity. A test run for this case has demonstrated that the ISL data rate will become the limiting factor for satellite capacity once it is installed, and in addition it will cause a higher cost. So the Pareto optimal design has no ISL.

The next design that we will test is Pareto optimal design #15. This is a random choice, except the design variable values of this design is close to the design of Globalstar. The normalized sensitivity values are listed in Table 2.17 and illustrated in Figure 2-10.

i	Variable	Sensitivity of system total capacity with respect to design variables	Sensitivity of life-cycle cost with respect to design variables
1	constellation type	0.1539	0.1459
2	altitude	-1.8645	-0.5989
3	min elevation	0.0597	0.0772
4	diversity	1.2121	0.6061
5	sat xmit pwr	0.6866	0.2499
6	edge cell spot beam gain	5.9578	0.1575
7	inter sat link	-0.7320	0.5415
8	multiple access scheme	-0.9040	0
9	sat lifetime	0	1.68E-5

Table 2.17: Normalized sensitivity of Pareto optimal design #15

The sensitivity analysis shows that the system total capacity of Pareto optimal design #15 is also most sensitive to orbital altitude and edge cell gain. Different from design #1, the life-cycle cost is most sensitive to orbital altitude, diversity, and ISL.

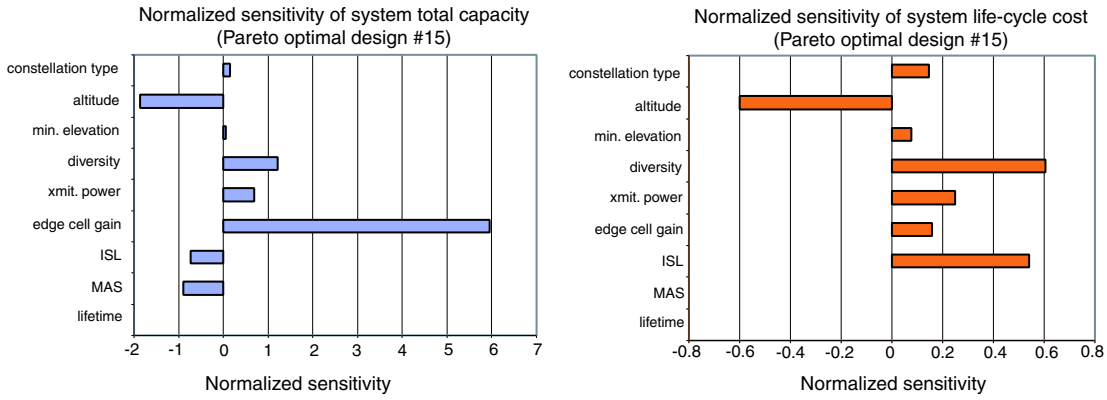

Figure 2-10: Graphical illustration of normalized sensitivity of Pareto optimal design #15

Different from design #1, design #15 is between the high capacity-high cost corner and the low capacity-low cost corner of the objective space. Some of its design variable values including constellation type, orbital altitude and elevation angle are pushed to the design range boundary to minimize system capacity and cost. The other design variables do not show a trend of maximizing or minimizing the capacity or cost. Once again, if ISL is installed, its data rate will become a limiting factor to satellite capacity, same as design #1.

If the result of the sensitivity analysis is acceptable, then Loop B of the trade space exploration methodology shown in Figure 2-1 is complete. Otherwise, more loops are necessary until a satisfactory result is obtained.

2.7 Summary of System Architectural Trade Space Exploration

This chapter has illustrated a comprehensive methodology of exploring the trade space of a complex multi-input, multi-output, and multi-disciplinary system design. We first identify the design variables, constants, policy constraints, and requirements as inputs, and the objectives and benchmarking parameters as outputs. Then we go through an inner loop that creates a system model for the real system. This

loop maps different modules of the model to different physical or functional aspects of the real-world system, implements and integrates the modules, and at the end benchmarks the model with the real-world system. With the model's fidelity proved by the benchmarking, we run a full-factorial run that generates a set of designs covering the entire design space. From this set of designs, we identify the Pareto optimal designs and the utopia point. The Pareto optimal designs provide a pool from which the system designers can select the final design based on demand or budget constraints. The utopia point will be used in the next chapter to measure objective space migration caused by technology infusion. At the end, we perform sensitivity analysis on the Pareto optimal solutions. Thus we have completed the outer loop of the trade space exploration methodology.

Chapter 3

Impact of Technology Infusion

3.1 Introduction

In Chapter 2, the trade space of LEO communication satellite constellations is produced using system model LEOcomsatcon. A full-factorial run made with the model generates the baseline objective space. In this objective space, the Pareto optimal solutions along the Pareto front are found. But the trade space is not unalterable. The baseline trade space we have seen represents the possible designs implemented with current technologies and under current policy constraints. If newer technologies are implemented or the policy constraints are changed, the trade space would shift accordingly. By comparing the Pareto optimality of the new trade space with that of the baseline case, we will be able to gain insight of the effects that the new technologies or policy constraints would have on the system. The implementation of new technologies to the system is done through technology infusion interface (TII) that will be integrated into the model. Impact of policy constraint changes will be discussed in Chapter 4 using real-world examples.

3.2 Motivation for Technology Infusion Study

Technology advancement is a common phenomenon of the modern age. System designers take advantage of these technologies to improve system performance. But

there is a consequence to the use of new technologies: often the system designers can select only one or two technologies from a set of new technologies due to limited budget or technology compatibility issue. This makes the new technologies at competition with each other. To make things more complicated, a new technology will typically improve system performance, but sometimes it may increase the system performance in one direction at the sacrifice of the performance in another direction or improve one sub-system's performance at the sacrifice of another sub-system's performance. In addition, any performance improvement typically comes at higher economic expense. The understanding of the trade-offs between costs, system performance in different directions, and the sub-system performances is important in deciding whether to implement the technology and also in understanding how to prepare for the impact brought by technology implementation. Technology infusion study will help us to understand these relations that appear to be complicated at the first glance, and therefore provide the criteria for evaluating new technologies. Technology infusion is a quantitative study on the effects the new technologies bring to the system. It will help the system designers to make the technology selection. It will also help the system designers to convey the rationales of the selection to decision-making bodies such as the board of a company or national parliament.

3.3 Technology Infusion Framework

The quantitative technology infusion framework consists of six steps as illustrated in Figure 3-1.[dWCSM03]

1. Explore the baseline trade space using system simulation.

2. Identify, classify, and model candidate new technologies whose effects on the system will be studied.

3. Develop technology infusion interface (TII) through which the new technologies are implemented to the system and affect the system without violating the integrity of the system model.

4. Assess the effects of individual new technology on the system.

5. Assess the effects of combinations of new technologies on the system.

6. Post-process and interpret the results from step 4 and 5.

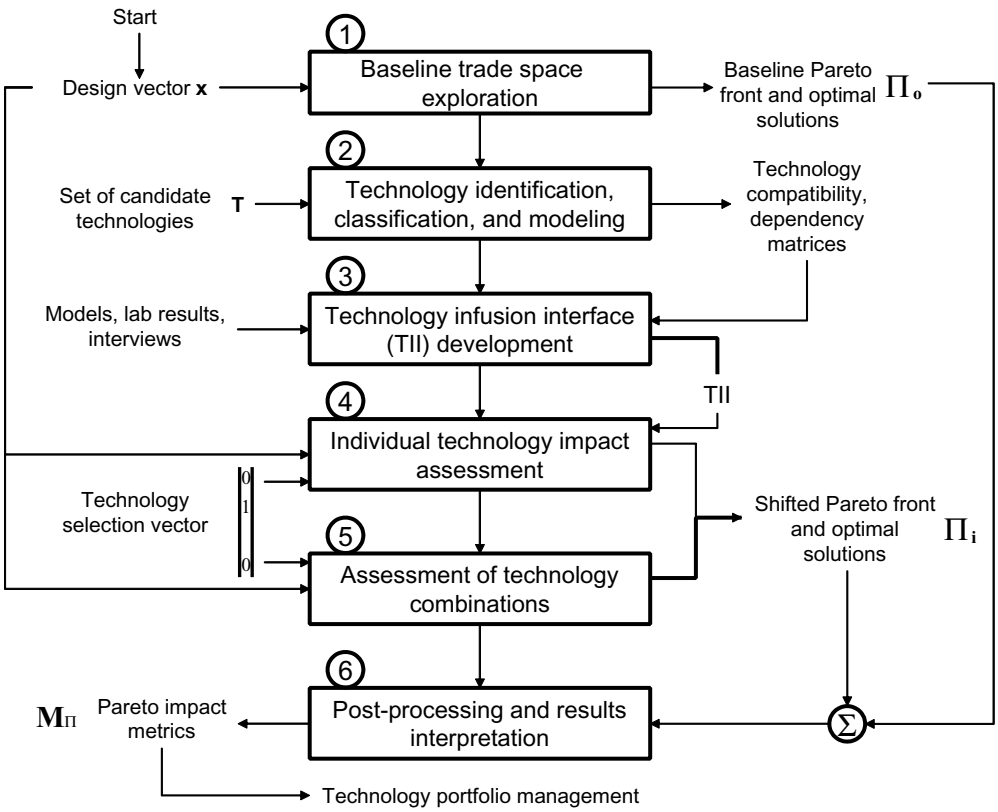

Figure 3-1: Quantitative technology infusion study framework

This framework is applicable to a variety of systems. In the sections below, we will go through the six steps in the framework and use LEO communication satellite constellation system as example.

3.4 Technology Infusion and Its Application to LEO Satellite Communication Constellation System

3.4.1 Baseline Trade Space Exploration (Step 1)

This step has been accomplished in Chapter 2. From the baseline objective space, we have identified the Pareto front and Pareto optimal designs. The design inputs for the Pareto optimal designs are listed in Table 2.14, the matching objectives and utopia distances are listed in Table 2.15. The entire objective space and the Pareto front are plotted in Figure 2-7.

3.4.2 Technology Identification, Classification, and Modelling (Step 2)

The second step consists of identifying, classifying, and quantitatively modelling the new technologies that potentially can be infused into the baseline system. The potential technologies represent cutting-edge technologies in the industry. They should have reached certain maturity in development so that their effects on the system performance and cost can be assessed. The new technologies form the new technology vector $\mathbf{T} = [T_1, T_2, ..., T_n]^{\mathrm{T}}$. The maturity of each new technology must be assessed. The NASA technology readiness level (TRL) forms a well-established scale for the maturity assessment. The definitions of NASA TRL are listed in Table 3.5.[LW92]

Among the new technologies, there are two types of relations we need to clearly understand before we simulate their implementation to the system: compatibility-relationship and dependency-relationship. Some technologies are mutually incompatible so they cannot be applied to the system simultaneously. An example of this exclusiveness in spacecraft is gravity gradient stabilization and high-angular resolution optical payloads. The compatibility relation between the new technologies can be expressed in form of compatibility matrix $\mathbf{T_c}$. With the technologies as both the row and column entries, the compatibility matrix is symmetric and has zero entries for technologies that are compatible and a 1 for technologies that are mutually exclusive.

Technology readiness level	Definition	Relative risk level
1	Basic principles observed	High
2	Conceptual design formulated	High
3	Conceptual design tested analytically or experimentally	Moderate
4	Critical function/characteristic demonstrated	Moderate
5	Component or breadboard tested in relevant environment	Low
6	Prototype/engineering model tested in relevant environment	Low
7	Engineering model tested in space	Low
8	Full operational capability	Low

Table 3.1: NASA Technology Readiness Level (TRL)

In the sample compatibility matrix shown in Figure 3-2, T_1 and T_3 are incompatible, and T_2 and T_5 are incompatible.

$$\mathbf{T_c} = \begin{array}{c} \\ T_1 \\ T_2 \\ T_3 \\ T_4 \\ T_5 \end{array} \begin{array}{c} \begin{array}{ccccc} T_1 & T_2 & T_3 & T_4 & T_5 \end{array} \\ \begin{bmatrix} - & 0 & 1 & 0 & 0 \\ & - & 0 & 0 & 1 \\ & & - & 0 & 0 \\ & & & - & 0 \\ & & & & - \end{bmatrix} \end{array}$$

Figure 3-2: A sample technology compatibility matrix

Another relationship between technologies is dependency. That is, a technology can be applied only after another technology is applied first. This relation is represented by the technology dependency matrix $\mathbf{T_d}$. If a cell in the matrix is 1, the technology of that column depends on the technology of that row. In the example shown in Figure 3-3, T_2 depends on T_4, T_3 depends on T_2, and T_5 depends on T_1:

Technology compatibility-relationship and dependency-relationship are useful in deciding which individual technology or combination of technologies to be tested. Af-

$$\mathbf{T_d} = \begin{array}{c} \\ T_1 \\ T_2 \\ T_3 \\ T_4 \\ T_5 \end{array} \begin{array}{c} \begin{array}{ccccc} T_1 & T_2 & T_3 & T_4 & T_5 \end{array} \\ \begin{bmatrix} 0 & 0 & 0 & 0 & 1 \\ 0 & 0 & 1 & 0 & 0 \\ 0 & 0 & 0 & 0 & 0 \\ 0 & 1 & 0 & 0 & 0 \\ 0 & 0 & 0 & 0 & 0 \end{bmatrix} \end{array}$$

Figure 3-3: A sample technology dependency matrix

ter the technology selection, each technology must be modelled quantitatively. There are three avenues to generating such quantitative modelling:

1. Physics-based bottom-up reproduction of new technologies in the simulation environment

2. Data from prototype/benchtop tests of new technologies

3. Empirical relationships of new technologies' performance and cost based on expert interviews

For this study, the third avenue is mainly taken with partial help from the second avenue. There are a few reasons for this approach. The new technologies are often in the process of being developed, ranging anywhere from conceptual design to prototype testing. Their technical details are still maturing and cannot be determined with certainty. This increases the difficulty in modelling them in computer simulations. In addition, in contrast to mature technologies, information on technical details of these new technologies is more difficult to obtain due to business proprietary protection policies. So it may be the more credible approach to leap-frog the technical details and assess technology impacts directly from the opinions of the experts working on these technologies. The experts make their assessment based on mostly the second avenue, data from prototype testing. Since we typically do not have direct access to these data, interviewing the experts who did the testing is the only way of obtaining them.

Since we use the expert inerview approach, we should be conscious of two consequent issues. The first issue is that the technology to be tested must reach a TRL of at least 5. The reason is that at TRL 3 or 4, although analysis or experiment has been conducted and even critical function and characteristic have been demonstrated, the test environment is irrelevant to the working environment, and therefore the test result cannot be extrapolated reliably. So in our opinion a TRL of 5 is a prerequisite for basing the technology infusion study on interviews with experts.

The second issue of using the third approach is that the expert interviewed, if personally involved in creating the new technology, may give an overly optimistic assessment either because s/he is emotionally attached to the technology or because s/he has a personal stake in the success of the technology. To cope with this problem, whenever allowed by the circumstances, multiple interviews from different stakeholders on the same technology should be conducted to average out personal bias. Although this study has not been able to interview multiple stakeholders on any of the technology studied because of time constraints, this kind of interviews should be conducted in the future as follow-up to the study.

Four new technologies are selected for this study. They are optical inter-satellite link (OISL), asynchronous transfer mode (ATM), large deployable reflector (LDR), and digital/analog beam forming (DBF/ABF). These technologies represent the most forward-looking development trends in space-based communication. They are currently under development in Communications Research Laboratory (CRL) and Next-generation LEO System Research Center (NeLS) in Japan, as well as other laboratories around the world. The technical and cost specifications of these technologies were obtained mainly during interviews conducted in Japan in the summer of 2002 by this author. An analysis of these technologies and its modelling follows in the subsequent sections.

Optical Inter-Satellite Link (OISL)

Inter-satellite link (ISL) enables satellite-to-satellite data transfer free of reliance on ground-based gateway. Each Iridium satellite has four ISL's for both intra-orbital

plane and inter-orbital plane data transfer. OISL is a significant improvement over ISL with the following three advantages:

1. Using laser beam instead of the radio frequency (RF) wave, OISL has a much higher data rate.

2. Because laser beam has a very small divergence on the scale of 0.0001 degree, inter-transmission interference is negligible. Therefore OISL can have virtually any bandwidth.

3. Compared with RF ISL, OISL is lighter, more compact, and consumes less power.

The disadvantage of OISL is that the small beam width requires much higher pointing, acquisition, and tracking accuracy. Currently, OISL is under development in U.S., Japan, and Europe. In 2001, European Space Agency (ESA) launched its advanced telecommunication technology test satellite, Artemis, that carries an optical ISL named SILEX (Semi-conductor laser Inter-satellite Link EXperiment). National Space Development Agency of Japan (NASDA) plans to launch Optical Inter-orbit Communications Engineering Test Satellite (OICETS) in 2005. OICETS will carry with it Laser Utilizing Communications Equipment (LUCE). ESA and NASDA have agreed to demonstrate the optical inter-satellite link capability between Artemis and OICETS.

The effects that OISL has on the satellite system is summarized in Table 3.2.[Koy02] Appendix B shows a derivation of the data. It should be noted that the development cost refers to the cost incurred by integrating the technology into the system.

If Iridium's RF ISL's are replaced by OISL's, the mass of Iridium in reality would become 689kg - 309kg = 380kg. The satellite mass of Iridium without ISL is given as 425kg by the simulation. But since the simulation has over-predicted the mass of Iridium with ISL (856kg vs. 689kg), it is likely to over-predict the mass of Iridium without ISL as well. If the ratio of weight between the predicted Iridium with ISL and the actual Iridium with ISL is about the same as the ratio between the predicted

Figure 3-4: Artist impression of OISL demonstration between OICETS and Artemis (Copyright: NASDA)

Iridium without ISL and the actual Iridium without ISL, the actual Iridium without ISL mass is more likely to be around 340kg. The difference between Iridium with OISL mass and the Iridium without ISL is about 40kg, smaller than the mass of OISL of 117kg given by the expert interview. We should be aware of this discrepancy and be reserved about the data on the OISL.

Asynchronous Transfer Mode (ATM)

Asynchronous transfer mode is suitable for high bandwidth transfer of multimedia signals because its scheme has fixed packet length (53 bytes) and is flexible in capacity allocation to each connection. Multiple logical connections are multiplexed over a single physical layer with each connection allocated the amount of resources it needs. Thus no network resource is under- or over-utilized. ATM system has a higher utilization of communication traffic capacity than conventional system.[LWJ00]

Employing ATM technology aboard satellites has been under active study by several countries. Examples of satellites carrying ATM include the Advanced Com-

	30 Mbps RF ISL (4 links)	300 Mbps RF ISL (4 links)	10 Gbps optical ISL (4 links)	Increase from 30 Mbps RF ISL to optical ISL	Increase from 300 Mbps RF ISL to optical ISL
Development cost (million $)	13.56	16.95	25.42	11.86	8.47
First unit cost (million $)	29.49	31.19	67.80	38.31	36.61
Weight (kg)	426	480	117	-309	-363

Table 3.2: Effects of OISL on the satellite system

munications Technology Satellite (ACTS) launched into geosynchronous orbit in 1993 by the U.S. ACTS is designed for tests of multiple spot beam antennas and advanced on-board switching and processing systems. Another example is the Wideband Internetworking Engineering Test and Demonstration Satellite (WINDS) developed by NASDA and CRL. Equipped with high-gain antennas and high-speed ATM, WINDS will transmit fast internet signals for households with portable ground equipment. WINDS is planned to be launched into geosynchronous orbit in 2005. Teledesic, a broadband LEO constellation system intended to provide internet access, has planned to use an operational version of ATM.

ATM ranks 7 in NASA TRL because its engineering model has been tested in space aboard ACTS and other satellites. Its effect on the system is summarized in Table 3.3.[Kad02]

	ATM
Development cost (million $)	40.0
First unit cost (million $)	12.5
Weight (kg)	100.0
Increase to communication capacity	$\times 1.5$

Table 3.3: Effects of ATM on the satellite system

Large Deployable Reflector (LDR)

The most notable technology carried by NASDA's Engineering Test Satellite VIII (ETS-VIII) is the large deployable reflector (LDR). According to NASDA publication,

"LDR uses a modular structure to meet the requirements of reflector surface preciseness (2.4mm RMS) and antenna-diameter expandability. Each hexagon shaped module, similar to automatic umbrella, has a deployable truss structure.

LDR consists of 14 modules. The outside dimension is 19m × 17m at largest and folds to 1m (diameter) × 4m (height) during launch. ETS-VIII is equipped with 2 LDRs, one for transmission and the other for reception."

The large surface area of LDR increases the gain of the satellite transmitter and receiver, and therefore is critical in realizing mobile satellite communication with hand-held terminals. NASDA is to launch ETS-VIII into the geostationary orbit in 2004.

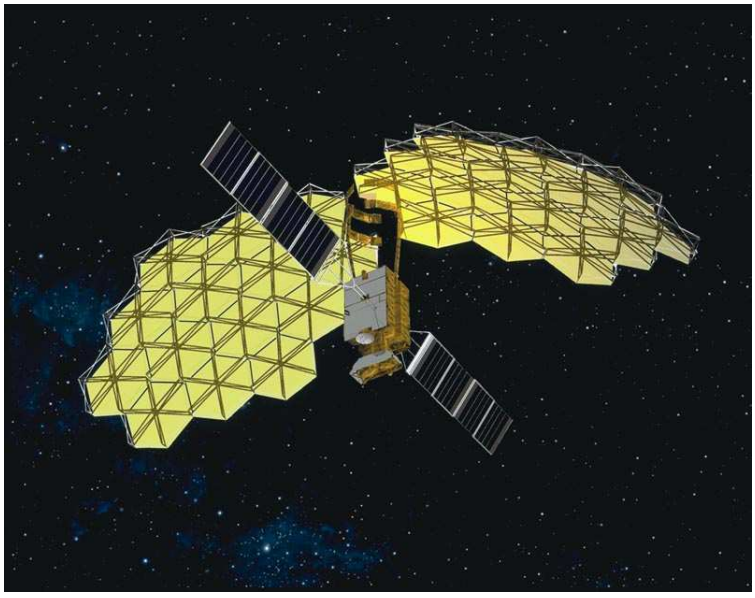

Figure 3-5: Artist impression of ETS-VIII in space with LDR deployed (Copyright: NASDA)

LDR has a TRL of 6 since its engineering model has been tested on the ground. Its effects on the system is summarized in Table 3.4.[Hom02] The LDR deployed on ETS-VIII is about 18-meter in diameter. Because the capacity effect of LDR is

exclusively through its larger gain which will be accounted in the capacity calculation, therefore item "Increase to communication" in Table 3.4is listed as 0.

	LDR
Development cost (million $)	84.7
First unit cost (million $)	7.5
Weight (kg)	$9.173D_{sat}^{1.403}$
Increase to communication capacity	0
Antenna gain	$\left(\frac{D_{sat}}{\lambda}\pi\right)^2$

Table 3.4: Effects of LDR on the satellite system (λ is wavelength)

Figure 3-6: LDR engineering model deployment test (Copyright: NASDA)

Digital/Analog Beam Forming (DBF/ABF)

For multiple spotbeam LEO satellites, because the cells on the ground move at the same speed as the satellite, cell handover is required when the user is shifted from one cell to another. If the duration of a user's staying in a cell is short ($<$ 30 secs), the

rapid shifting of cells demands a handover capability that is not practical with current clock speed in the CPU aboard the satellite. To overcome this problem, beam forming is developed to enable the satellite to anchor its footprint to the ground. Analog beam forming (ABF) employs a small mechanically steered antenna for each spotbeam. For relatively high frequency transmission, the size of this antenna will be too big to be practical, so that digital beam forming (DBF) is preferred. DBF is more complex, consumes more power, and more expensive, but it has the advantage of mechanical simplicity and programming flexibility.[Suz02]

Teledesic mentioned above and SkyBridge, a GEO-LEO combined system for broadband service complementary to terrestrial system, have been planned to use ABF. On the other hand, NeLSTAR, a test satellite developed by NeLS in Japan, plans to use DBF.

DBF/ABF ranks level 6 in TRL as its prototype has been built and tested on the ground.

DBF cost consists of costs of elements, up-converters, calculators, controller, front-end, solid state power amplifiers (SSPA), heaters, and integration. ABF cost consists of costs of elements, up-converters, controller, beam forming networks (BFN), SSPA, heater, and integration. For detailed calculation of the first unit cost of DBF/ABF, see Appendix D. The development cost of DBF/ABF is about twice the cost of first unit. No significant mass is added.[Ori02]

To summarize, the TRL classifications of the four technologies at the time this literature is written are listed in Table 3.5.

Applying the technology compatibility matrix to the four technologies, we have the matrix shown in Figure 3-7. Clearly, all four technologies are mutually compatible.

There are three dependency relations among the four technologies:

1. ATM will increase system capacity and therefore increase the traffic capacity demand on the ISLs. If RF ISL has been used for the original system, the ISL might not be able to handle this higher capacity brought by ATM. In the situation of ISL inefficient capacity, OISL should be implemented to fully utilize the capacity increase.

Index	Technology	Current development	TRL classification
T_1	OISL	Engineering model to be tested in space between Artemis and OICETS	6
T_2	ATM	Engineering model tested in space aboard ACTS and other satellites	7
T_3	LDR	Operational capability aboard Thruaya	8
T_4	DBF/ABF	DBF achieves operational capability aboard Thruaya. ABF prototype tested on ground.	8 for DBF and 6 for ABF

Table 3.5: TRL classification of the four new technologies

$$\mathbf{T_c} = \begin{array}{c} \\ T_1 \\ T_2 \\ T_3 \\ T_4 \end{array} \begin{array}{c} \begin{array}{cccc} T_1 & T_2 & T_3 & T_4 \end{array} \\ \begin{bmatrix} - & 0 & 0 & 0 \\ & - & 0 & 0 \\ & & - & 0 \\ & & & - \end{bmatrix} \end{array}$$

Figure 3-7: Compatibility matrix for the four technologies studied

2. By increasing transmitter and receiver gain, LDR increases the traffic flow of the system. It might require OISL for the same reason as dependency relation 1.

3. LDR will increase spotbeam gain, decrease spotbeam beamwidth, and thus reduce the footprint size of the spotbeam on the ground. Sometimes this footprint becomes so small that the user duration in a cell is less than 30 seconds. In this situation, user handover between spotbeams becomes difficult, and the implementation of beam forming (DBF/ABF) is required to anchor the spotbeam to the ground to avoid the user handover.

It should be noted that these dependency relations are conditional. Whether they exist or not depends on the technical thresholds that are expressed in quantitative

terms. For relations 1 and 2, the threshold is the comparison between ISL data rate requirement and available ISL data rate capacity. For relation 3, the threshold is the 30 seconds duration for which the user stays in a cell. Relations 1 and 2 are specially complicated because OISL is not required for the system's technical validity. It is required only if the capacity increase brought by ATM or LDR is to be fully utilized. Implementing OISL could be a mixed blessing because it will increase the system cost at the same time of increasing performance. Whether the increase in performance is worth the increase in cost is not clearly answered. Understanding the complexity brought by technology infusion is exactly the purpose of this study. We will examine the effects brought by individual technology and combinations of technologies on the system in later sections of this chapter.

The dependency matrix for the four technologies is shown in Figure 3-8

$$\mathbf{T_d} = \begin{array}{c} \\ T_1 \\ T_2 \\ T_3 \\ T_4 \end{array} \begin{array}{c} \begin{array}{cccc} T_1 & T_2 & T_3 & T_4 \end{array} \\ \begin{bmatrix} - & 1 & 1 & 0 \\ 0 & - & 0 & 0 \\ 0 & 0 & - & 0 \\ 0 & 0 & 1 & - \end{bmatrix} \end{array}$$

Figure 3-8: Dependency matrix for the four technologies studied

It should be noticed that the first three technologies, OISL, ATM, and LDR are not required for system technical validity under any circumstances. In other words, they are "luxury" technologies that will improve the system's performance but not needed for the system to operate properly. The fourth technology, DBF/ABF, is not a luxury technology under certain circumstances. When the duration of a user in a cell is less than 30 seconds, DBF/ABF must be used to avoid user handover between cells; otherwise, the system does not operate properly.

With understanding of the quantitative effects the new technologies have on the system and the relations between the technologies, we are ready to infuse these effects into the system simulation that we have developed in Chapter 2. To achieve this goal,

we will introduce the development of technology infusion interface (TII) in the next step.

3.4.3 Technology Infusion Interface (TII) Development (Step 3)

The purpose of TII is to simulate the effects of new technologies on the system in real-world by infusing the technologies quantitatively into the system model. The technology infusion in the simulation environment mirrors the technology infusion in the real-world. One goal of the TII is to be modular and avoid recoding of the other parts of the system system model every time a new technology needs to be investigated. Figure 3-9 shows a diagram of the TII.

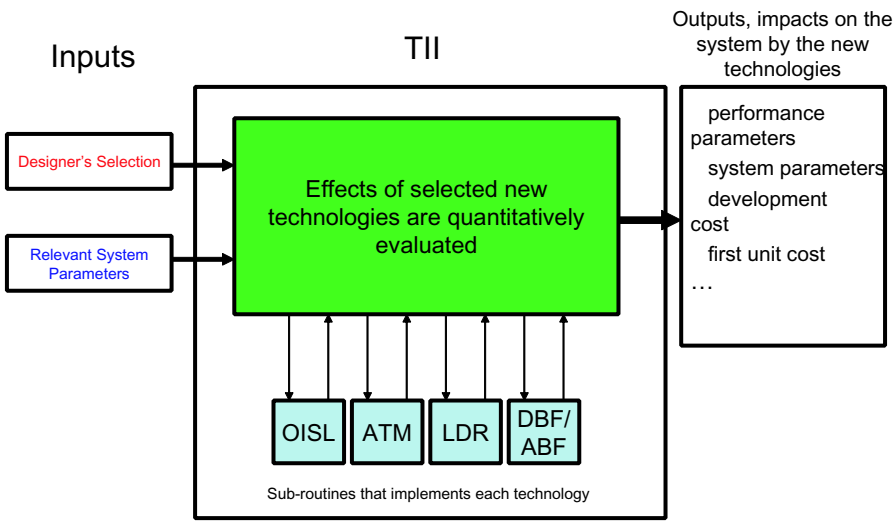

Figure 3-9: Technology infusion interface (TII) structure diagram

The TII has two types of inputs: designer's selection and relevant system parameters. Designer's selection flags which new technologies the designer selects to test. Relevant system parameters are the technical parameters needed to model the technologies. They include some of the design variables, constants, and parameters calculated by modules executed before technology infusion interface is called into action.

Inside TII, subroutines representing the selected technologies are called into action. Each subroutine evaluates the quantitative changes the new technology brings to the system according to the data listed in step 2 above. To smooth the interaction between TII and the model, these impacts are summarized as the change in performance parameters (for example, system capacity change brought by ATM), change in system parameters (for example, change in satellite mass and change in antenna gain), change in development cost, and change in first unit cost. These changes are outputs of TII, and they are made to be among the standard inputs of the modules that are executed after TII. Inside each module, the changes are accounted in all calculations of the system. It should be noticed that even if TII is re-programmed, as long as the TII outputs and module inputs are unchanged, there is no need to make change inside the modules. The model with TII added is illustrated in Figure 3-10.

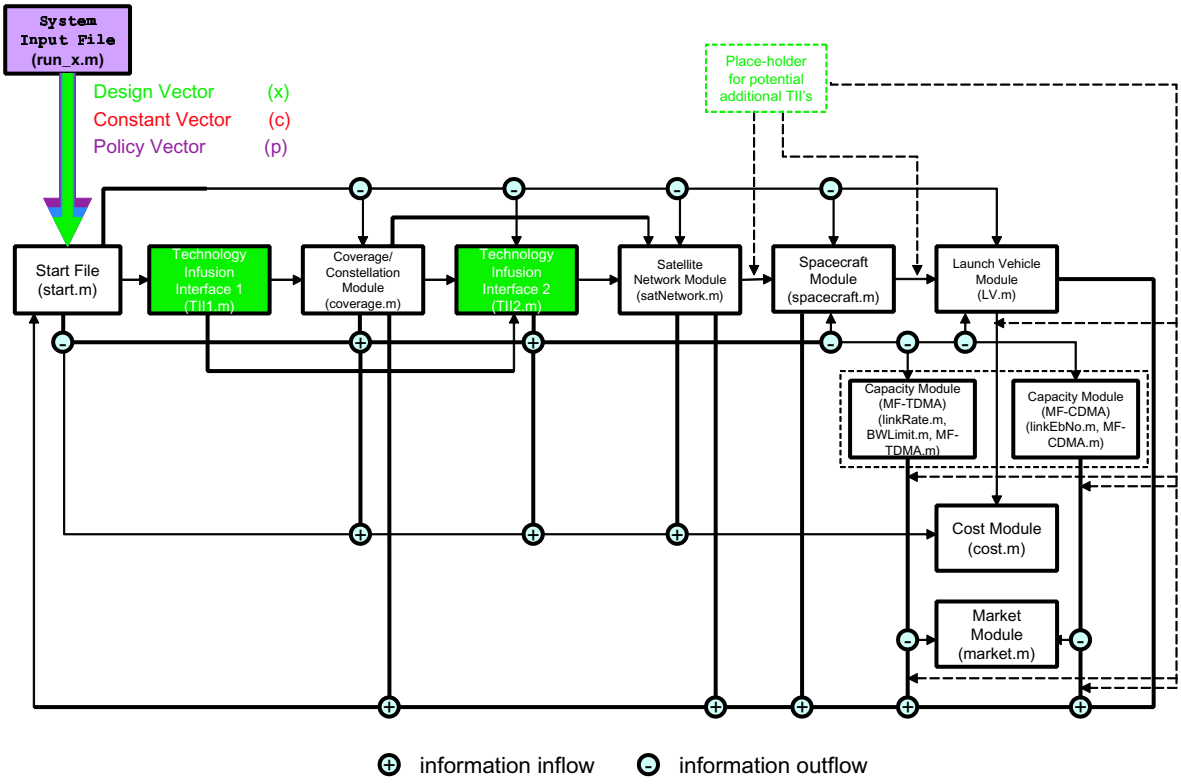

Figure 3-10: System model with technology infusion interface

The reason that there are both TII 1 and TII 2 is that the implementation of DBF/ABF requires some system parameters calculated in the coverage module, in-

cluding cell duration and number of cells. But among the inputs of coverage module are parameters that may be affected by infusion of other technologies. For example, the edge cell gain of antenna would be affected by the infusion of LDR. Therefore the system model is structured so that the infusion of LDR and other technologies are implemented before the coverage module, and the infusion of DBF/ABF is implemented after the coverage module. In Figure 3-10, place holder for additional TII's is illustrated. These additional TII's can be added to capture new technology improvements made to any of the major modules if potential new spacecraft, launch vehicle, or communication technologies have to be analyzed. In principle, the TII would interrogate and intervene in the simulation flow after each of the main modules.

With the TII implemented into the model, we are ready to assess the impact of new technologies on the system. First, let's look at individual technology impact.

3.4.4 Assess the Effect of Individual Technology Infusion (Step 4)

In this phase, we select technology T_i individually to be infused into the system. The new technology will be selected through TII. Full-factorial runs with the same inputs as the baseline case will be conducted with the addition of technology infusion. The objective spaces of these individual technology infusion cases are constructed and their Pareto front $\mathbf{\Pi_i}$ and Pareto optimal solutions are found.

The technologies we will infuse are OISL, ATM, LDR, and DBF/ABF. Figure 3-11, 3-12, 3-13, and 3-14 show the objective spaces and Pareto fronts of the system with these technologies infused respectively. It also shows the baseline objective space and Pareto front on the same plot for comparison. The first impression is that the Pareto fronts of OISL and DBF/ABF cases retreat away from the Utopia point. The Pareto fronts of ATM and LDR cross with the baseline Pareto front several times at the higher-capacity, higher cost corner of the objective space, while the baseline case dominate at the lower-capacity, lower cost corner.

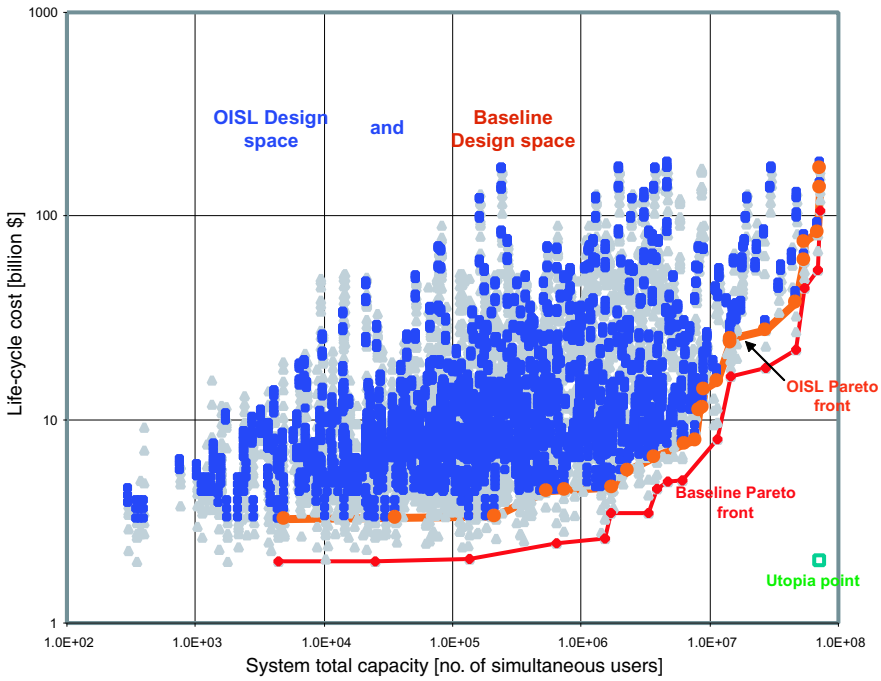

Figure 3-11: OISL-infused objective space and Pareto front

3.4.5 Assess the Effect of Technology Combinations (Step 5)

Assessing the effects of individual technology infusion alone is not enough. As mentioned above, there are dependency relations between the technologies. Sometimes, in order to fully utilize the additional performance brought by one technology, another technology must also be implemented. The dependency relations between ATM and OISL, and LDR and OISL are examples of this situation. At other times, in order to make the implementation of one technology feasible, another technology must be implemented. For example, the dependency relation between LDR and DBF/ABF. Therefore it is very important to evaluate technology infusion in combinations of technologies that have dependency relations. In this section, we will test four combinations: OISL+ATM, OISL+ LDR, LDR+DBF/ABF, and LDR+DBF/ABF+OISL.

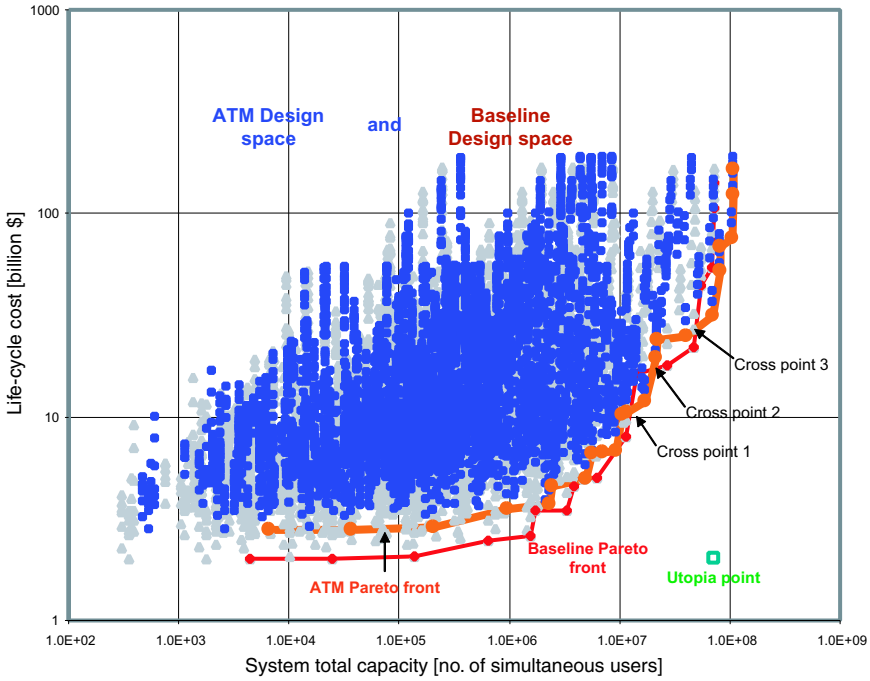

Figure 3-12: ATM-infused objective space and Pareto front

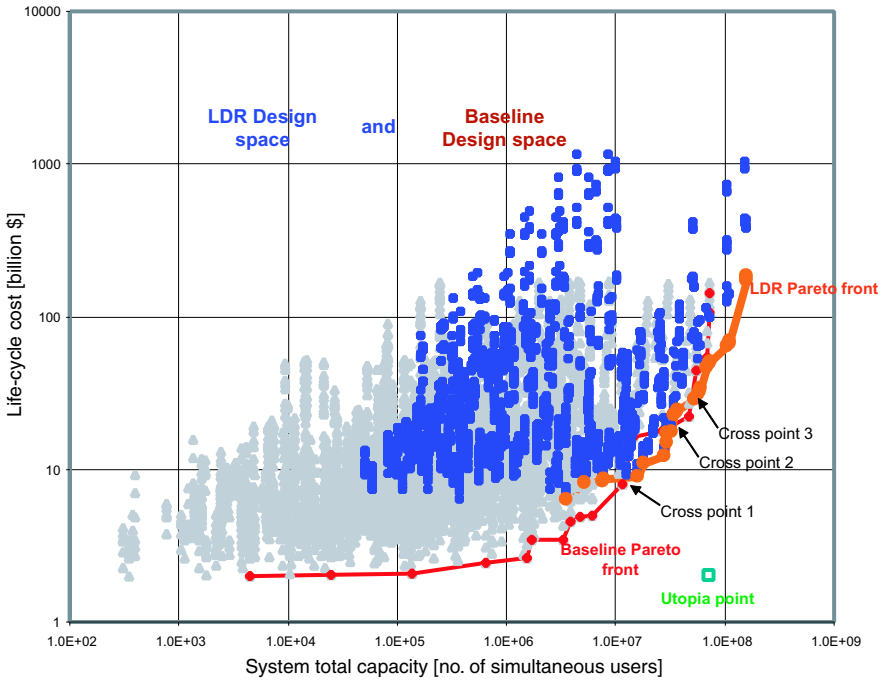

Figure 3-13: LDR-infused objective space and Pareto front

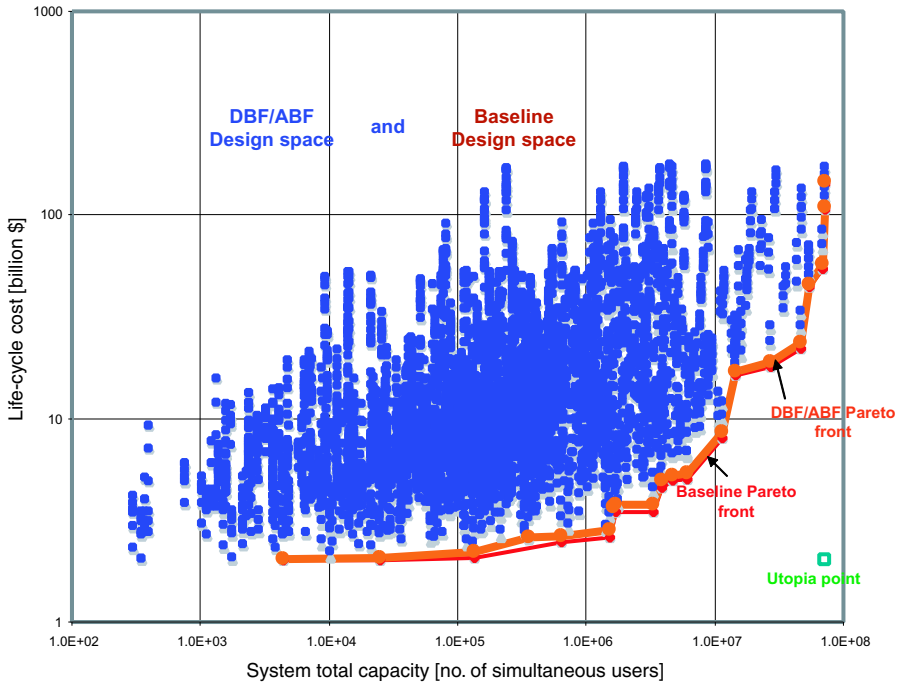

Figure 3-14: DBF/ABF-infused objective space and Pareto front

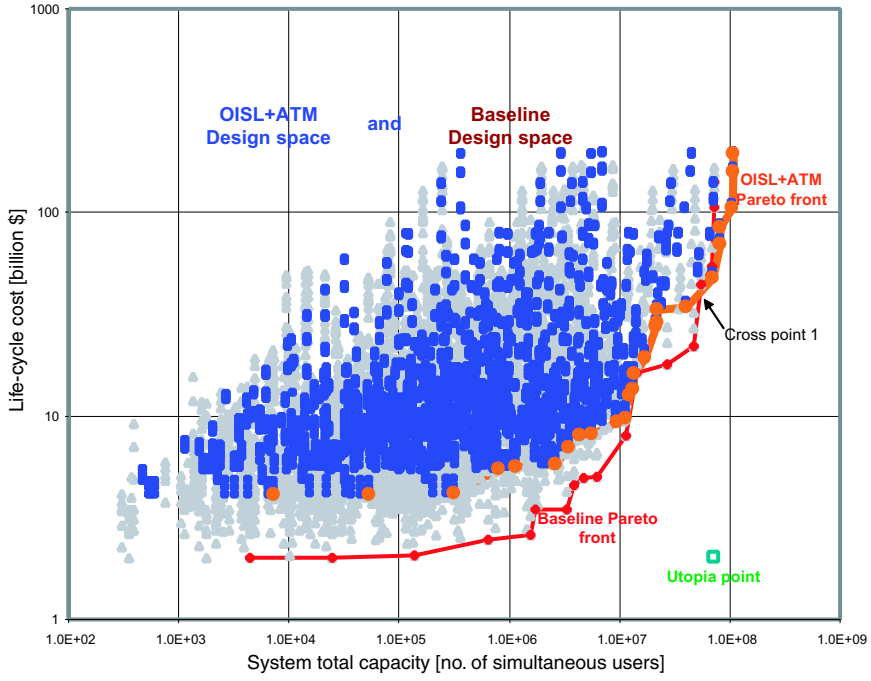

Figure 3-15: OISL+ATM-infused objective space and Pareto front

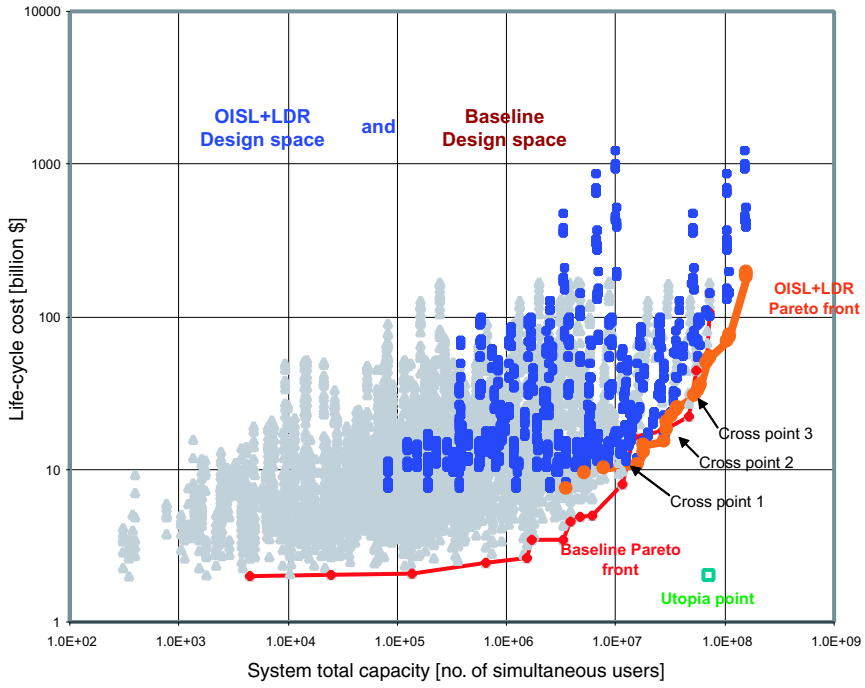

Figure 3-16: OISL+LDR-infused objective space and Pareto front

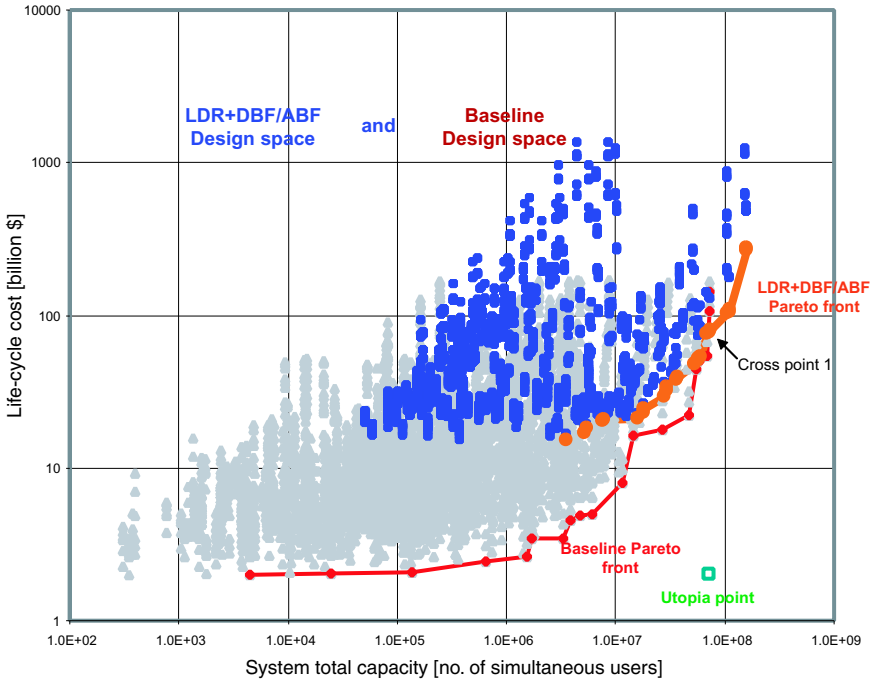

Figure 3-17: LDR+DBF/ABF-infused objective space and Pareto front

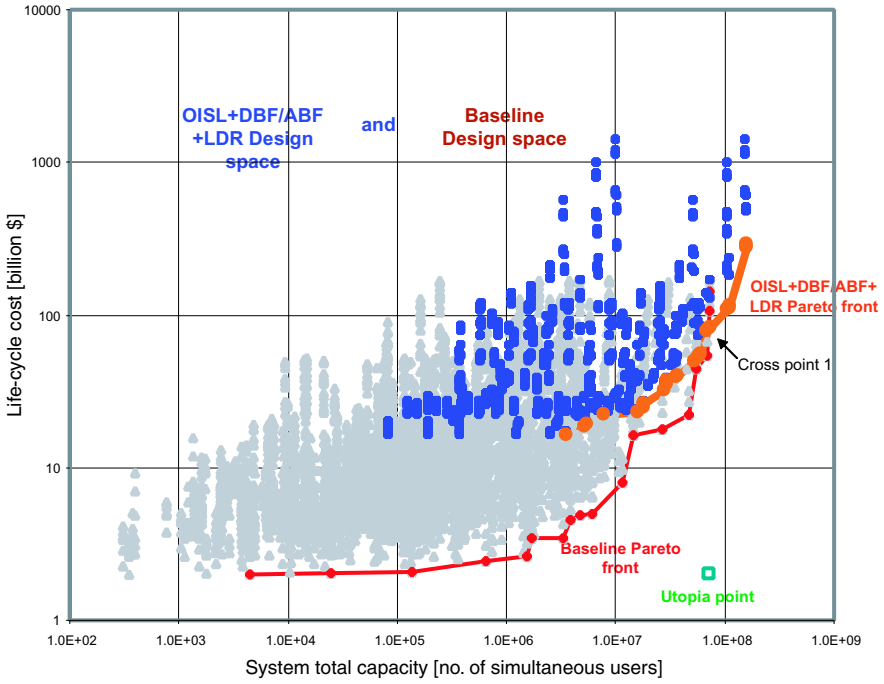

Figure 3-18: LDR+DBF/ABF+OISL-infused objective space and Pareto front

3.4.6 Post-Processing and Result Interpretation (Step 6)

In order to compare the relative benefit of technologies on a common scale, we define four metrics of technology impact, which are derived from the shift in the baseline Pareto front, Π_0, relative to a Pareto front perturbed by technology T_i, Π_i. The four metrics are shown graphically in Figure 3-19. The four metrics, δ_{min}, μ, υ, and χ are computed in normalized objective space $J_i/J_{i\ max}$.

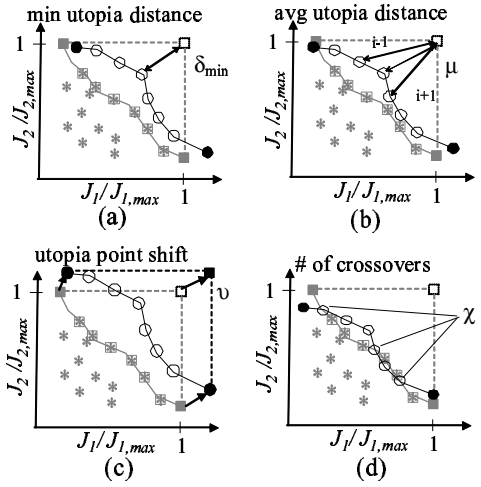

Figure 3-19: Pareto impact metrics

The first metric is the normalized, minimum distance from the Pareto solutions of the technology-infused objective space to the utopia point determined in the baseline case.

$$\delta_{min} = \min \left(\sqrt{\sum_{i=1}^{m} \left(\frac{J_i(x_k) - J_i^{utopia}}{J_{i,worst} - J_i^{utopia}} \right)^2} \right) \ \forall\, k = 1, 2, ..., N \tag{3.1}$$

where $J_i(x_k)$'s are the objectives of the kth technology infused Pareto optimal design, and J_i^{utopia}'s are the objectives of the utopia point of the baseline trade space. The difference is normalized with difference between the worst value of the objectives $J_{i,worst}$ and J_i^{utopia} of the baseline Pareto designs. There are N Pareto optimal solutions in the technology-infused objective space.

The second scalar metrics is the averaged distance, μ, to the utopia point, from

all the Pareto optimal solutions.

$$\mu = \frac{1}{N}\sum_{k=1}^{N}\left(\sqrt{\sum_{i=1}^{m}\left(\frac{J_i(x_k) - J_i^{utopia}}{J_{i,worst} - J_i^{utopia}}\right)^2}\right) \quad \forall\, k = 1, 2, ..., N \tag{3.2}$$

The third metric captures the shift between the baseline utopia point and the technology-infused utopia point. This is captured as the vector from the baseline utopia point to the technology-infused utopia point in normalized objective space. This captures the ability of a new technology to extend the current state-of-the-art. For the satellite case, υ_1 represents system total capacity and υ_2 represents life-cycle cost.

$$\upsilon = \left[\frac{J_1^{utopia}(\tau) - J_1^{utopia}}{|J_{1,worst} - J_1^{utopia}|} \cdots \frac{J_m^{utopia}(\tau) - J_m^{utopia}}{|J_{m,worst} - J_m^{utopia}|}\right]^T \tag{3.3}$$

Another way to evaluate the technologies is to analyze the geometric relation between the Pareto front of the technology-infused objective space and the baseline Pareto front. When the two Pareto fronts cross each other, one design is surpassing the other in becoming closer to the utopia point. When this crossing happens several times for two designs, it means a design is superior in some ranges of the objective space and the other design is superior in the other ranges. If there is no crossover, then one design is clearly superior to the other technology across the entire objective space. Thus, the number of crossover points is the fourth Pareto impact metric, χ.

The Pareto impact metrics for the four individual technologies and four combinations of technologies are summarized in Table 4.1.

Now each technology or technology combination is ready to be examined based on technology metrics and the Pareto plots displayed in step 4 and 5.

OISL alone does not improve the Pareto optimality. Both of its minimum utopia distance and average utopia distance increase from the baseline case. Its utopia point shifts toward higher cost but with no capacity increase. This result is not surprising. OISL offers two advantages: First, it increases ISL data rate so that ISL will not be the network bottleneck; Second, it reduces the weight of ISL if RF ISL has been used on

Technology	δ_{min}	μ	υ	χ
Baseline	0.309	0.803	(0,0)	-
OISL	0.404	0.819	$(0, 6.9 \times 10^{-3})$	0
ATM	0.161	0.778	$(0.50, 4.2 \times 10^{-3})$	3
LDR	0.037	0.587	$(1.22, 3.5 \times 10^{-3})$	3
DBF/ABF	0.322	0.823	$(0, 1.5 \times 10^{-4})$	0
OISL+ATM	0.232	0.801	$(0.50, 0.011)$	1
OISL+LDR	0.043	0.584	$(1.22, 4.6 \times 10^{-3})$	3
LDR+DBF/ABF	0.052	0.598	$(1.22, 9.07 \times 10^{-3})$	1
LDR+DBF/ABF+OISL	0.057	0.587	$(1.22, 0.01)$	1

Table 3.6: Pareto impact metrics of eight individual technologies and technology-combinations

the baseline design. But in the baseline case, as shown in Chapter 2, none of the Pareto optimal designs uses ISL, which means none of the Pareto optimal design is able to utilize the advantages offered by OISL. Although some designs that use ISL benefit from the implementation of OISL, they nevertheless cannot yet reach the Pareto front. On the other hand, the implementation of OISL involves the inevitable development and unit costs. Therefore, with no performance improvement and increased cost, the Pareto optimality of the trade space infused with OISL deteriorates from the baseline case. With no crossover point, the Pareto front of OISL-infused objective space is clearly dominated by the baseline Pareto front throughout the entire objective space.

ATM increases both system capacity and life-cycle cost. This is expected because ATM increases system capacity to all including the Pareto optimal designs but also increases costs. The ATM-infused Pareto front has three crossovers with the baseline Pareto front. This means in some ranges the ATM-infused designs dominate the baseline designs, especially in the high capacity, high cost range. An intuitive explanation for this is that the capacity improvement brought by ATM is consistently 50% of the original capacity, no matter the capacity is high or low. But the development cost will be evened out for large systems with many satellites and high capacity. The average unit cost will also decrease for large systems as a result of the learning curve. Therefore that in general, the ATM has advantage over the baseline case at high capacity, high cost range. Both the minimum and average utopia distances reduce

from the baseline case.

LDR has both increased system capacity and life-cycle cost. The objective space plot of LDR in Figure 3-13 illustrates two trends: First, the LDR-infused objective space is sparse compared with the baseline design because many of the designs implemented with LDR are too heavy to be carried by any available launch vehicle, so they become technically invalid and do not appear in the objective space; Second, the LDR-infused objective space migrates significantly to the higher-capacity, higher-cost region. The second trend will be seen over and over again in the other technologies or combinations of technologies examined later. Both the minimum and average utopia distances of the LDR objective space decrease from the baseline case.

Similar as OISL, DBF/ABF is the only other individual technology that has both increased minimum and average utopia distance from the baseline case. The reason is that none of the baseline designs has a cell duration less than 30 seconds; DBF/ABF does not benefit any of the designs. On the other hand, DBF/ABF brings higher development and unit costs to the systems. Therefore, the DBF/ABF-infused Pareto front is dominated by the baseline Pareto front almost everywhere.

The combination of ATM and OISL has lowered minimum utopia distance but increased average utopia distance from the baseline case. But compared with the ATM case, the minimum and average utopia distances of the ATM+OISL case are higher. The ATM+OISL case has the same utopia shift as the ATM case in the capacity direction but even more shift in the cost direction. It is not difficult to realize that ATM brings the increase in capacity, and ATM and OISL together bring the increase in cost. Although the increased capacity brought by ATM may make OISL more "useful" for some designs in relaying data between satellites, these designs cannot yet reach the Pareto optimality.

The combinations of LDR with OISL, DBF/ABF, and OISL+DBF/ABF have the similar tendency: LDR brings increased capacity, and the technologies together increase the cost. DBF/ABF is not utilized even with LDR implemented because the runs show that none of the designs has a cell duration less than 30 seconds. OISL again is able to improve some designs that have ISL as the capacity bottleneck but

is not able to alter the Pareto optimality because the Pareto optimal solutions are exclusively designs without ISL.

Except the cases of individual technologies of OISL and DBF/ABF, all the other cases show a trend of the baseline designs dominating in the low-capacity, low-cost corner (lower left corner) and the technology-infused designs dominating in the higher-capacity, higher-cost corner (upper right corner). Bringing performance improvement at a higher cost is typically what we expect of a new technology.

3.5 Summary of Technology Infusion Study

We have seen the different effects on trade space optimality by the infusion of new technologies into the system. The following lessons have been learned:

1. The Pareto front plots show that the baseline case is advantageous in some ranges while the new technologies infused systems are advantageous in other ranges. The bottom line is that traditional (baseline) technologies appear to be favorable for smaller, low capacity systems, while high capacity systems such as the ones under development at NeLS in Japan could potentially utilize the advantage brought by the newer technologies such as OISL. This suggests that both "traditional" technologies such as RF ISL and OISL will co-exist in the future - at least for a while.

2. It is meaningless to study the effect a new technology has on one single design because this particular design itself might not be Pareto optimal. The technology may improve this design, but if the design is not on the Pareto front, then the designer should modify the design to make it Pareto optimal first, and then seek the effect the new technology may have on the design. For example, OISL may improve many baseline designs that have ISL as the capacity bottleneck. But if the Pareto optimal designs do not include any designs with ISL, then OISL is not able to alter the Pareto optimality of the trade space.

3. In cases where the baseline Pareto front crosses with the technology-infused

Pareto front, whether or not to implement the technology depends on non-technical considerations such as market demand and budget constraints. As illustrated in Figure 3-20, when there are two Pareto fronts, the Pareto front that crosses with the constraint at a point closer to the utopia point is selected. For example, the capacity market demand represented by the vertical line intercepts the LDR-infused Pareto front at point A and the baseline Pareto front at point A'. Point A should be selected because it is closer to utopia point than A'; LDR should be implemented. The budget constraint represented by the horizontal line intercepts the LDR-infused Pareto front at point B' and the baseline Pareto front at point B. Because B is closer to utopia point than B', point B should be selected; LDR should not be implemented.

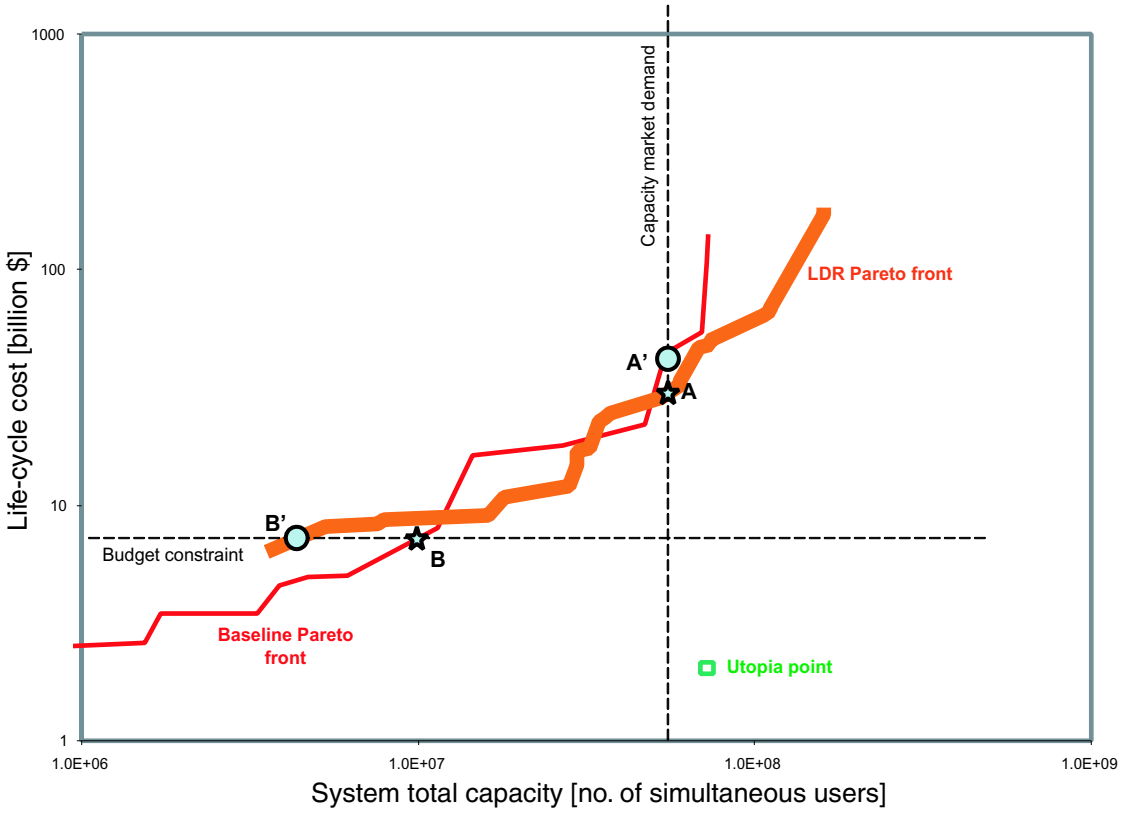

Figure 3-20: Technology infusion decision under constraints

4. When we need to consider multiple technologies, we are looking at multiple

design spaces each of which is infused with a different technology. As illustrated in Figure 3-21, areas A, B, and C represent objective spaces of a system infused with three different technologies a, b, and c. Each objective space has its own Pareto front. All these technology-infused Pareto fronts together form a big Pareto by connecting the segments closest to the utopia point. Using this big Pareto front, we can select the technology to implement. This big Pareto front is called S-Pareto front. The intercepting point between the S-Pareto front and the constraint is where the design should take place. Mattson and Messac first introduced the S-Pareto front concept. [MM02] But they refer to S-Pareto front as the joint Pareto front for the objective spaces of three different design concepts, with each concept having its own parametric model. The distinction here is that objective spaces A, B, and C represent the same system with the same parametric model infused with three different technologies.

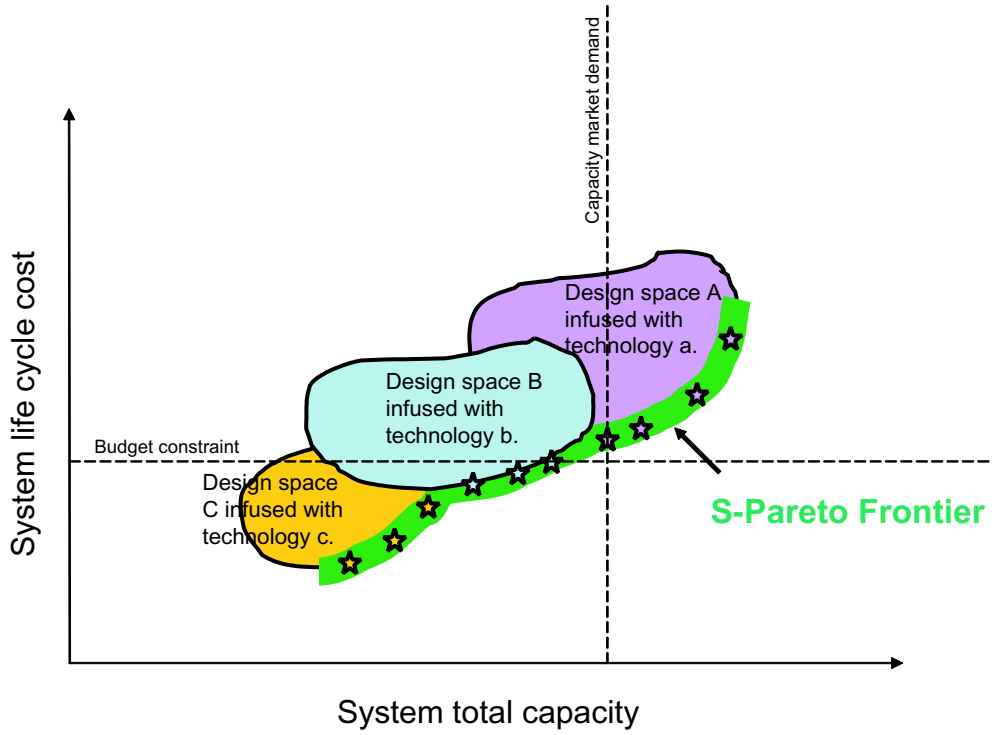

If there are N technologies available,

then A, B, C, D… = [T_1, T_2, T_3,…, T_N]

Figure 3-21: Technology selection on S-Pareto front

Chapter 4

Impact of Policy Implementation

4.1 Introduction

New technologies are not the only things that can change the trade space of a system. Past experience has shown that engineering systems are also susceptible to the influence of technology-related policies. In Chapter 2, the inputs of the model include policy constraints. Changing these constraints will significantly alter the trade space, and therefore the Pareto optimal solutions.

Technology infusion and policy implementation impact the system model in fundamentally different ways. While technology infusion must be modelled in detail "inside" the system - by interacting with the existing physics of the system and changing internally dependent system technical parameters and cost factors - policy acts mainly from the "outside" by imposing constraints and changing fixed parameter assumption. Compared with technologies, policies belong to a different dimension and have more of an "external" effect on the system.

Here we consider two policy constraints. The first one is use of foreign launch vehicles. The second one is allocation of frequency bandwidth. We will first look at the historical background of these issues. Then we will introduce policy impact study framework that is similar to the technology infusion study framework. The framework will examine quantitatively how the policy constraints affect the trade space of the system and how the Pareto optimality changes accordingly. A policy

infusion interface (PII) is developed to add the effects of the policies to the system in a fashion similar as the TII .

4.2 Motivation for Policy Implementation Study

The interactions between technology and policy have been pervasive throughout history. An example for technology's effect on policy is the shaping of the international political landscape by nuclear weapon since the beginning of the Cold War. An example of policy's impact on technology is that the bundling of additional tasks onto the space shuttle design in order to gain political support complicated the design. Here we attempt to provide a measurement of the policy impact on engineering system in terms of the quantitative change in performance-versus-cost brought by the policy decisions. These quantitative changes can serve as reference in policy-related decision-making. Future work is in order to understand how the results shown by the policy implementation study will impact the policy decision process.

4.3 Policy Implementation Study Framework

The quantitative policy impact framework consists of five steps as illustrated in Figure 4-1.

1. Explore the baseline trade space using simulation based on system model.

2. Policy identification and modelling.

3. Develop policy infusion interface (PII) through which the effect of the policies are added to the system without violating the integrity of the system model.

4. Assess the impact of each policy on the system.

5. Post-process and interpret the results from step 4.

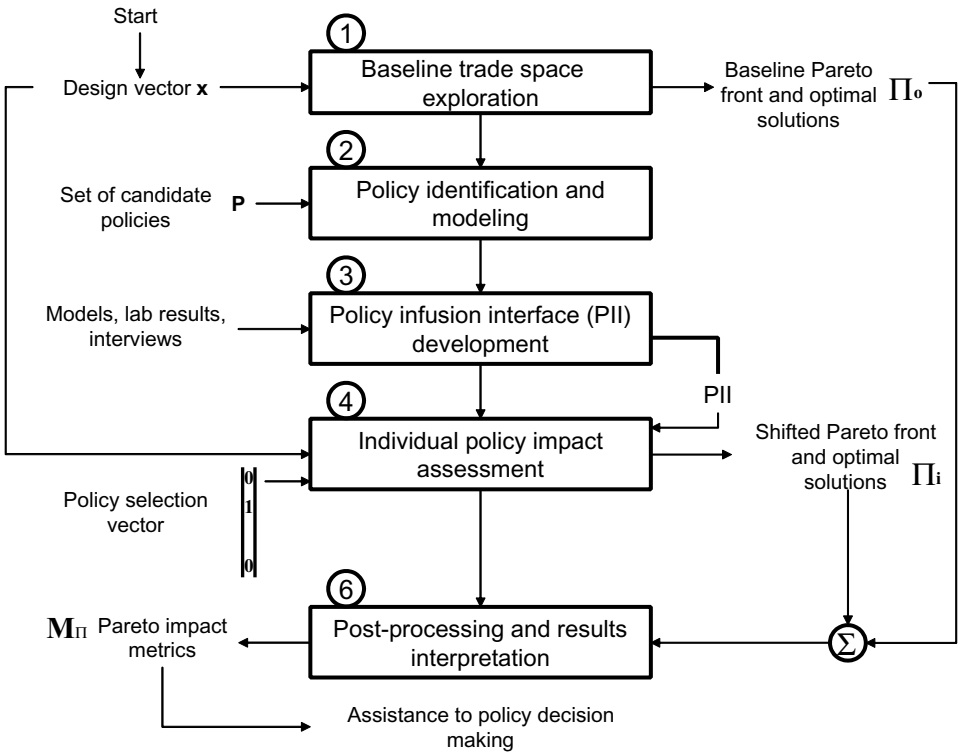

Figure 4-1: Quantitative policy impact study framework

4.4 Policy Impact and Its Application to LEO Satellite Communication Constellation System

4.4.1 Baseline Trade Space Exploration (Step 1)

This step has been accomplished in Chapter 2. A baseline trade space has been generated using the model developed in Chapter 2. The Pareto optimal solution set of the objective space have been identified.

4.4.2 Policy Identification and Modelling (Step 2)

Two major policy issues related to LEO satellite communication system are identified by this study - the use of foreign launch vehicles and frequency bandwidth allocation. These two issues will be discussed in the following sections.

Policy Issue for the Use of Foreign Launch Vehicles

Before a U.S. company launches its satellites aboard a foreign launch vehicle, it needs to obtain an export license from the U.S. government. The licensing jurisdiction was in the hands of the Commerce Department until the 1998 National Defense Authorization Act transferred it to the State Department. The Congress made this change due to its concern that the Commerce Department was not able to prevent sensitive dual-use technologies aboard the satellites from leaking to foreign governments. The licensing process at State Department is slow and conservative. It likely leads to the refusal of the use of foreign launch vehicles, even those that are equally capable but cheaper compared to the U.S. launch vehicles. This will inevitably increase the launch cost of the system, especially for LEO constellations that require multiple launches to deploy the entire constellation. We will examine the effect of not using foreign launch vehicles on the trade space.

As introduced in Chapter 2, the policy constraint variable FLV is initialized in the system input file. The modelling of the ban on foreign launch vehicles is done by turning FLV on or off. Then the modified value is wired into the launch vehicle module through the PII.

Policy Issue for the Frequency Bandwidth Allocation

Same as land, clean air, water, iron, and forest, radio frequency is a natural resource vital to the industrial and commercial activities of the human society. As we have entered the information age and continue to charge forward at full speed in technological development and utilization, this resource is going to be more important than ever. Frequency is not only important, but also desirable because it is a limited resource. Just as for many other limited resources, regulations, both on the international and national levels, are needed to ensure efficient and fair use of frequency.

Why Frequency Is a Limited Resource

As carriers of radio signals, frequency is a limited resource. The section on satellite capacity calculation in Chapter 2 has given the mathematical expressions for this

limitedness. Described in words, the reasons for frequency as a limited resource are the following:

1. When two signals occupying the same frequency band come into time and spatial proximity (same time, same location), interference occurs between the two signals and may make one or both signals unintelligible.

2. Signal transmission requires a certain data rate. When everything else fixed, there is a linearly proportional relation between the data rate and the bandwidth of the frequency carrier. That is, the larger the frequency bandwidth is, the higher the data rate is. Therefore, for signal transmitting applications, especially for broadband applications, it is desirable to occupy a wide band of frequency.

3. Physical properties of different bands make them suitable for different applications. Because low-frequency signals follow the curvature of the earth surface or bounce off the ionosphere, low-frequency bands are suitable for long-range over-the-horizon transmission. Signals at higher frequency bands are less susceptible to the attenuation caused by travelling through space, so they are excellent for line-of-sight transmission. At the highest frequency bands, signals are subject to severe atmosphere attenuation and absorption. Therefore frequencies that are too high are not desirable by radio frequency applications.

Why Regulation Is Necessary

Frequency allocation involves users, service providers, and manufacturers of huge geographical and national diversity. Rather than leaving the issue to be solved by the invisible hand of the market, regulatory bodies on the national and international levels are needed to maximize efficiency. Four points for the justification of uniform regulations are summarized here[Wit91]:

1. Applications utilizing communication and navigation devices often travel across multiple regions. If regionalized frequency bands for the same device are all different from each other, to match these different frequency bands, the device

would be complicated in production and usage. Standardization of the bands brings efficiency to both the producers and users of the devices.

2. For communication systems whose transmissions reach multiple regions, for example, global positioning system and satellite broadcast, across-region (sometimes international) uniformity is needed for these systems to operate because technically the system cannot switch its frequency band when the transmission propagates from one area to another.

3. Human safety services should be given high priority in frequency band allocation and be protected from other transmissions. This protection is typically not available in a free-market environment without regulatory intervention.

4. Cooperation is needed to avoid across-border interference and to achieve maximum aggregate technical efficiency for all transmitters involved.

The Current International Regulatory Regime

The current international regulatory regime is the International Telecommunication Union (ITU), a specialized agency of the United Nations. The organization is streamlined into three sectors: radiocommunication sector (ITU-R), telecommunication standardization sector (ITU-T), and telecommunication development sector (ITU-D). The current structure of ITU is listed as in Figure 4-2.

The plenipotentiary conference is the supreme authority of the organization. It is formed by delegates from the member states. It sets the basic policies and strategies for the Union, and reserves the rights of amending the Constitution and the Convention at the conferences. The Constitution "sets out the objectives of the Union, defines the frame within which it is to operate and states major principles governing the conduct of telecommunications services. It is to become the basic instrument of the Union. Amendment will require the vote of two thirds of the delegations accredited to a plenipotentiary conference."[Wit91] The Constitution is subject to the ratification by governments of the member states. The Convention, revised from the former International Telecommunication Convention, sets out the way in which the

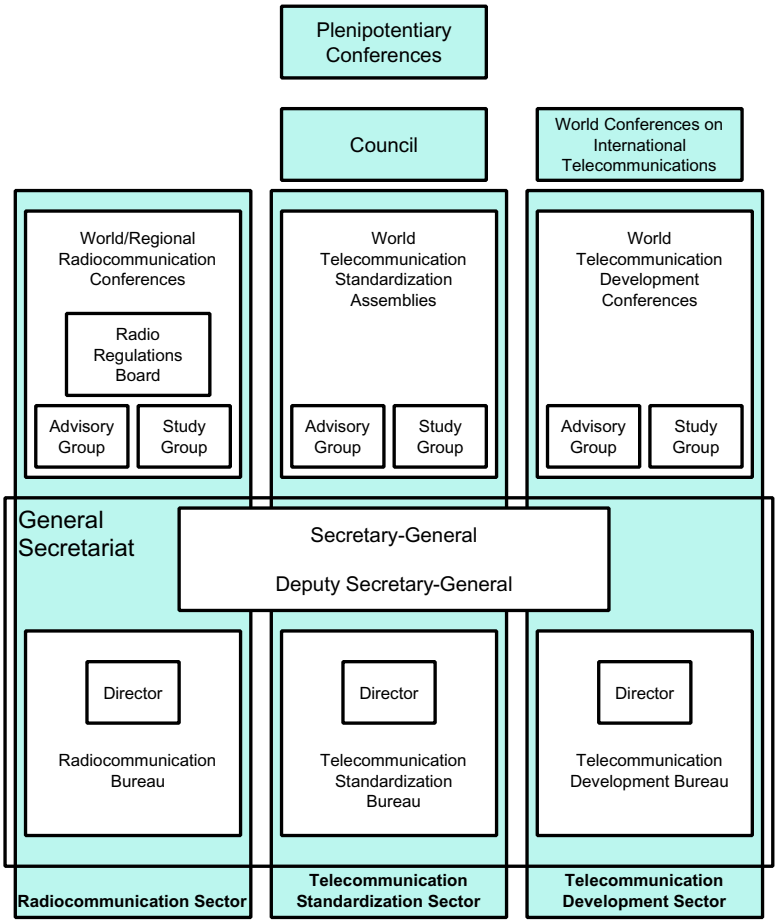

Figure 4-2: Current structure of the ITU

ITU carries out its work. Amendments of the Convention are subject to a simple majority vote at the plenipotentiary conference. The Convention is also subject to the ratification by member states.

The plenipotentiary conference also elects members to the Council and decides the number of seats in the Council. The Council, also known as the Administrative Council, meet annually during the intervals between the plenipotentiary conferences. Its duty is to ensure that the activities, policies, and strategies fully respond to the need of its members. The Council is also in charge of carrying out the daily running of organization and facilitates the implementation of the Constitution, Convention, and Administrative Regulations.

The World Conference on International Telecommunications, taking part of the

responsibility of the former Administrative Conferences, is empowered to revise the International Telecommunication Regulations. The Regulations are "an international treaty governing the provision and operation of public telecommunication services, as well as the underlying transport mechanisms used to provide them. The regulations provide a broad, basic framework for telecommunication administrations and operators in the provision of international telecommunication services."[oIT03]

Under the top governing body of ITU are three sectors in radiocommunication (ITU-R), telecommunication standardization (ITU-T), and telecommunication development (ITU-D). Among the three sectors, the one of concern to this paper is the Radio Communication Sector. As shown in Figure 1, the Radio Communication Sector is divided into two - the World/Regional Radiocommunication Conferences and the Radiocommunication Bureau under the General Secretariat. The Radiocommunication Conference is tasked to review and revise the Radio Regulations (RR). The Radio Regulations "set out the agreements and procedures regulating the allocation of frequency bands to services, the international registration of frequency assignments and the various technical measures that have been given mandatory force in order to increase the efficiency with which the radio spectrum can be used."[Wit91] The RR covers frequency assignments for both terrestrial systems, as well as geostationary-satellites and non-geostationary orbital satellites. The Radiocommunication Bureau is the executive branch of the Radiocommunication Sector.

Frequency Allocation and Assignment

The Radio Regulations have allocated the frequency bands from 9kHz to 275GHz to various types of usages, in a way that the physical character of the allocated band best fits the technical requirement of the service. The allocation plan is recorded in the international Table of Frequency Allocations.

Member states of the ITU need to implement the international Table of Frequency Allocations only if a frequency band it assigns may cause interference to another station that operates in accordance with the Radio Regulations. A country can draw up its own national frequency allocation table. When drawing up such national table, appreciation should be given to the existing pattern of frequency usage in neighboring

countries, and to an efficient utilization of the bandwidth. International frequency allocation needs to be incorporated into the national plan only for:

- Those that will be needed for the country's international links.
- Those that will be needed by ships and aircraft, civil and military, for terrestrial and satellite communication and radiodetermination.
- Those under which ITU frequency plans, of interest to the country, have been or are going to be drawn up.
- Those which are allocated in the international Table of Frequency Allocations to one service only.

Outside the above-listed usage, the country has the freedom to draw up the allocation plan as it sees fit.

Frequency Allocation in the United States

In the United States, the Communication Act of 1934 defined the principles for spectrum management.[Eco93] According to the Act, Federal Communications Commission (FCC) was established to manage the frequency allocation for non-federal government users. The FCC reports to the Congress. On the other hand, the President of the United States has the power to allocate frequency for federal government-related usage. The President delegates the power to the Secretary of Commerce, and executed by the National Telecommunications and Information Administration (NTIA). The Inter-department Radio Advisory Committee (IRAC) advises the NTIA and acts as a linkage between FCC and NTIA.

The task of NTIA is on both domestic and international levels. On the domestic level, NTIA manages the availability of frequency bands before assigning it to applicants, prevents harmful interference, studies efficient use of the spectrum, and maintain a database for up-to-date frequency uses.[BC80] On the international level, NTIA helps the State Department on the U.S. positions at ITU conferences.

The FCC shares the NTIA's responsibility for the non-federal sector. Jointly, the NTIA and FCC plot the frequency allocation for domestic usage. Finalized in 1996,

the allocation covers frequency spectrum from 0 all the way to 400GHz. Complex as it is, the chart spreads over 88 letter-size pages.

In the making of the domestic allocation plan, the FCC and NTIA need to incorporate the international allocation when the U.S. usage may cause interference to neighboring countries' telecommunication activities or if the usage is of an international nature, as described at the end of Section II.

It should be noted that in the United States, as well as several other countries, a relatively new way of frequency allocation has been introduced - auction. By auction, the government puts a certain bandwidth on sale, and the highest bidder will obtain the usage and management rights of this bandwidth. The advantages of this form of allocation is that attaching an economic value to the band will ensure the buyer's sincerity in wanting the band and its competence in utilizing it. The government will gain a revenue from the auction, too. The downside is, as someone argues, that auction will disadvantage communications that have much social benefits but less economic profitability, for example, some public TV programming.[Eco93] Appropriate selection of the bandwidth to be auctioned is important in maximizing the economic benefit while preserving the social values.

Development of Frequency Allotment in Space

As the activities in space by the United States, the Soviet Union, and the European countries increased, especially in communication, meteorology, and navigation, frequency allocation in the space was brought up to the agenda of ITU. In 1963, the members came together to formulate a frequency plan in space. Although the Soviet Union, the IFRB, and developing countries such as Israel preferred to keep the allocation based on current usage interim so developing countries could apply for bands after developing their space capability, the developed countries led by the U.S. managed to pass a Conference Recommendation that made the allocation permanent unless it was revised by another conference. Therefore, the 1963 space frequency allotment achieved the same legitimacy as the other plans made by the Union earlier, although the moral principles of justice and equity in the use of the spectrum was acknowledged in Recommendation 10A of the conference. The wording of the

Recommendation left possibility for future revision of the plan.

The problem of the sharing of the spectrum by developing countries was later resolved through the founding of the International Telecommunications Satellite Consortium (INTELSAT) in 1969, in which all members countries including both developed and developing countries jointly operate global communication satellite system.

Because the Space Conference decided that the space systems share and use the same frequency bands with the terrestrial systems with equal rights, it became necessary to coordinate between the space systems and the earth stations and among space systems. To achieve the coordination between space systems, Article 7 of the CCIR Recommendations detailed requirements such as power limits and flux density of the space-based transmitters, and the minimum elevation angle from the satellite to the earth station. To coordinate between space system, Resolution 1A by the Space Conference outlined that an administration that plans to establish an international satellite system should file detailed technical data of the system to the weekly circular for all members. A member is allowed 90 days to comment on any harmful interference the newly planned system may cause to its own satellite system. If a comment is received, the administration concerned shall make solutions satisfactory to the administration that has made the comment. If no agreement between the two administrations can be achieved, the IFRB will provide assistance.[Fin]

Current Bandwidth Allocation for Satellite Communication

Satellites mostly operate in the C-band of 4-8 GHz, Ku-band of 11-17 GHz, K-band of 18-27 GHz, and Ka-band of 20-30 GHz. Except C-band, the other bands are exclusively reserved for satellite communication. Because the majority of the Ku-band has been in use around the world by systems deployed previously, the new broadband systems that came out in 1995 applied for the Ka-band. In late 1997, a new round of band application for broadband systems aimed at the V-band of 40-50 GHz. These new applications represent a trend of booking early for systems to be developed in the distant future.

Iridium's communication between satellite and user terminal uses the L band, while Globalstar uses both L and S bands. Their frequencies are listed in Table 2.3

and Table 2.4. Figure 4-3 shows the bandwidth allocation of these two systems.

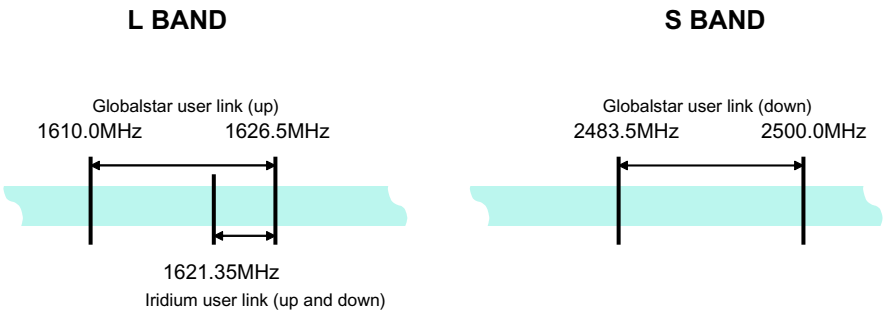

Figure 4-3: Bandwidth allocation of Iridium and Globalstar in the L and S bands

4.4.3 Policy Implementation Interface (PII) Development (Step 3)

Similar to TII, PII is integrated into the computer model so the user can specify what policy constraints to implement. The user has two options: If the "Use U.S. launch vehicle only" option is selected, then all the foreign launch vehicles in the launch vehicle module are "turned off" and not available for selection; if the "Different bandwidth allocation" option is selected, then the simulation will ask the user to specify the lower and upper bounds of the new bandwidth.

The integration of PII into the system model is relatively simple compared with the TII because PII modifies none of the system parameters except the FLV and frequencies upper and lower bounds in start file.

4.4.4 Assess the Effect of Policy Impact (Step 4)

Two full-factorial runs are made with PII option 1 and 2 selected, respectively. The impact of option 1, "Use U.S. launch vehicle only", on the baseline objective space is illustrated in Figure 4-4.

The Pareto front implemented with the ban on foreign launch vehicle is so close to the baseline Pareto front that they can be barely distinguished in the graph. Indeed, the policy implemented Pareto front is slightly moved away from the utopia point.

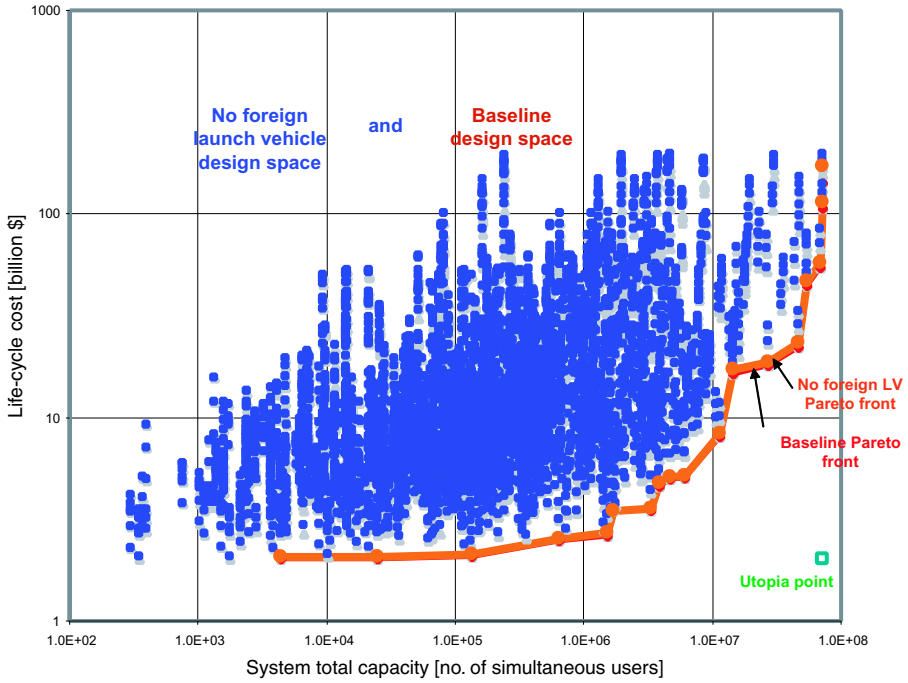

Figure 4-4: Objective space shift caused by using no foreign launch vehicles

The impact of option 2 "Different bandwidth allocation" is illustrated in Figure 4-5. The case is run with downlink bandwidth 2000-2005.15 MHz. The bandwidth is the same as the baseline case, but the band is shifted toward higher frequencies compared with the baseline case.

4.4.5 Post-Processing and Result Interpretation (Step 5)

The Pareto impact metrics for the two policy constraint changes are listed in Table 4.1

Technology	δ_{min}	μ	v	χ
Baseline	0.309	0.803	(0,0)	-
No foreign launch vehicle	0.288	0.801	$(0, 3.0 \times 10^{-4})$	0
Downlink bandwidth 2000-2005.15 MHz	0.319	0.833	$(-6.1 \times 10^{-3}, -1.3 \times 10^{-5})$	0

Table 4.1: Pareto impact metrics of two policy constraint changes

The constraint on the use of foreign launch vehicles has increased both minimum

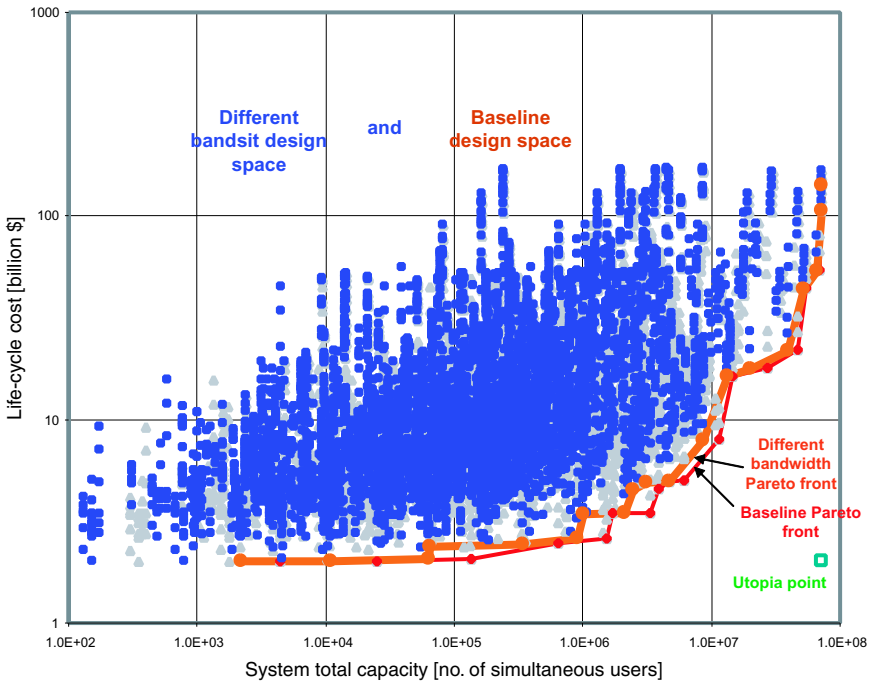

Figure 4-5: Objective space shift caused by using a different downlink bandwidth

and average utopia distances. This is no surprise because using U.S. launch vehicles has no effect on the system performance but has a higher launch cost. The restriction has no effect on any other part of the system.

The downlink bandwidth change has also increased both minimum and average utopia distances. The effect of a different bandwidth is more to predict because the frequency will affect multiple system parameters such as antenna size and capacity. For this particular case of shifting to 2000-2005.15 MHz, the objective space shifts toward a lower life-cycle cost, lower total capacity region, as indicated by the utopia point shift. A closer look shows that these effects are mainly caused by the following two reasons:

1. Higher frequency will require larger antennas, as shown by Equations A.6 and A.7. Larger antenna will increase the mass and volume of the satellite, which might lead to higher launch cost. Larger antenna will also increase the cross-section area of the spacecraft in orbit, which leads to higher drag and more

orbital maintenance fuel,and this will in turn increase the satellite mass and volume. This "vicious cycle" will lead to a satellite wet mass larger than the baseline case. Its effect on the total life-cycle cost might or might not be significant. More significantly than the increase in satellite mass, a larger antenna requires higher RDT&E cost, as shown by Equation A.70, and higher theoretical first unit (TFU) cost, as shown by Equation A.76. In the cost estimating relationship provided in Chapter 2, the antenna RDT&E cost is factored into the total hardware cost of the RDT&E phase as shown in Equation A.75. The antenna TFU cost is factored into the TFU hardware cost as shown in Equation A.81. Therefore, the increase in frequency will raise the system life-cycle cost.

2. In capacity calculation, frequency has two kinds of effects on the result. The first one is demonstrated by Equation 4.1, which shows that the transmission loss due to attenuation in space is inversely proportional to the frequency f of the transmission. So a higher frequency will slightly reduce the space loss of the transmission. But on the other hand, a higher frequency might lead to higher system noise temperature T_s. Higher noise temperature will increase the interference to the transmission, and therefore reduce the data rate of the system when the E_b/N_0 requirement is fixed. The change of system temperature with frequency is shown in Table 4.2.[LW92]. Actually, shown by the table, 2.0GHz is a threshold at which system noise temperature increases from 25.7 dB-K to 27.4 dB-K for downlink. This means that when the downlink bandwidth shifts form 1621.35 to 1626.5MHz, system noise temperature is increased. Therefore, the combined effect of reduced space loss and increased system temperature is a reduced system capacity.

$$L_s = \left(\frac{c}{4\pi S f}\right)^2 \tag{4.1}$$

An interesting study to perform is to simulate Iridium and Globalstar assuming no foreign launch vehicle is allowed to be used. The result show that the total life-cycle

	Frequency (GHz)					
		Downlink		Crosslink	Uplink	
	0.2	2-12	20	60	0.2-20	40
System Noise Temp. (dB-K)	25.7	28.6	27.4	32.5	31.1	32.6

Table 4.2: Typical system noise temperature, T_s, in satellite communication links in clear weather

cost of Iridium increases from $5.49 to $5.73 billion. The life-cycle cost of Globalstar increased from $3.59 to $3.62 billion. Apparently this cost penalty is because that the U.S. launch vehicles are more expensive. But there is a more subtle effect not captured by the simulation: relying on Delta or Atlas alone, the constellations could not have been launched as quickly due to the limited launch rate of the U.S. launch infrastructure. Thus, there is a second cost penalty due to the delayed completion of the constellation.

4.5 Summary of Policy Impact Study

Similar as technology infusion, policy impact can alter the trade space of the baseline case. The shift can be visualized using Figure 4-4 and Figure 4-5 as shown above. Under certain market or budget constraints, policy decision-makers can compare the advantage and disadvantage of the policy implementation. This will assist the final decision-making.

Policy issues other than ban on foreign launch vehicles and frequency bandwidth allocation can be simulated as well with modification to the PII and the system model itself. An example for such a issue is the influence on the constellation if gateways cannot be placed in some countries.

Chapter 5

Summary and Recommendation for Future Work

5.1 Summary of the Current Research Work

The purpose of the research is to test the effects of implementing new technologies and new policy constraints on LEO communication satellite constellation system. The research process is divided into three stages. Each stage is summarized in the sub-sections below.

5.1.1 Summary of Trade Space Exploration

The first stage is to build a computer simulation that can reasonably predict the system characteristics when design inputs are given. This stage consists of the following steps:

1. Define architectural design space inputs that include design variables, constants, policy constraints, and requirements, and outputs that include objectives and benchmarking parameters.

2. Build mapping functions between inputs and outputs, and subdivide them into modules that match the system's physical or functional characters. Define module interface.

3. Implement and integrate the modules based on constellation geometry, network theory, astrophysics, communication theory, cost estimating relationships, and market estimation.

4. Benchmark the simulation against the data of existing systems. If the results generated by the simulation are not satisfying, reiterate to step 2 until the results converge onto the exiting systems.

5. Perform a trade space exploration by full factorial run that covers the entire possible range of design variables.

6. Identify and postprocess the Pareto optimal solutions. If no acceptable Pareto optimal solution is found, reiterate back to step 1.

As a result of the first stage, a system simulation with reasonable fidelity is made. A full factorial run populates the trade space with 5,832 designs that represent the full range of all design variables. Among these 5,832 designs, 18 are Pareto optimal. Thus a baseline case is obtained.

5.1.2 Summary of Technology Infusion Study

The second stage of the research is to implement selected new technologies into the simulation and observe how the objective space and the Pareto optimal solutions change with each technology implementation. This stage is also a multiple step approach starting from the trade space exploration results of stage 1.

1. Trade space exploration.

2. Identify potential new technologies and classify them using NASA technology readiness level (TRL). Four new technology are to be implemented: OISL, ATM, LDR, and DBF/ABF. Their compatibility and dependency relations are checked. Then their physical and cost effects on the system are modelled using empirical relations obtained from interviews with experts who are directly involved in the research and development of the technologies.

3. These effects are exerted to the simulation through technology infusion interface (TII) without violating the integrity of the simulation.

4. Make new full-factorial runs of the system infused with individual technology. Observe how the implementation affects the objective space and Pareto optimal solution set.

5. Make full-factorial runs of the system infused with combinations of technologies. Observe how the objective space and Pareto optimal solution set are affected.

6. Postprocess the new Pareto optimal solutions. Four metrics are used to measure the new optimal solution sets against the baseline case: minimum utopia distance, average utopia distance, utopia point shift, and number of crossovers of Pareto fronts. Interpret the results.

The results show the general trend that new technologies bring higher performance at higher monetary cost. The significance of Pareto optimality in testing technological improvement, implementation decision made under market or budget constraint, and technology selection using the S-Pareto front are discussed.

5.1.3 Summary of Policy Impact Study

The third stage of the research is to exert the impact of policy decisions into the simulation and observe how the objective space and Pareto optimal solution set change with each policy implementation. This stage has steps similar to the technology infusion study.

1. Trade space exploration.

2. Identify and model potential policies. Two policy decisions are to be implemented: ban on using foreign launch vehicles and frequency bandwidth allocation.

3. These effects are exerted to the simulation through policy infusion interface (PII) without violating the integrity of the simulation.

4. Make new full-factorial runs of the system implemented with individual policy. Observe how the implementation affects the objective space and Pareto optimal solution set.

5. Postprocess the new Pareto optimal solutions. The same four metrics are used to measure the new optimal solution sets against the baseline case as in the technology infusion study. Interpret the results.

The run results show that the ban on foreign launch vehicles will increase the system cost without changing the system performance. The effect of frequency allocation change depends on the exact frequency bandwidth allocated. In the particular case tested, where the downlink frequency bandwidth changes from 1621.35-1626.5 MHz to 2000-2005.15 MHz, the new Pareto front moves away from the utopia point.

5.2 Conclusions

At the end of the study, we can draw the following conclusions (Conclusions 4, 5, 6, and 7 have been mentioned in Chapter 3 but deserve to be mentioned here again for their importance):

5.2.1 Globalstar and Iridium yet to Reach Pareto Optimality

The financial failure of Globalstar and Iridium is mainly caused by the loss of the intended market for the two systems. But from a system perspective, neither system is on the Pareto optimal front of the trade space. As shown by the baseline trade space analysis, the Pareto optimal designs that have a similar capacity as the two systems have costs around $2 billion, much lower than the $3.3 billion for Globalstar and $5.7 billion for Iridium. The designs for both the Globalstar and Iridium systems can be modified to reach the Pareto optimality.

5.2.2 Feasibility of Modelling of Complex Engineering Systems

System modelling of complex engineering systems in multiple modular form is feasible. Even with simplifying assumptions, the model can still represent the real-world system with a satisfying fidelity. A successful model of the system provides the platform on which the trade space analysis, technology infusion and policy impact studies can be performed.

5.2.3 Cost as a Design Objective

Lowering cost should be a design objective from the initial stage of the design process, and should be integrated into the system design optimization. Not taking cost into serious consideration from the beginning might be the reason that some real-world systems are not on the Pareto optimal front of the objective space. Lack of consideration for cost is a problem inherent to the "spin-off" model that characterized the technology development in the United States during the Cold War era, where technologies were first developed for defense usage, and then transferred to the civilian market. To be more competitive in today's international market, cost needs to be a driving factor in the design process, rather than being neglected and only passively accounted at the end of the process. One way of accounting the cost during design is to use cost as one dimension in the objective space, and find the Pareto optimal solutions in this objective space, as illustrated in this thesis.

5.2.4 Comparison between Traditional and New Technologies

The Pareto front plots show that the baseline case is advantageous in some ranges while the new technologies infused systems are advantageous in other ranges. The bottom line is that traditional (baseline) technologies appear to be favorable for smaller, low capacity systems, while high capacity systems such as the ones under develop-

ment at NeLS in Japan could potentially utilize the advantage brought by the newer technologies such as OISL. This suggests that both "traditional" technologies such as RF ISL and OISL will co-exist in the future - at least for a while.

5.2.5 Testing New Technology on Pareto Optimal Designs

It is meaningless to study the effect a new technology has on one single design because this particular design itself might not be Pareto optimal. The technology may improve this design, but if the design is not on the Pareto front, then the designer should modify the design to make it Pareto optimal first, and then seek the effect the new technology may have on the design. For example, OISL may improve many baseline designs that have ISL as the capacity bottleneck. But if the Pareto optimal designs do not include any designs with ISL, then OISL is not able to alter the Pareto optimality of the trade space.

5.2.6 Technology Selection under Non-Technical Constraints

If one Pareto front is closer to the utopia point than another Pareto front across the entire objective space, then the designs represented by the former Pareto front should be chosen over the designs represented by the latter Pareto front. But in cases where the baseline Pareto front crosses with the technology-infused Pareto front, whether or not to implement the technology depends on non-technical considerations such as market demand and budget constraints. As illustrated in Figure 5-1, when there are two Pareto fronts, the Pareto front that crosses with the constraint at a point closer to the utopia point is selected. For example, the capacity market demand represented by the vertical line intercepts the LDR-infused Pareto front at point A and the baseline Pareto front at point A'. Point A should be selected because it is closer to utopia point than A'; LDR should be implemented. The budget constraint represented by the horizontal line intercepts the LDR-infused Pareto front at point B' and the baseline Pareto front at point B. Because B is closer to utopia point than B', point B should be selected; LDR should not be implemented.

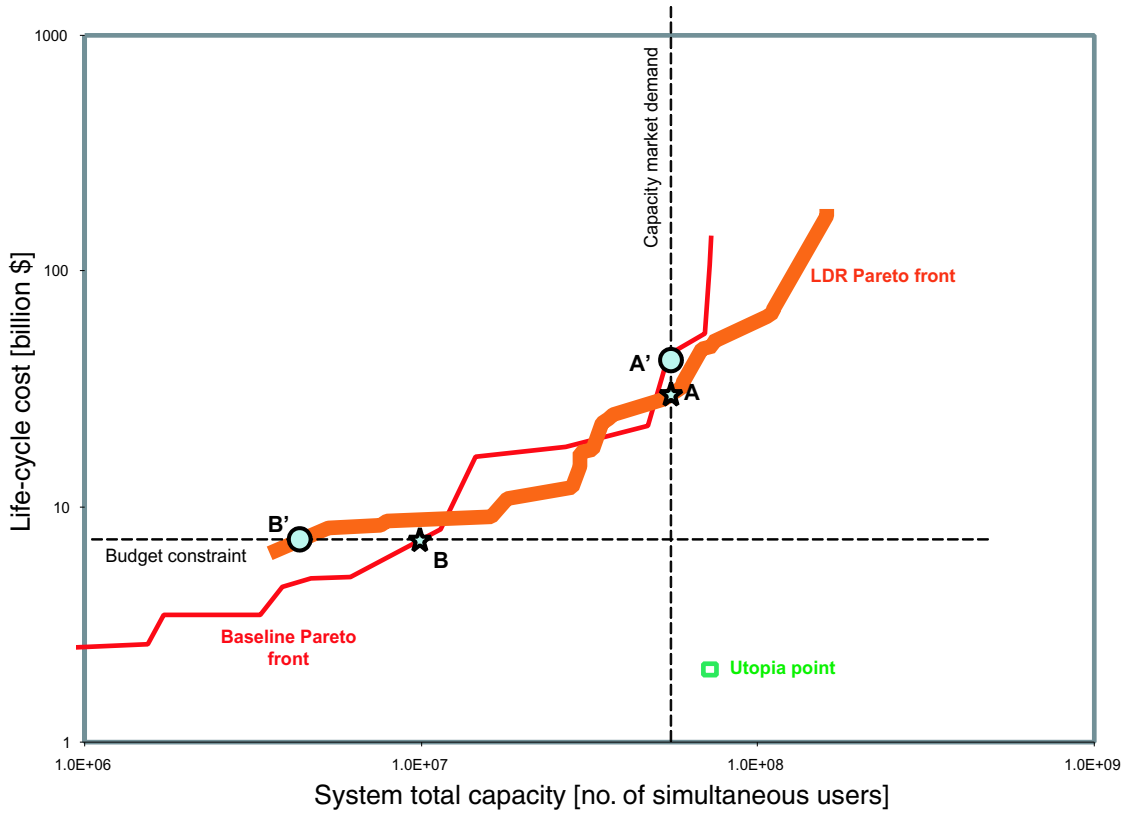

Figure 5-1: Technology infusion decision under constraints

5.2.7 Use of S-Pareto Front in Selection from Multiple Technologies

When we need to consider multiple technologies, we are looking at multiple design spaces each of which is infused with a different technology. As illustrated in Figure 5-2, areas A, B, and C represent objective spaces of a system infused with three different technologies a, b, and c. Each objective space has its own Pareto front. All these technology-infused Pareto fronts together form a big Pareto by connecting the segments closest to the utopia point. Using this big Pareto front, we can select the technology to implement. This big Pareto front is called S-Pareto front. The intercepting point between the S-Pareto front and the constraint is where the design should take place.

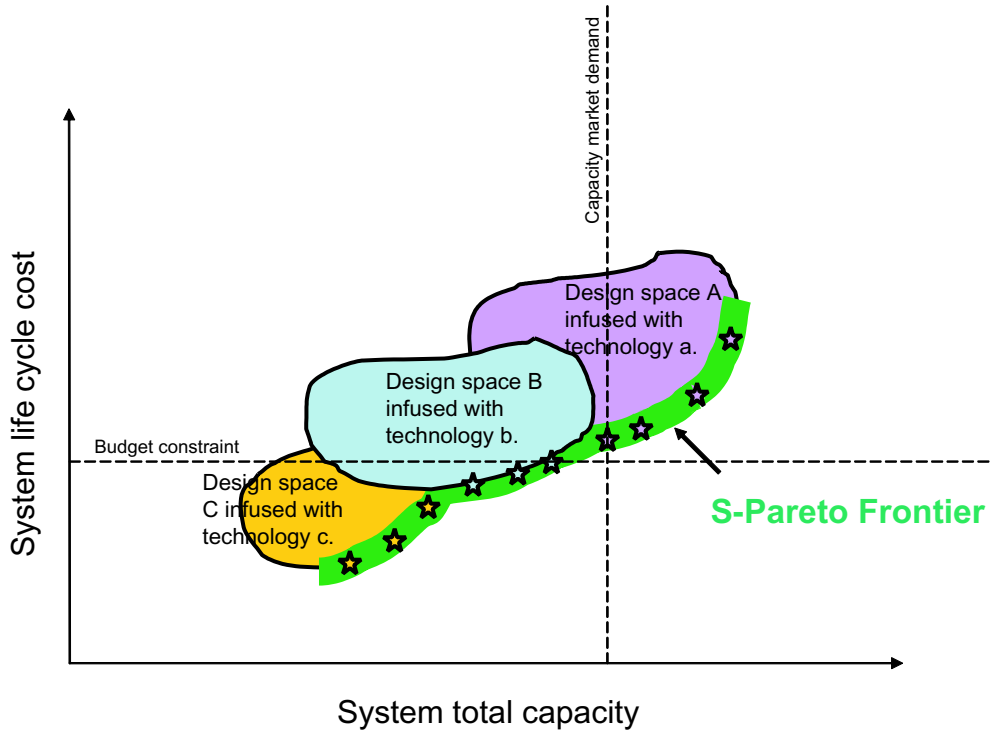

If there are N technologies available,

then A, B, C, D… = [T_1, T_2, T_3,…, T_N]

Figure 5-2: Technology selection on S-Pareto front

5.2.8 The Difference between the Modelings of Technology Infusion and of Policy Implementation

The modelling of technology infusion is fundamentally different from the modelling of policy implementation. Technology infusion changes the system's physics on the sub-system level, and brings direct cost effect. Policy implementation constrains the design by limiting the design space. So technology infusion needs to be modelled "inside" the system, while the effects of policy implementation are exerted from the outside. The difference between technology infusion and policy implementation is reflected in the difficulty of their modelling in the system model. On one hand, technology infusion interface alters the internal parameters passed to the modules of the system. On the other hand, policy implementation only changes policy constraints

in the start file.

5.3 Recommendation on Future Work

The research has been conducted within a time span of two years. A few recommendations are made for future work as continuation of current research.

5.3.1 Test of Trade Space Formed by Performance Metrics and Life-Cycle Cost

For the goals we set up at the onset of the research, there is one of them yet to be accomplished. We have examined the system trade space formed by capacity and life-cycle cost. But we have not looked at the trade space formed by system performance and life-cycle cost. The performance includes metrics used to measure the quality of the communication, the reliability, or user's satisfaction.

5.3.2 Finer Discretization of Design Variables and Use of Optimization Algorithms

The discretization of the design variables should be finer in further study of the Pareto optimization of the trade space. Because the size of the trade space grows exponentially with the discretization, full-factorial run of all the designs will be unrealistically time consuming. Therefore optimization algorithms proposed by Jilla and Miller should be used in search of the optimal solutions.

5.3.3 Different Mission Types and Systems

The current research holds satisfying voice communication as the mission objective. Other mission objectives, however, can also be set for LEO systems. For example, high-bandwidth, multiple-media communication will bring different requirements and physical characters to the system. Although the system model needs to be modified,

the same methodologies for technology infusion and policy impact studies can be used to explore new mission types and new systems.

5.3.4 Technology and Policy Uncertainty

Uncertainty is inherent in the prediction of future technologies and policy decisions. How to incorporate these uncertainties into the technology infusion and policy impact studies will be an interesting topic yet to be explored. The study may yield different technology infusion or policy impact results together with the probability associated with each scenario. Thus the decision-makers are able to select the technology portfolio and policy decision that shield them from the risk of unrecoverable loss.

5.3.5 "Fuzzy" Pareto Fronts

"Fuzzy" Pareto fronts can be built as a function of TRL level. Lower TRL level should result in a "fuzzier" Pareto front. This offers a different way to look at the effect of technology uncertainty on the system trade space.

5.3.6 Additional Objectives

In the current research, the two main objectives by which the system is evaluated are system capacity and life-cycle cost. Additional objectives should be used to measure the merit of systems. For example, reliability is an important quality of the system that could be modelled with additions to the simulation.

5.3.7 Additional New Technologies and Policy Issues

The technologies and policy issues tested in this thesis are just samples taken from the real-world. There are other new technologies and policies that can be examined using the modified simulation and same methodologies. Examples for new technologies are satellite IP network and new launch vehicle. An example for policy issue is the placement of ground gateways in foreign countries.

5.3.8 Identification of Disruptive Technologies in History and Reconstruction of Their Pareto Front Evolution

It will be interesting to study the disruptive technologies in history using the methodologies proposed in this research. First we need to identify what are the disruptive technologies in history, model the systems that use these technologies in computer simulation, and then construct the systems' trade space, and see how the disruptive technologies have evolved the Pareto fronts. This study might provide insight for the pattern of successful technology innovations. The historical data for many other systems can only be more abundant than LEO satellite constellation system. These systems include automobiles, airplanes, household machines, and consumer electronics.

5.3.9 The Impact of Policy Implementation Study on Policy Decision-Making Process

How will the results of the policy implementation study impact the real-world policy decision-making process? This can be a topic of study for a technology policy study. What will be information be most effectively delivered? How well will the policy decision-making body receive the information? What kind of impact will the results cause? These questions are yet to be answered.

5.4 Generalizability to Other Systems

At the end of this thesis, I would like to add a few words on technology infusion and policy impact on systems other than LEO satellite communication constellations. I believe that the same methodology can be used for any system that can be modelled in computer simulation and whose performance and cost can be quantified. For example, how has the use of jet engine revolutionized the airline industry? Much of this impact can be quantified: cost, profit, number of passengers travelled per year, mileage travelled, etc. Is it possible to model the airline industry and populate the

trade space? I think it should be doable.

For systems that cannot be modelled or quantified, technology infusion and policy impact will still be valid topics of study except that the methodology has to be changed. For example, how has nuclear weapon, the result of a technological advancement, reshaped the landscape of international political system? Or how has steel-reinforced concrete stimulated changes in architectural design of buildings? These are interesting topics to be studied, although the exact approach is yet to be formulated.

Appendix A

Description of Computer Model Modules

A.1 System Input File (SIF)

In system input file (SIF), design variables, constants, and policy constraints are initialized and bundled into their vector forms **x**, **c**, and **p**.

There are two types of SIF. One of them represents a particular design. In this type of SIF, each design variable has only a single value. The design vector is one-dimensional. Another kind of SIF represents a group of possible designs. In this type of SIF, each design variable has an array of different values. Therefore the design vector is a two-dimensional vector. Specified by hardware, policy constraints, and requirements, the parameters in **c**, **p**, and **r** always have just a single value in both types of SIF. An example for the first kind of SIF is the input file for Iridium system, which contains exactly the design parameters of the system. It will make the start file call all the modules only once before it obtains the simulation results for Iridium. The second kind of SIF calls the modules multiple times until it finishes performing an exhaustive combination of all the design values.

It should be noted that in the two-dimensional design vector, design variables do not need to contain the same number of values as each other. For example, orbital altitude can have five values at 500km, 750km, 1,000km, 1,250km, and 1,500km,

while minimum elevation angle has four values at 5^o, 15^o, 25^o, and 35^o. Figure A-1 demonstrates the difference between the two types of design vectors.

SIF passes the bundled vectors to the start file.

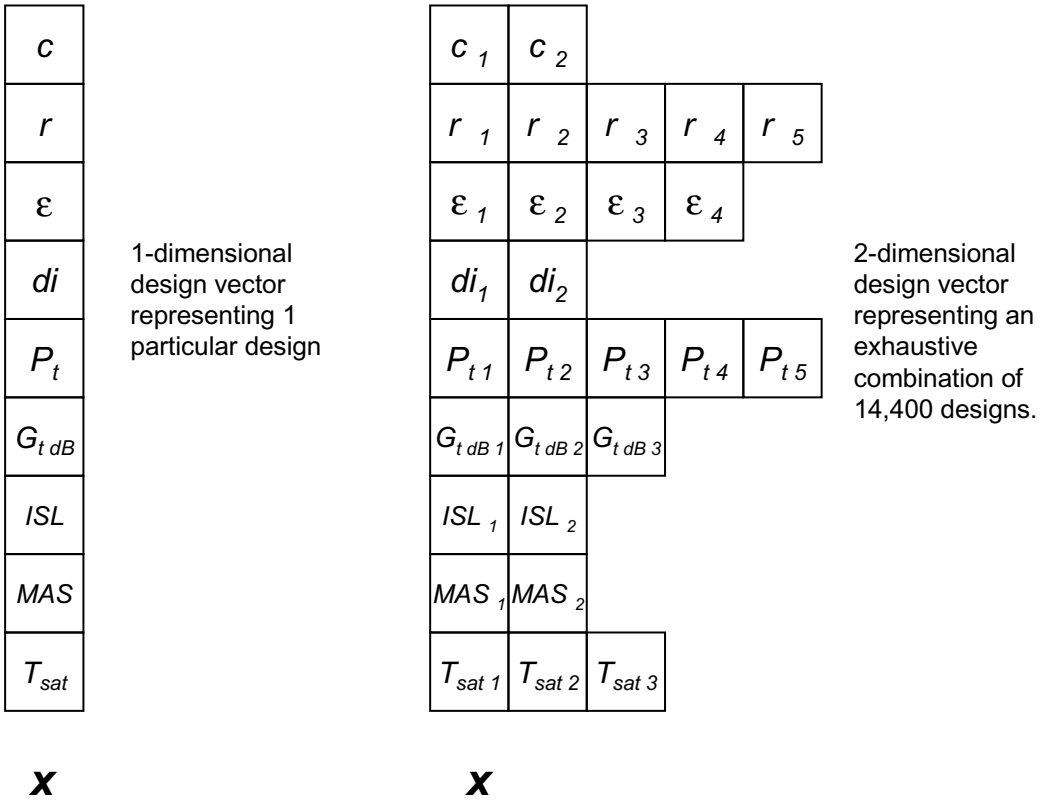

Figure A-1: Structure of the system input files

A.2 Start File (SF)

After inputting design, constant, and policy vectors from system input file, start file first unbundles the vectors and assigns their values to local variables. It also keeps track of the size of each design variable. For example, "alti = x.r;" assigns the value(s) of orbital altitude from the design vector to the local variable called alti. Then, "alti_n = length(x.r);" assigns the size of alti to alti_n. There is no need to track the size of the constants and policy constraints since they always have a size of 1.

After unbundling the design, constant, and policy vectors, SF first checks whether

the antenna size required by the user-defined transmitter antenna gain (a design variable) is larger than 3-meter. This checking is done in sub-routine `LDRcheck.m`. If the size of the antenna is larger than 3-meter, `LDRcheck.m` will ask the user to enter lower value(s) for the transmitter gain, and return the new value(s) as well as the variable dimension to SF. The assumption here is that an antenna larger than 3-meter requires the large deployable reflector (LDR) technology. After calling `LDRcheck.m`, SF will ask the user to select the new technologies to be used for technology infusion study. Technology infusion, including the infusion of LDR, is covered in Chapter 3. For this part ignoring it does not violate the integrity of the simulator.

Using the design variable size information obtained when unbundling the design vector, SF runs an exhaustive combination of all selected values of design variables. In terminologies of optimization, this is a full-factorial run. In MATLAB, we achieve a full-factorial run through a nested for-loop. Each for-loop represents one design variable, iterating through all values of this design variable. The 1-dimensional design vector example in Figure A-1 has nine for-loops with one for-loop for each design variable. Altogether it makes one run. The 2-dimensional design vector example has also nine for-loops, with respectively 2, 5, 4, 2, 5, 3, 2, 2, 3 iterations for each for-loop. Altogether it makes 14,400 runs.

The rest of the model is run almost entirely inside the nested for-loops except some post-processing. From the point of view of SF, it simply keeps track of the number of runs, makes calls to a series of subroutines and functions, and directs the traffic of information among them, and collects and post-processes outputs from the subroutines and functions that are of interests to the user of the simulation.

Inside the nested for-loops, SF first stores the number of runs in a variable named result_ count. Based on the relation defined in Table 2.5, it then calls the subroutine named requirements in which the requirements are calibrated. Then SF makes calls to the following functions: `coverage.m` (CCM), `satNetwork.m` (SNM), `spacecraft.m` (SM), `LV.m` (LVM), either `linkRate.m` followed by `MF_TDMA.m` or `linkEbNo.m` followed by `MF_CDMA.m` depending on the type of multiple access scheme (CM), `cost.m` (TCM), and `market.m` (MM). After the execution of these functions, SF stores values of the

objectives into vector J and values of the benchmarking metrics into vector B. After the nested for-loops end, post-processing procedures of finding the Pareto optimal solutions and finding the utopia point are carried out. In the following sections, we will go through each function called inside the nested for-loops.

A.3 Coverage/Constellation Module (CCM)

CCM calculates the geometry and size of the constellation. The inputs of this module are the following: constellation type, orbital altitude, minimum elevation angle, diversity, satellite antenna spot beam gain, and the average frequency of the downlink bandwidth. The outputs of the module are the following: inclination angle, number of satellites in the optimal constellation design, number of orbital planes in the design, beamwidth of the edge cell spot beam, number of cells, the distance from a satellite to the center of its edge cell, orbital period, duration of a beam over a center cell, satellite antenna dimension, and footprint area.

CCM starts with the calculation of some basic constellation geometric parameters including the satellite nadir angle ϑ and the corresponding central angle ψ as in the following equations, where R_e stands for the earth radius, r for orbital altitude measured from the center of earth, and ε for minimum elevation angle.[LWJ00]

$$\vartheta = \arcsin\left(\frac{R_e}{r}\cos\varepsilon\right) \tag{A.1}$$

$$\psi = \arccos\left(\frac{R_e}{r}\cos\varepsilon\right) - \varepsilon \tag{A.2}$$

To calculate the geometry of polar or Walker constellation, depending on which type of constellation the design uses, CCM calls `polar.m` or `walker_lang.m`.

In `polar.m`, the minimum number of planes P that provides a central angle ψ_{min} that is smaller than the central angle calculated in equation A.2 is found by iterating the following equation with incremental values for number of planes P.

$$\psi_{min} = \frac{\pi - (P-1)\psi}{P+1} \tag{A.3}$$

The number of satellites per plane S is then found to be

$$S = \left\lceil \frac{\pi}{\arccos\left[\frac{\cos\psi}{\cos\left(\frac{\pi-(P-1)\psi}{P+1}\right)}\right]} \right\rceil \tag{A.4}$$

If S obtained is not an integer, the smallest integer larger than S is used. The total number of satellites in the constellation is simply

$$N_{sat} = S \times P \tag{A.5}$$

The geometry of a polar constellation is shown in Figure A-2.

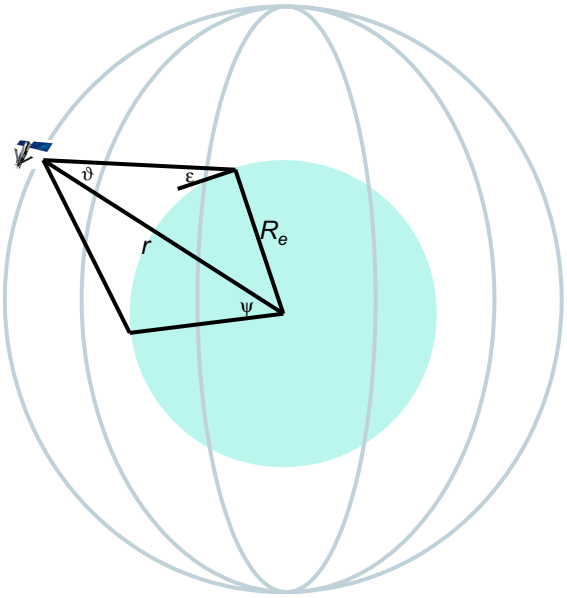

Figure A-2: Geometry of a polar constellation

It should be noticed that the calculation above gives the polar constellation a diversity of one, or single-fold coverage. If the constellation provides multiple diversity coverage, then the numbers of both the planes P and satellites N_{sat} should increase accordingly. The number of planes is the smallest integer equal to or larger than the product of its original value and diversity. Then the final number of satellites is the

product of the number of planes and the number of satellites per plane. This is done at the end of `polar.m`.

If it is `walker_ lang.m` that is called, then the file employs a numerical optimization of Walker constellation designs developed by Lang and Adams.[LA97] The optimization is not a simple function where we can plug in orbital altitude and minimum elevation and come up with $N/P/F$ (This is a classic way of representing the geometry of a Walker constellation, where N is the same as N_{sat}, P is the number of planes, and F is the phasing factor that determines the angular offset between the satellites in adjacent orbital planes). Numerical optimization of P/F and inclination for each value of N_{sat} needs to be performed. By optimization, we mean the configuration that requires the smallest value of ψ to achieve continuous global coverage. This will be the constellation that can be operated at the lowest altitude and still give global coverage. Conversely, at the same altitude, it will offer the largest values of elevation angle and still achieve coverage. The result has been a table of optimal constellations. The tables contain the best P/F and inclination values for each N_{sat}, along with the minimum value of ψ to achieve global coverage. The file `walker_ lang.m` goes through the following steps to find an optimal Walker constellation:

1. Compute central angle ψ using equation A.2.

2. Select the appropriate table (diversity of 1, 2, or 3).

3. Scan down the table to the first entry (lowest number of satellites) for which the table value of ψ (required) is less than the value in step1 (available). This is the optimal constellation for the design. The $N/P/F$ and inclination are given in the table. Read the value of N from the table. For value of P, assume each orbital plane contains 6 satellites, and set P as the lowest integer larger than or equal to N/6.

4. If the diversity number is between 1, 2, or 3, then interpolate between the values given in the table.

At the end, `walker_ lang.m` returns the value of optimal $N/P/F$ and inclination I to `coverage.m`. The geometry of a Walker constellation is shown in Figure A-3.

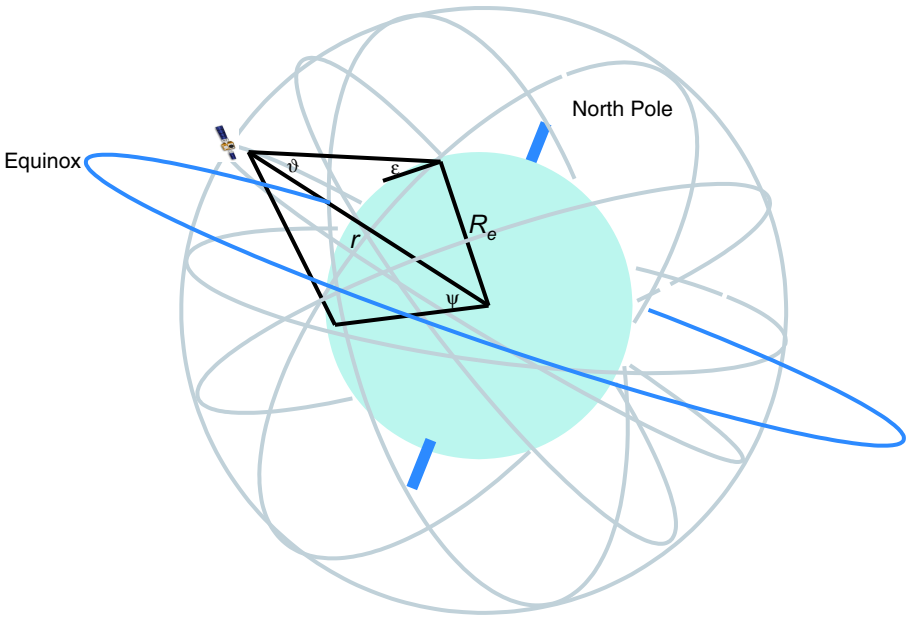

Figure A-3: Geometry of a Walker constellation

After calculating the formation of the constellation, the module finds the dimension of satellite transmitter. First, the wavelength λ of the transmission is the division between the speed of light c and the average frequency of the downlink bandwidth f

$$\lambda = c/f \tag{A.6}$$

Then, using $G_{t\ edge}$ the edge cell gain converted from $G_{t\ dB}$, the dimension of satellite transmitter is

$$D_{sat\ t} = \lambda\sqrt{G_{t\ edge}}/\pi \tag{A.7}$$

Another calculation is dedicated to find the number of cells in the footprint of a satellite. First, the beamwidth θ_{edge} of an edge cell is found to be

$$\theta_{edge} = \frac{35\pi}{\sqrt{G_{t\ edge}}} \tag{A.8}$$

And footprint area and slant range are respectively found to be

$$A_{foot} = 2\pi R_e^2(1 - \cos\psi) \tag{A.9}$$

and

$$R_{slant} = \sqrt{{R_e}^2 + r^2 - 2R_e r\cos\psi} \tag{A.10}$$

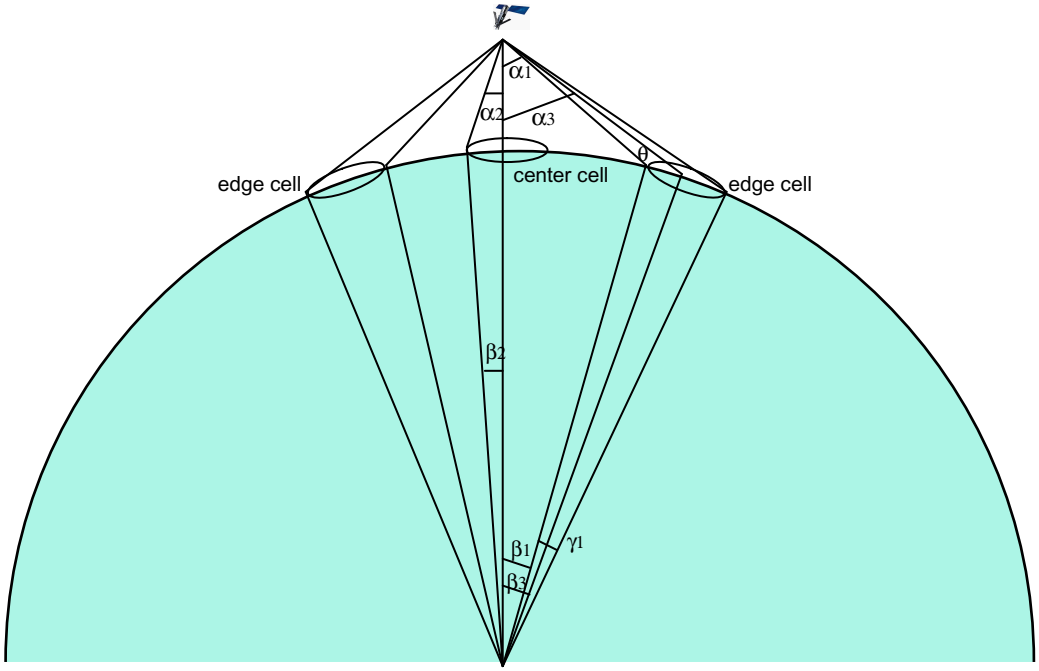

Figure A-4: Geometry involved in calculating single satellite coverage

Figure A-4 will help the understanding of the following geometric derivation. Basically, we will try to find the hexagonal areas of the edge cell and center cell. Then we divide the footprint area with the average of the two hexagonal areas to estimate the total number of cells in the footprint.

$$\alpha_1 = \vartheta - 2\theta_{edge} \tag{A.11}$$

β_1 is the earth centered angle corresponding to α_1.

$$\beta_1 = \arcsin\left(\frac{r}{R_e}\sin\alpha_1\right) - \alpha_1 \tag{A.12}$$

so that

$$\gamma_1 = \psi - \beta_1 \tag{A.13}$$

Radius of the edge cell is

$$r_{edge\ cell} = 1/2 R_e \gamma_1 \tag{A.14}$$

Circular area of the edge cell is

$$A_{edge\ cell} = 2\pi {R_e}^2 \left(1 - \cos\left(\gamma_1/2\right)\right) \tag{A.15}$$

And the hexagonal area inscribed by the circle is

$$A_{edge\ hexa} = \frac{3}{\pi}\sin\left(\frac{\pi}{3}\right) A_{edge\ cell} \tag{A.16}$$

Because the distance from the edge cell to the satellite is larger than the distance from the center cell to the satellite, in order to keep the same cell area, the edge cell beam width needs to be narrower than the center cell beam width. In other words, the gain of the edge cell spot beam needs to be larger than the gain of the center cell spot beam. Iridium's edge cell gain is 6dB larger than the center cell. We can estimate this to be the general case and get

$$G_{tcenterdB} = G_{t\ dB} - 6 \tag{A.17}$$

Beamwidth of the center cell spot beam is

$$\theta_{center} = \frac{35\pi}{\sqrt{G_{t\ center}}} \tag{A.18}$$

Let

$$\alpha_2 = \theta_{center} \tag{A.19}$$

and

$$\beta_2 = \arcsin\left(\frac{r}{R_e}\sin\alpha_2\right) - \alpha_2 \tag{A.20}$$

Radius of the center cell is

$$r_{center\ cell} = 1/2 R_e \beta_2 \tag{A.21}$$

Circular area of the edge cell is

$$A_{center\ cell} = 2\pi {R_e}^2 \left(1 - \cos\left(\beta_2/2\right)\right) \tag{A.22}$$

And the corresponding hexagonal area is

$$A_{center\ hexa} = \frac{3}{\pi}\sin\left(\frac{\pi}{3}\right) A_{center\ cell} \tag{A.23}$$

Then the cell number per footprint is estimated to be

$$N_{cell} = 2\left(\frac{A_{foot}}{(A_{center\ hexa} + A_{edge\ hexa})/2}\right) \tag{A.24}$$

The nearest integer value of the fraction in the parentheses is used. The factor of 2 is to compensate the overlapping of cells in the footprint.

Besides number of cells per footprint, this module also takes care the calculation of the distance from satellite to the center of an edge cell, orbital period, and duration of a beam over a center cell for use in later modules.

To find the distance from satellite to the center of edge cell,

$$\alpha_3 = \vartheta - \theta_{edge} \tag{A.25}$$

β_3 is the earth centered angle corresponding to α_3.

$$\beta_3 = \arcsin\left(\frac{r}{R_e} sin\alpha_3\right) - \alpha_3 \tag{A.26}$$

The distance is

$$D_{edge} = \sqrt{R_e^2 + r^2 - 2R_e r\cos\beta_3} \tag{A.27}$$

To find the orbital period in minutes,

$$T_{orbit} = \frac{1}{60}\left(2\pi\sqrt{r^3/GM_{earth}}\right) \tag{A.28}$$

where GM_{earth} is the Earth's gravitational constant (=398601km^{3}sec^{-2}).

To find the duration of a beam over a center cell, orbital angular velocity of satellite in (rad/s) is

$$\omega_{cir} = 631.34812 r^{-3/2} \tag{A.29}$$

Central angle of a center cell is $2\beta_2$. Then cell duration T_{cell} is

$$T_{cell} = 2\beta_2/\omega_{cir} \tag{A.30}$$

Upon finishing all the calculations, CCM passes the values of the outputs back to SF. SF calls the next module, the satellite network module.

A.4 Satellite Network Module (SNM)

SNM does some calculation that scales the network. The inputs of the module include constellation type, the Boolean variable representing the availability of ISL, number of satellites, number of orbital planes, and the footprint area. The last three inputs are outputs from CCM. The outputs of SNM include gateway thousand lines of code, number of gateways, and number of personnel staffed at the gateways.

Gateway thousand lines of code is an important parameter useful for estimating system life-cycle cost. In this study, it is estimated to be 6.3 thousand lines per

gateway for LEO systems. This estimation is based on the FCC filings of four systems including ARIES, Globalstar, ORBCOMM, and Starnet.

In estimating the number of gateways, two assumptions are made. The first assumption is that for system without ISL, the number of gateways is inversely proportional to the footprint area. The reasoning behind this assumption is simple: theoretically for systems without ISL, in the footprint of a satellite, there should be at least one gateway at anytime. The total area of coverage is constant, that is, the total land mass of the earth. If the footprint is larger, then fewer gateways are needed to cover the entire land on the earth. In the original design of Globalstar, 50 gateways are planned for 48 footprints. This confirms the assumption made above. For non-ISL systems with footprint A_{foot} different from that of Globalstar $A_{footGlobalstar}$, the number of gateways needed can be estimated as

$$N_{GW} = 50 \times \frac{A_{foot\ Globalstar}}{A_{foot}} \tag{A.31}$$

The footprint area of Globalstar is about 26.4 million square kilometers. The solution of N_{GW} is taken at the nearest integer value.

The second assumption is that for systems with ISL, two gateways are needed per orbital plane. Although in theory an ISL system needs just one gateway to interface the space segment with the ground segment, in practice each orbital plane should have two gateways to diverge the communication traffic. Indeed this is the design adopted by Iridium. Therefore if P is the number of planes, then the number of gateways for an ISL system is simply

$$N_{GW} = 2P \tag{A.32}$$

The number of personnel is estimated assuming at any moment there are three personnel members stationed at each gateway on a eight-hour rotating schedule. So the total number of personnel at all gateways are

$$N_{personnel} = N_{GW} \times 3 \times \left(\frac{24\text{hrs.}}{8\text{hrs.}}\right) \tag{A.33}$$

After the above calculations, SNM passes the output values back to SF.

A.5 Spacecraft Module (SM)

The next module called by SF is SM. The inputs of this module are satellite transmitter power, ISL, thousand lines of code of gateway, apogee kick motor specific impulse, station keeping engine specific impulse, orbital altitude, space life of the system, ISL datarate, and satellite transmitter antenna dimension. The outputs of the module are satellite mass, injection fuel mass, antenna weight, communication electronics weight, spacecraft bus dry weight, beginning of life power, apogee kick motor type, apogee kick motor dry weight, apogee kick motor impulse, and flight software thousand lines of code.

Although SM has multiple outputs, its major product is the satellite in-orbit wet mass. This mass is important to launch vehicle selection and cost estimation in later modules. To estimate this mass, a combination of analogy with existing system, scaling from existing systems, and budgeting by components is used. SM first estimates the relationship between the dry mass of spacecraft without ISL and its payload power based on data from the FCC filings of twenty-three LEO personal communication systems collected by Phil Springmann in November 2002

$$M_{dry} = 11.025 P_t^{0.6076} \tag{A.34}$$

The data are shown in Figure A-5.

After the spacecraft dry mass, the antenna weight is estimated from the transmitter antenna dimension. The relationship between antenna weight and antenna size is estimated based on data provided in SMAD[LW92] as what follows

$$M_{ant} = 9.1734 D_{sat\ t}^{1.4029} \tag{A.35}$$

The data are shown in Figure A-6.

Because the mass of the receiver antenna is assumed to be same as the transmitter,

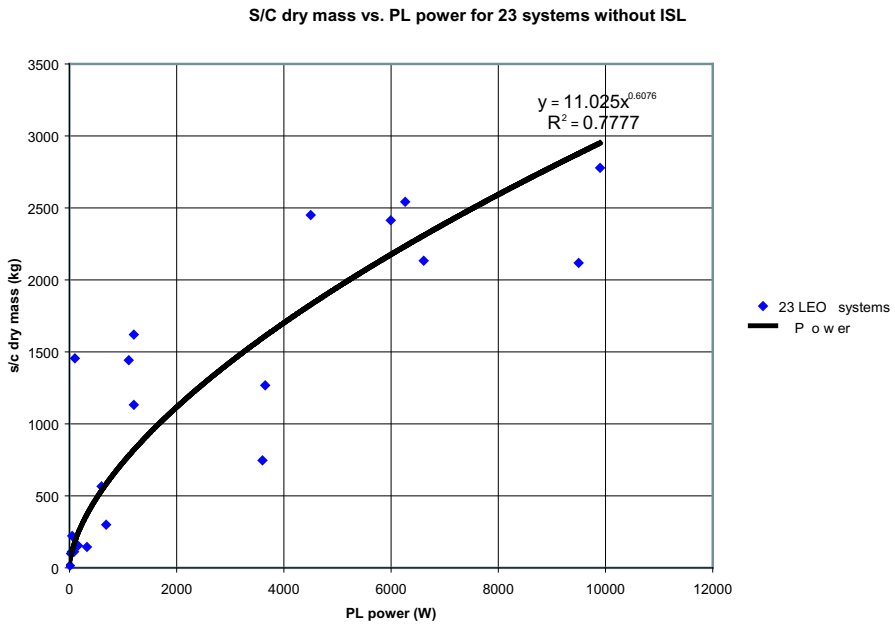

Figure A-5: Relationship between spacecraft dry mass and payload power for satellites with no ISL, based on the FCC filings of 23 LEO personal communication systems.

a factor of 2 is added to represent both antennas.

An estimation of the ISL weight is made based on information provided by Yoshisada Koyama at Next-Generation LEO System Research Center (NeLS) in Japan.[Koy02] The assumption is that the ISL system of a satellite has four links, two for intra-plane transmission and two for inter-plane transmission. The mass is estimated to be 426 kg for a radio frequency (RF) ISL with data rate lower than 100 Mbps, 480 kg for an RF ISL with data rate higher than 100 Mbps, and 117 kg for an optical ISL (OISL) with data rate of 10 Gbps. Appendix B shows a detailed breakdown of the estimation.

Using the dry mass of spacecraft without ISL and mass of ISL (if applicable) as initial value, M_{sat} goes through an iteration in which the significant portions of the spacecraft fuel mass are added. An iteration is used because the deorbiting and station-keeping fuels added at later steps of the calculation will affect the spacecraft cross-section area calculated at earlier step. It has been shown that M_{sat} typically converges to within 0.01% of its final value in less than 10 iterations. The structure of the iteration is shown below.

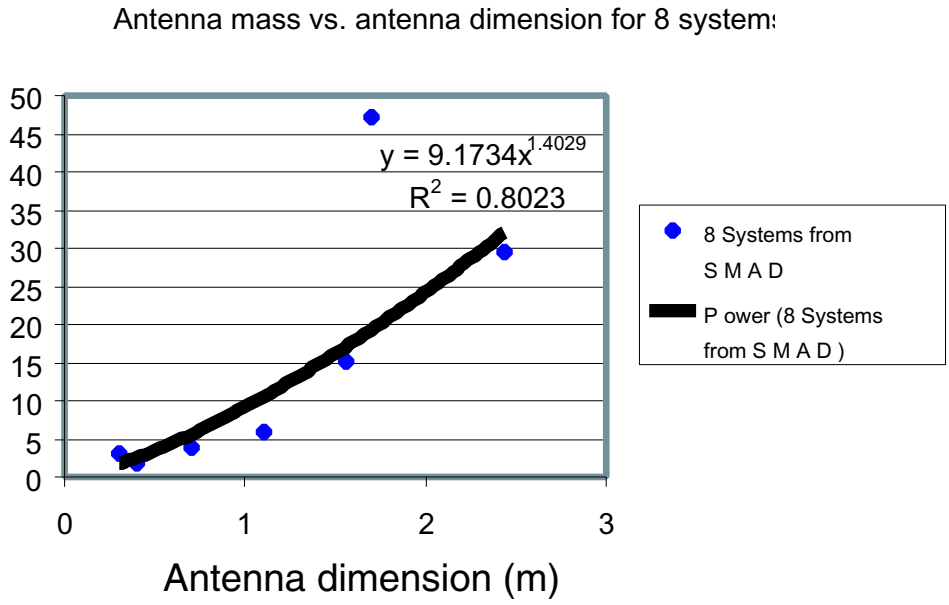

Figure A-6: Relationship between antenna mass and antenna dimension based on the data of 8 systems provided in SMAD

As shown in Figure A-7, the first step in the iteration is to find the volume and cross-section area of the satellite. This step is done in a subroutine named `scgeometry.m`. Based on data from fifteen LEO communication systems collected by Springmann, the average density of this type of spacecraft is found to be 234.18 kg/m^3. Since the volume will later be used in finding the satellite stowage capacity of rocket fairings, we include the entire mass of the satellite, including the antenna, to find the volume

$$V_{sat} = \frac{M_{sat}}{234.18\text{kg/m}^3} \tag{A.36}$$

Next, we find the cross-section area of the satellite in orbit. Since in orbit the antennas are often unfolded from the spacecraft, we will account antenna area separately from spacecraft cross-section area. Assuming spherical shape of spacecraft and circular shape of antennas, the total cross-section area of the spacecraft and antennas is

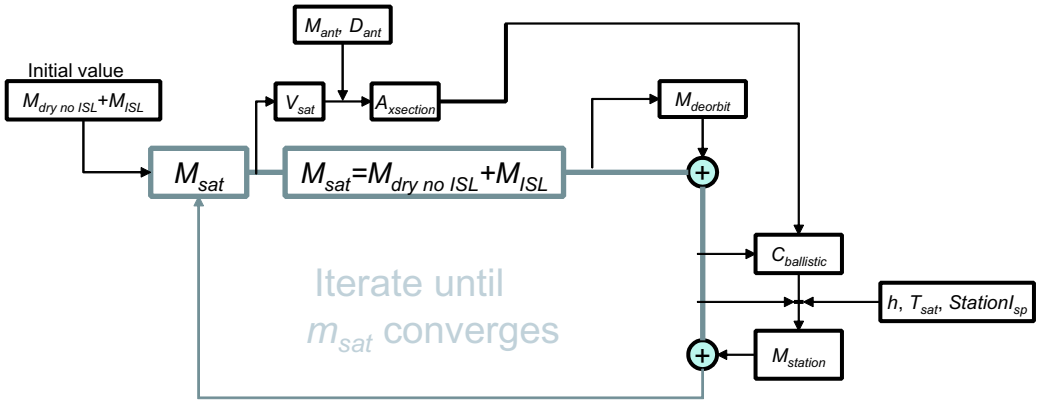

Figure A-7: Iterations to find satellite mass

$$A_{xsection} = \pi \left(\frac{3}{4\pi} \frac{M_{sat} - M_{ant}}{234.18 \text{kg/m}^3} \right)^{\frac{2}{3}} + 2\pi \left(\frac{D_{sat}\, t}{2} \right)^2 \tag{A.37}$$

Again, a factor of 2 is added to represent both the transmitter and receiver.

The third step is to add deorbiting fuel mass to satellite mass. The deorbiting fuel mass is found in subroutine `deorbit.m`. First the delta V for deorbiting is suggested by equation (6-54) in SMAD.

$$\Delta V_{deorbit} \approx V \left(1 - \sqrt{\frac{2R_E}{R_E + r}} \right) \tag{A.38}$$

where R_E is earth radius and r earth-centered orbital radius.

This equation assumes the deorbiting process brings the satellite from its original orbital altitude to the earth surface. But the FCC filings of both Iridium and Globalstar suggest that a ΔV much smaller than defined by Equation A.38 is needed. In practice, the decommissioned satellite is propelled only to an altitude low enough to avoid collision with the other satellites in the constellation, and the rest of the descending is natural decay due to atmosphere drag. In the simulation, It is assumed that the satellite is thrust to 90% of its original orbital altitude. So Equation A.38 becomes

$$\Delta V_{deorbit} \approx V \left(1 - \sqrt{\frac{2(R_E + 0.9h)}{(R_E + 0.9h) + r}} \right) \tag{A.39}$$

To find the fuel needed for deorbiting, we first find the sum of fuel and satellite using equation

$$M_{fuel+sat} = M_{sat} e^{\Delta V_{deorbit}/g I_{sp\ station}} \tag{A.40}$$

The specific impulse of station-keeping thruster is used because the same thruster is assumed to be used for decommission, as what often happens in practice. Then the fuel mass is found simply by

$$M_{fuel} = M_{fuel+sat} - M_{sat} \tag{A.41}$$

The value of deorbiting fuel mass is returned to `spacecraft.m` and added to total satellite mass.

The next step is to find station-keeping fuel mass. For satellites with circular orbit at low altitude, the most significant disturbance comes from atmosphere drag. The other disturbances due to earth's oblateness and third-body interaction are negligibly small compared with drag. The first thing to be found is ballistic coefficient $C_{ballistic}$. In `ballistic.m`, the cross-section area calculated earlier is used. According to SMAD, an approximate value of 2.2 should be used for drag coefficient C_d. Then ballistic coefficient $C_{ballistic}$ is

$$C_{ballistic} = \frac{M_{sat}}{C_d A_{xsection}} \tag{A.42}$$

After `ballistic.m`, `station.m` is called. In `station.m`, the density at the particular orbital altitude is interpolated through atmosphere density data that is available in SMAD. Then the mean ΔV per year required to maintain altitude (in m/s per year) is

$$\Delta V_{station} = \frac{\pi \rho r V}{C_{ballistic} T_{orbit}} \tag{A.43}$$

where r is orbital radius in meter, V orbital velocity in m/s, $C_{ballistic}$ ballistic coefficient in kg/m^2, and T_{orbit} orbital period in year. This equation can be found in

column 6 on the back sheet of SMAD.

After knowing the ΔV required for station-keeping, the station-keeping fuel mass is calculated using Equation A.40 and A.41 as described above. This mass is added to satellite mass.

The calculation of station-keeping fuel mass concludes the iteration. The iteration loops until the mass of satellite converges. Although the satellite includes orbital injection fuel at launch, but the injection fuel does not affect the iterative calculation of satellite mass when the satellite is in orbit because it has been used up when the satellite enters the orbit.

It should be noted that the order of calculations on different masses is designed to be the reverse of their order of removal from the satellite during its life. The dry mass and ISL mass (if applicable) are the original masses of the satellite. Deorbiting fuel stays on satellite throughout satellite's lifetime and is used only at the end of it; therefore its mass is the next to be calculated and added to total satellite mass. The station-keeping fuel is consumed throughout the lifetime of the satellite, and its mass is the last to be calculated and added to satellite mass. The orbit injection fuel is used up before the satellite enters the orbit; therefore its mass is not included in the iterative calculation. Indeed, it is the first thing to be calculated outside the iteration.

The calculation of orbital injection fuel depends not only on characteristics of the spacecraft and orbit but also on the launch vehicle employed to send the spacecraft to the injection orbit from where the injection will happen. Different launch vehicles vary from each other in flight profile. Even the same launch vehicle has different versions that are customized to be mission-specific. It is difficult to make a generic calculation for the injection fuel requirement for a specific design. This rough estimation is based on available data of existing systems. In its FCC filing, the original design of Iridium uses 17.5 kg of fuel to inject 323.2 kg of in-orbit wet mass. The original design of Globalstar uses 30 kg of fuel to inject 232.0 kg of in-orbit wet mass. The average of the two systems is 23.75 kg of injection fuel for 277.6 kg in-orbit wet mass. A reasonable assumption is that the injection fuel mass is linearly proportional to in-

orbit wet mass. So the following relation for a ballpark estimation of injection fuel mass is derived

$$M_{insertion} \approx 23.75 \times \frac{M_{sat}}{277.6} \tag{A.44}$$

Together with a few other inputs, $M_{insertion}$ is plugged into `insertion.m`. In `insertion.m`, we find the impulse and dry weight of the apogee kick motor (AKM) that propels the orbit injection. These two quantities will be useful in finding the life-cycle cost of the system. First, the $\Delta V_{insertion}$ for orbital insertion is found using equation (17-6) in SMAD

$$\Delta V_{insertion} = g I_{sp\ insertion} \ln \frac{M_{sat} + M_{insertion}}{M_{sat}} \tag{A.45}$$

Then the impulse for the AKM in kg·m/s is

$$J_{AKM} = M_{sat} \Delta V_{insertion} \tag{A.46}$$

But the cost model that will be used later requires J_{AKM} in kg·s, so we use a modified equation

$$\hat{J_{AKM}} = M_{sat} \Delta V_{insertion} / g \tag{A.47}$$

Since AKM is typically a solid-fuel motor, its dry weight can be estimated using data on solid rocket motors provided in Table 17-7 in SMAD. Based on 12 existing motors, a relation can be found between the dry weight and the total impulse of the motor, as illustrated in Figure A-8.

In mathematical form, the relation is

$$AKMDW = 2 \times 10^{-5} J_{AKM} \tag{A.48}$$

The quantities calculated in `insertion.m` are returned to `spacecraft.m`.

A few more parameters are prepared for use in estimating the system life-cycle cost. These parameters are communication electronics weight (CEW), spacecraft bus

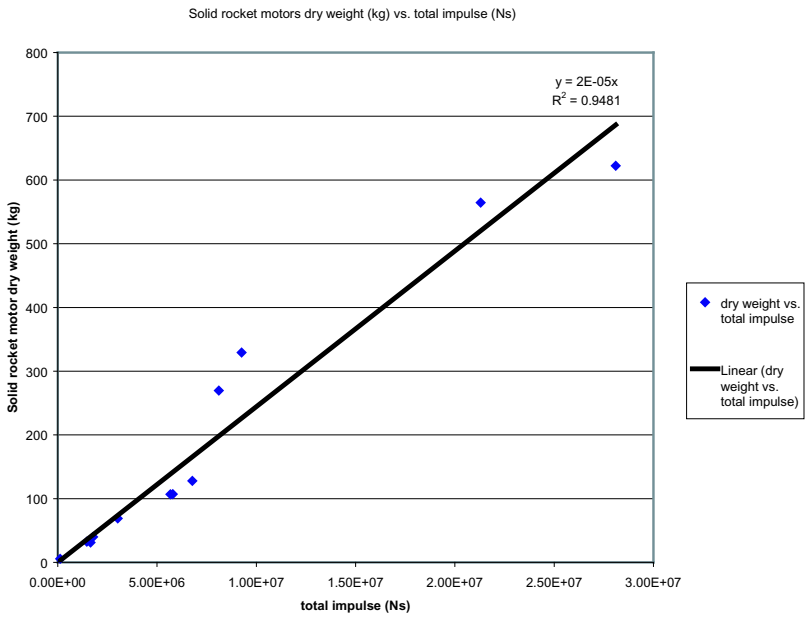

Figure A-8: Solid motor dry weight vs. total impulse

dry weight ($SCBDW$), beginning of life power (BLP), and flight software thousand lines of code ($FSKLOC$). Based on data from existing systems, basic scaling relations are found to be

$$CEW = 0.27 M_{sat} \tag{A.49}$$

$$SCBDW = 0.436 M_{sat} \tag{A.50}$$

$$BLP = 2.61 P_t \tag{A.51}$$

$FSKLOC$ is approximated equal to gateway thousand lines of code that has been calculated in `satNetwork.m`.

This concludes all the calculations in `spacecraft.m`. The module returns all useful values to the start file (SF).

It is worth noticing that Springmann and de Weck have developed a parametric

scaling model methodology to estimate the spacecraft power, dry mass, and wet mass for non-geosynchronous communication satellites.[SdW04] Although it is not used in this thesis, the methodology might be used in the future as a reference point for spacecraft attributes prediction.

A.6 Launch Vehicle Module (LVM)

The LVM checks six launch vehicles against the satellite mass and volume and select the ones that are capable of launching the satellites to the designed orbit. Among the capable launch vehicles, the module selects the one with lowest launch cost. The inputs of the module are satellite mass (including insertion fuel mass), orbital inclination angle, orbital altitude, and number of satellites in the constellation. The outputs that are of interests to this research are the name of the selected launch vehicle, number of satellites per vehicle, number of launches, selected launch site, launch success ratio of the selected launch vehicle, launch cost, and counter of capable vehicles. In the code, extra outputs are given for the purpose of launch image generation in Satellite Tool Kit. Irrelevant to the research, they will not be covered.

The six launch vehicles are: Ariane 5 (Europe), Atlas IIIA (U.S.A.), Delta II 7920 (U.S.A.), H-IIA 202 (Japan), Long March 2C (China), and Pegasus XL (U.S.A.). and . Except Long March 2C and Ariane 5, the launch capability data are from International Reference Guide to Space Launch Systems published by AIAA.[IJH99] The data on Long March 2C and Ariane 5 are from the official website of their service providers, respectively.[oLVTCowEv03, Web03]

The launch capability data of a vehicle are typically given in diagram as shown in Figure A-9. The diagram is specifically for launching into circular orbits. The x-axis stands for orbital altitude and the y-axis stands for payload mass that the vehicle is capable to send up. Each curve represents a different orbital inclination angle. The highest curve is the lower bound of orbital inclination the launch vehicle is able to reach, while the lowest curve is the higher bound (Unless it is a sun synchronous orbit [SSO]. In this case, the curve above the SSO should be read for higher bound). The

altitude bound of vehicle can also be read straightforwardly from the diagram. Thus, the diagram provides two bounds we need to measure against: the inclination bounds and the altitude bounds.

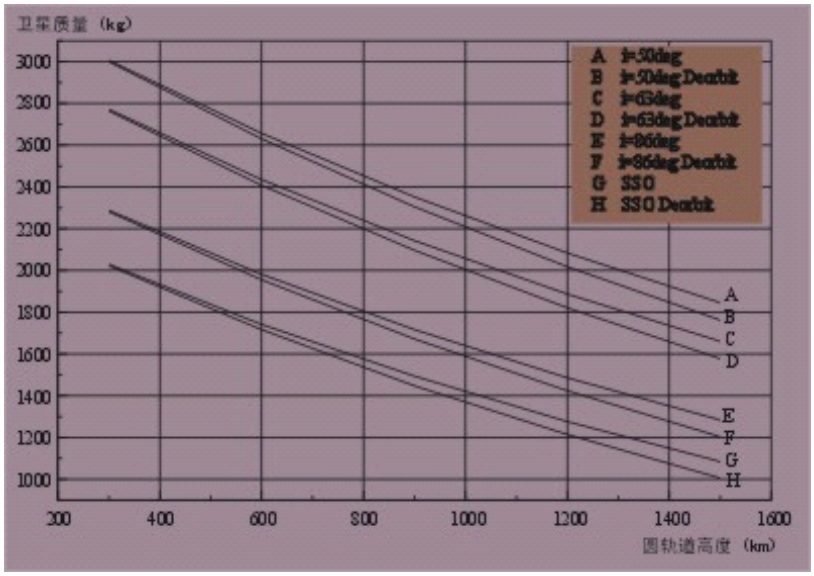

Figure A-9: Launch capability of Long March 2C. Copyright: China Academy of Launch Vehicle Technology

The other physical limit on launch capability is dimensions of the launch vehicle's fairing. Fairing is where the payload of the launch vehicle is stored. The satellite to be launched must fit into the fairing or otherwise it cannot be launched even if its mass is lower than the vehicle's lifting capability. Figure A-10 shows a typical fairing diagram. From the data provided by the diagram, the volume of the fairing can be easily estimated. By comparing the volume of the satellite with the internal volume of the fairing, we will know whether the fairing can accommodate the satellite.

LVM checks the satellite design against the three limits mentioned above: inclination, altitude, and fairing dimension. If the satellite design is within the range of these limits, then we interpolate its launch capability diagram as shown in Figure A-9 to find the payload mass the launch vehicle can lift to the designed orbital altitude. If the payload mass is larger than satellite mass and the fairing volume is larger than satellite volume, then the launch vehicle is recognized as a capable vehicle and added to a data array that records capable launch vehicles. To find how many satellites can

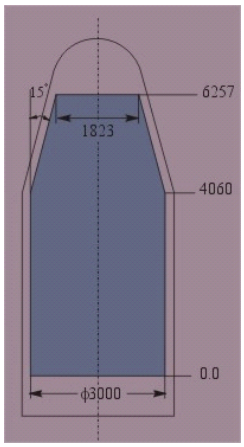

Figure A-10: Fairing dimensions of Long March 2C. Copyright: China Academy of Launch Vehicle Technology

be sent up per vehicle (SPV), we use the following simple expression, in which MPL is payload mass, $V_{fairing}$ is fairing volume, M_{sat} is satellite mass including insertion fuel, and $Vsat$ is satellite volume including insertion fuel, so that the lower of the mass limit and volume limit is taken.

$$SPV = \min\left(\left\lfloor \frac{M_{PL}}{M_{sat}} \right\rfloor, \left\lfloor \frac{V_{fairing}}{V_{sat}} \right\rfloor\right) \tag{A.52}$$

The number of launches to send up the entire constellation is found as

$$N_{launch} = \left\lceil \frac{N_{sat}}{SPV} \right\rceil \tag{A.53}$$

The information sources for launch capabilities also give the cost per launch for each launch vehicle. Then the total launch cost C_{launch} is simply

$$C_{launch} = C_{per\ launch} N_{launch} \tag{A.54}$$

After checking the capabilities of all six launch vehicles, the array recording the capable launch vehicles and their cost information is scanned. The capable vehicle with lowest cost is chosen to be the selected launch vehicle for the design, and its information and technical data are returned to SF.

Since launch vehicles such as Ariane 5 can lift 6 tons of payload to the geostationary transfer orbit (STO), it is hard to imagine any design is unable to find a launch vehicle capable of lifting it to the much lower LEO orbits. In the unlikely event that the satellite cannot find a capable launch vehicle, SF will set its capacity in term of simultaneous users supported by a satellite to zero. Otherwise, the satellite capacity needs to be calculated in the capacity modules as described in the following section.

A.7 Capacity Modules (CM)

The capacity modules calculate the number of simultaneous users a satellite can support. Each of the MF-TDMA and MF-CDMA schemes requires a different approach in capacity calculation. Therefore, CM is divided into five subroutines. The first three subroutines together calculate the capacity of MF-TDMA scheme, and the rest two subroutines together calculate the capacity of MF-CDMA scheme. Before introducing the computer codes, we will look at the mathematical equations for the capacity calculation. In the paragraphs below, I will just give the final equations used in the code. The paper "Basic Capacity Calculation Methods and Benchmarking for MF-TDMA and MF-CDMA Communication Satellites (AIAA2003-2277) describes the physics behind these equations and derives results that confirm the calculation of the modules. The paper is attached as Appendix C.[CdW03]

For MF-TDMA, we first need to find the total data rate for FDMA carriers per cell. There are two possible limits on the data rate - power limit and bandwidth limit. The FDMA data rate per FDMA carrier due to power limit can be calculated using link budgeting, where R_{FDMA} stands for data rate per FDMA carrier, $Power_{cell}$ for transmitter power per cell, N_{FDMA} for number of FDMA carriers per cell, G_t for transmitter gain, G_r for receiver gain, k for Boltzmann's constant, T_s for system temperature, E_b/N_0 for bit energy to noise ratio, L_{tot} for total loss along the transmission path, and $Margin$ for link margin

$$R_{FDMA} = \frac{\frac{Power_{cell}}{N_{FDMA}} G_t G_r L_{tot}}{kT_s(E_b/N_0)Margin} \tag{A.55}$$

Moving N_{FDMA} to the left-hand side of the equation gives the total data rate of all the FDMA carriers per cell defined by power limit

$$R_{FDMA}N_{FDMA} = \frac{Power_{cell}G_tG_rL_{tot}}{kT_s(E_b/N_0)Margin} \tag{A.56}$$

To find data rate per cell due to bandwidth limit, we first write the data rate per FDMA channel defined by bandwidth limit. Let BW_{cell} denotes bandwidth per cell (= satellite bandwidth / cluster size; cluster size is the number of bands for a satellite), M denotes signal modulation level, β for Nyquist filter rolloff factor, normally ranging from 0.2 to 0.5, B_T for frequency channel bandwidth, and B_g for guard bandwidth, then

$$R_{FDMA} = \frac{\frac{BW_{cell}}{N_{FDMA}}\log_2 M}{1+\beta}\left(\frac{B_T}{B_T+B_g}\right) \tag{A.57}$$

Moving N_{FDMA} to the left-hand side of the equation gives the total data rate of all the FDMA carriers per cell defined by bandwidth limit

$$R_{FDMA}N_{FDMA} = \frac{BW_{cell}\log_2 M}{1+\beta}\left(\frac{B_T}{B_T+B_g}\right) \tag{A.58}$$

In this equation, we already know BW_{cell}; M is 4 if QPSK is used, and β is set to 0.26 as a constant. In Iridium, the frequency domain is divided so that

$$\frac{B_T}{B_T+B_g} = \frac{41.67\text{MB}}{41.67\text{MB}+1.236\text{MB}} = 0.9712 \tag{A.59}$$

We assume this division applies to all MF-TDMA systems and use the value of 0.9712 in Equation A.58.

To find the number of TDMA channels, we refer to the geometry of time distribution as shown in Figure C-2. In the geometry, let FL denote frame length, FIL denote framing time slot length, TGL denote total guard slot length, and R_{user} denote individual user datarate. It is not difficult to perceive the following relation

$$N_{TDMA} = \frac{R_{FDMA}\left(1-\frac{FIL}{FL}\right)}{R_{user}\left(1+\frac{TGL}{FL-FIL-TGL}\right)} \tag{A.60}$$

Per theory of MF-TDMA modulation scheme, the total number of MF-TDMA channels is the product of N_{FDMA} and N_{TDMA}. Then we will get

$$\begin{aligned} N_{FDMA}N_{TDMA} &= N_{FDMA}\frac{R_{FDMA}\left(1-\frac{FIL}{FL}\right)}{R_{user}\left(1+\frac{TGL}{FL-FIL-TGL}\right)} \\ &= N_{FDMA}R_{FDMA}\frac{\left(1-\frac{FIL}{FL}\right)}{R_{user}\left(1+\frac{TGL}{FL-FIL-TGL}\right)} \end{aligned} \tag{A.61}$$

In this equation, $N_{FDMA}R_{FDMA}$ is the lower of the results from Equations A.56 and A.58. To find the fractional term in the equation, we use the design of Iridium and assume it is typical of MF-TDMA systems. In Iridium, the time domain is divided so that

$$\frac{1-\frac{FIL}{FL}}{1+\frac{TGL}{FL-FIL-TGL}} = \frac{1-0.192}{1+\frac{0.04}{1-0.192-0.04}} = 0.77 \tag{A.62}$$

Therefore, the capacity of a MF-TDMA system can be found. For Iridium, equation A.61 gives a capacity of 905 simultaneous users per satellite.

For MF-CDMA system, omitting the detailed derivations (for detailed derivations, see Appendix C), we arrive at an equation for the number of simultaneous users per cell N_c, where T denotes number of CDMA carriers in the satellite bandwidth, B_{sat} denotes satellite bandwidth, B_g denotes guard band between CDMA carriers, R_{user} denotes individual user data rate, a value of 0.5 represents the expected value of voice channel activity state, f denotes neighboring user interference factor, E_b/N_0 represents the ratio of bit energy to noise caused along the link, and E_b/I_{tot} represents the ratio of bit energy to noise including both N_0 and interference noise.

$$N_c = T + \left[\frac{B_{sat}-TB_g}{R_{user}}\frac{1}{\alpha(1+f)}\right]\left[\left(\frac{E_b}{I_{tot}}\right)^{-1} - \left(\frac{E_b}{N_0}\right)^{-1}\right] \tag{A.63}$$

and an equation for E_b/N_0 for each individual link is

$$\frac{E_b}{N_0} = \frac{\frac{Power_{cell}}{N_c}G_tG_rL_{tot}}{kT_sR_{user}Margin} \tag{A.64}$$

or, if move N_c to the left-hand side,

$$\frac{E_b}{N_0}N_c = \frac{Power_{cell}G_tG_rL_{tot}}{kT_sR_{user}Margin} \tag{A.65}$$

Substituting (A.64) into (A.63) and solve for N_c, we find the following expression

$$N_c = \frac{T + \frac{B_{sat}-TB_g}{R_{user}}\frac{1}{\alpha(1+f)}\frac{I_{tot}}{E_b}}{1 + \frac{B_{sat}-TB_g}{R_{user}}\frac{1}{\alpha(1+f)}\left(\frac{Power_{cell}G_tG_rL_{tot}}{kT_sR_{user}Margin}\right)^{-1}} \tag{A.66}$$

As mentioned before when introducing the equations, five subroutines are written to implement the above mathematical calculations into the model. The first three subroutines are for MF-TDMA, among which, the first subroutine `linkRate.m` returns the value of $R_{FDMA}N_{FDMA}$ in (A.56). The second subroutine `BWLimit.m` returns the value of $R_{FDMA}N_{FDMA}$ in (A.58). The lower of these two values defines the bound and is input into the third subroutine `MF_TDMA.m`, which uses (A.61) to find the total number of MF-TDMA channels supported by a satellite.

The next two subroutines find the capacity of a MF-CDMA system. The first of them `linkEbNo.m` gives $(E_b/N_0)N_c$ in (A.65). Substituting this result to the last subroutine `MF_CDMA.m`, N_c in (A.66) is calculated. The satellite capacity is the product of N_c and the number of cells N_{cell} calculated in (A.24).

$$C_{sat} = N_c \times N_{cell} \tag{A.67}$$

One more thing worth mentioning despite the omission of the derivation of the equations is convolutional coding. In convolutional coding, redundancy cleverly coded into transmitted information reduces transmit power required for a specific bit error probability. This reduction process has two important parameters, code rate r and constraint length K. Code rate r is defined by the ratio between the original information bits k and the redundantly coded content bits n,

$$R_c = k/n \tag{A.68}$$

The bit energy to mean total noise power spectral density ratio E_b/I_{tot} corresponding to several bit error probabilities, p_b, are listed in Table A.1 for soft-decision

Viterbi decoding.

	E_b/I_{tot}	$R_c =$	1/3		$R_c = 1/2$		$R_c =$	3/3	$R_c =$	3/4
p_b	uncoded	K=7	K=8	K=5	K=6	K=7	K=6	K=8	K=6	K=9
10^{-3}	6.8	4.2	4.4	3.3	3.5	3.8	2.9	3.1	2.6	2.6
10^{-5}	9.6	5.7	5.9	4.3	4.6	5.1	4.2	4.6	3.6	4.2
10^{-7}	11.3	6.2	6.5	4.9	5.3	5.8	4.7	5.2	3.9	4.8

Table A.1: Coding gain E_b/N_0 (dB-b^{-1}) for soft-decision Viterbi decoding, QPSK

From Table A.1, the values of E_b/N_0 in Equation (A.56) and of E_b/I_{tot} in Equation (A.66) can be read and used in the simulation.

The satellite capacity of either the MF-TDMA system or MF-CDMA system is returned to SF. Then in SF, the system capacity in term of the number of simultaneous users supported by the entire constellation is calculated. The calculation is slightly different for polar constellation and Walker constellation. Because satellites in the polar constellation all need to fly above the poles, at the poles there is a severe overlapping of satellites' footprints. This overlapping causes a reduction in the overall system capacity of polar constellation, which can be represented by the polar overlapping factor (POL)of 0.68. For Walker constellation, POL is 1 because Walker constellation covers only below certain latitude and never passes the poles. Therefore the system capacity equation is

$$C_{system} = C_{sat} \times N_{sat} \times POL \tag{A.69}$$

A.8 Total Cost Module (TCM)

The cost module methodically computes the present value of the life-cycle cost of the system. The method is modified on the basis of cost estimating relationships (CERs) in SMAD. A step-by-step introduction to the method will be given after we introduce the inputs and output of the module. The inputs include the number of satellites in the constellation, number of orbital planes, orbital altitude, antenna weight, communication electronics weight, spacecraft bus dry weight, satellite mass (wet weight),

beginning-of-life power, flight software thousand lines of code, ground software thousand lines of code, designed life of space segment, initial deployment time, number of gateways, number of operations and support personnel, AKM type, AKM dry weight, AKM impulse, discount rate, minimum launch cost, and ISL datarate. The output of the module is the total present value of the life-cycle cost (LCC) of the designed system. All cost terms in this module are in unit of thousand of U.S. dollars in fiscal year 2002.

In this module, it takes 16 steps to account for the LCC of the system. The first step sets space mission characteristics. Most of these characteristics are design variables, constants, or system parameters obtained in previous modules. There are two exceptions: payload type and number of spare spacecraft. For this study, the payload type is communication. A spare satellite is typically launched into each orbital plane at altitude lower than that of the regular orbit so that it is ready to replace a failed satellite in that orbital plane. Therefore the number of spare spacecraft is set to the number of orbital planes.

The second step accounts for the hardware cost of the research, development, test and evaluation (RDT&E) phase. As the name suggests, this phase occurs very early in the system life-cycle. It is a breakdown of the costs of antenna, communication electronics, spacecraft bus, and apogee kick motor. Each component's cost is in relation to the weight of that particular component except that the AKM cost is linear with the AKM impulse. These relations are from SMAD[LW92].

If antenna weight is M_{ant}, then the antenna RDT&E cost is found to be

$$C_{ant} = 1015 M_{ant}^{0.59} \tag{A.70}$$

The communication electronics cost is

$$C_{CE} = 917 CEW^{0.7} \tag{A.71}$$

where CEW is weight of communication electronics. The cost of spacecraft bus is based on SCBDW, the dry weight of spacecraft bus

$$C_{SCbus} = 16253 + 110SCBDW \tag{A.72}$$

The AKM weight depends on AKM impulse and also on the AKM type. If the AKM is spin-stabilized, then the cost is

$$C_{AKM} = 490 + 0.0518J_{AKM} \tag{A.73}$$

If the AKM is 3-axis stabilized, which is more popular for current LEO communication satellite design, then the cost is

$$C_{AKM} = 0.0156J_{AKM} \tag{A.74}$$

The total hardware cost of the RDT&E phase is the sum of the above component costs. Because the numerical values above are expressed in 1992 USD value, they have been converted them to 2002 USD value by the inflation rate of 1.369. Therefore the hardware cost is

$$RDTEHC = (C_{ant} + C_{CE} + C_{SCbus} + C_{AKM}) \times 1.369 \tag{A.75}$$

The third step is to find theoretical first unit (TFU) hardware cost. This step is similar as the previous step except the component costs are calculated differently as what follow

$$C_{ant} = 20 + 230M_{ant}^{0.59} \tag{A.76}$$

$$C_{CE} = 179CEW \tag{A.77}$$

$$C_{SCbus} = 185SCBDW^{0.77} \tag{A.78}$$

For spin-stabilized AKM,

$$C_{AKM} = 58AKMDW^{0.72} \tag{A.79}$$

For 3-axis stabilized AKM,

$$C_{AKM} = 0.0052J_{AKM} \tag{A.80}$$

The rest of step 3 is the same as step 2. The TFU hardware cost is

$$TFUHC = (C_{ant} + C_{CE} + C_{SCbus} + C_{AKM}) \times 1.369 \tag{A.81}$$

Step 4 is to find the hardware cost of every spacecraft produced. This step includes the learning curve phenomenon that accounts for production cost reduction as the production quantity increases. The reduction in cost is due to economies of scale, set up time, and human learning. The total production cost of N units is modelled as

$$C_N = TFU \times N^{1-\log_2(100\%/S)} \tag{A.82}$$

The learning curve slope S represents the percentage reduction in cumulative average cost when the number of production units is doubled. SMAD recommends the following values for learning curve slope.

Number of units	Learning curve slope
≤ 10	95%
$10 <$ and ≤ 50	90%
$50 <$	85%

Table A.2: Learning curve slope values

The cost of the first unit is C_1 given by equation A.82 with $N = 1$; the cost of the second unit is $C_2 - C_1$ where C_2 is given by equation A.82 with $N = 2$; the cost of the third unit is $C_3 - C_2 - C_1$, so on and so forth. The hardware costs of all units are assigned to elements of an array called **UHC**.

Step 5 finds aerospace ground equipment cost for RDT&E. This part of the cost covers the test and support equipment needed for assembly, development and ac-

ceptance testing and integration of satellite subsystems and satellite to the launch vehicle. The cost is expressed in a simple linear relation

$$AGEC = 0.11(RDTEHC + TFUHC) \tag{A.83}$$

Step 6 finds total program level cost for RDT&E and all units including TFU. First, program level cost for RDT&E is

$$PLC_{RDT\&E} = 0.36RDTEHC \tag{A.84}$$

Program level cost for all units is

$$PLC_u = \sum \mathbf{UHC} \tag{A.85}$$

Total program level cost is

$$PLC_{tot} = PLC_{RDT\&E} + PLC_u \tag{A.86}$$

Step 7 is to find launch operations and orbital support cost. For launch without the use of AKM, the cost per satellite is

$$LOOSC = 2.51M_{sat} \tag{A.87}$$

For launch with AKM, the cost per satellite is

$$LOOSC = 64 + 1.44M_{sat} \tag{A.88}$$

The total cost of all satellite units is

$$LOOSC_{tot} = LOOSC \times N_{sat} \times 1.369 \tag{A.89}$$

Step 8 finds flight software cost by scaling the thousand lines of code, assuming Ada source code is used.

$$C_{FS} = 375 \times FSKLOC \times 1.369 \tag{A.90}$$

Step 9 account for the minimum launch cost found in the launch vehicle module.

$$C_{LV} = C_{launch\ min} \tag{A.91}$$

Step 10 finds ground software cost assuming the language used is Unix-C.

$$C_{GS} = 190 \times GSKLOC \times 1.369 \tag{A.92}$$

Step 11 is to find total ground segment development cost, which is consisted of costs of all the gateways and two command centers. SMAD suggests that the cost of developing a gateway (or ground station) has a breakdown as listed in Table A.3.

Ground Station Element	Development Cost as Percent of Software Cost (%)
Facilities (FAC)	18
Equipment (EQ)	81
Software (SW)	100
Logistics	15
System level	
Management	18
Systems engineering	30
Product assurance	15
Integration and test	24

Table A.3: Ground segment development cost distribution

So the ground station development cost is simply

$$GSDC = (18 + 81 + 100 + 15 + 18 + 30 + 15 + 24)\% \times C_{GS} \tag{A.93}$$

In addition to gateways, the system also needs command centers to control network and satellite operations. Two command centers are assumed for the system. The command center cost (CCC) is the average of seven actual systems' command center costs drawn from their FCC filings. These seven systems are @contact, ARIES,

GEMnet, Globalstar, Orbcomm, Starnet, and VITA. The average cost is 11.856 million USD. Therefore the total ground segment development cost is the sum of the costs of all the gateways and two command centers.

$$GSDC_{tot} = N_{GW} \times GSDC + 2 \times CCC \tag{A.94}$$

Step 12 is to find initial development cost (IDC), which is the cost up to the onset of the service of the system. To get IDC, we need to sum up all the costs we have calculated previously.

$$\begin{aligned} IDC &= RDTEHC + \textstyle\sum_{i=1}^{size\ of\ UHC} \mathbf{UHC}_i + AGEC + PLC_{tot} \\ &\quad + LOOSC_{tot} + C_{FS} + GSDC_{tot} + C_{LV} \end{aligned} \tag{A.95}$$

In order to find the present value of the cost, a cost distribution over development time needs to be modelled first. To be clear, the life-cycle of the system consists of two stages. The first stage is the initial development time (IDT) that starts with the RDT&E stage of the system and extends till the deployment of the entire system. The second stage is the space segment life, which starts with the completion of system deployment and onset of service, and lasts until the end life of the satellites. In step 13, we look at the cost distribution in IDT. SMAD suggests the cost spreading by a function of the form

$$\begin{aligned} F(S) &= A[10 + S((15 - 4S)S - 20]S^2 + B[10 + S(6S - 15)]S^3 \\ &\quad + [1 - (A + B)](5 - 4S)S^4 \end{aligned} \tag{A.96}$$

where $F(S)$ is the fraction of cost consumed in time S, S is the fraction of the total time elapsed, and A and B are empirical coefficients. Coefficients A and B depend on percentage of expenditure at schedule midpoint. For project involving more than two satellites, 50% expenditure at schedule midpoint is suggested, and the corresponding A and B are 0 and 1.00. Using these values, it is easy to find the cost per year for

each year during the IDT. These values are stored in array $\mathbf{C_{year}}$. As mentioned above, we assume the IDT to be a constant of 5 years.

Step 14 gives operation and support cost per year during space segment lifetime. The yearly maintenance cost per gateway is

$$C_{maint} = 0.1 \times (SW + EQ + FAC)/year \tag{A.97}$$

For personnel cost, contractor labor is estimated to cost \$140K/staff year. The calculation is based on the assumption that 300 staff members are necessary in keeping the business running, in addition to the personnel at the gateways. Summing the maintenance and personnel costs, the total operation and support cost per year is

$$C_{OS\ per\ year} = C_{maint} \times N_{GW} + 140(N_{personnel} + 300) \tag{A.98}$$

In step 15, $C_{OS\ per\ year}$ is distributed over space segment lifetime. Because the maintenance and personnel costs are assumed to be constant throughout the years, we simply assign the value of $C_{OS\ per\ year}$ to each year in the space segment lifetime. Combining the initial deployment cost and the maintenance cost, C_{year} covers the entire life-cycle of the system.

$$C_{tot} = \sum_{i=1}^{size\ of\ C_{year}} \mathbf{C_{year}}_i \tag{A.99}$$

The value of the total cost thus obtained is the accounting cost of the entire system throughout its lifetime. It is returned to `SM.m` as the life-cycle cost.

A.9 Market Module (MM)

MM estimates the number of subscribers to the service provided by the satellite system per year, the total air time of the system, and the total amount of data transmitted throughout the system's lifetime. These are the outputs of the module. The inputs of the module are number of users supported per satellite, number of satellites in the system, footprint area, initial development time, space life of the

system, and data rate per user.

The first part of the module is to model the total global potential user (GPU_{tot}) throughout the space lifetime of the system. The global potential users are assumed to be distributed over the land area of the earth evenly for reasons explained shortly later in the same section. The number of potential user per unit area adds an upper bound to the number of subscribers to the system per unit area. The year 2004 is taken as the onset of the development of the system. The global potential user (GPU) in the first year of the service (in millions of subscribers) is

$$CPU_{1st\ year} = A + B(IDT + 1) \tag{A.100}$$

where A is the number of subscribers in 2003, B is the yearly increment of subscribers, IDT is the initial development time, and $IDT + 1$ is the first year of service. If we assume that the yearly increment in subscribers is constant, then the number of total potential users in the last year of the service is

$$CPU_{last\ year} = CPU_{1st\ year} + B(Life_{space} - 1) \tag{A.101}$$

The total number of global potential users throughout the lifetime of the system is

$$CPU_{tot} = (CPU_{1st\ year} + CPU_{last\ year})Life_{space}/2 \tag{A.102}$$

For this study, we model the market for both low-bandwidth satellite system and high-bandwidth system. If the user data rate is lower than 50 kbps, then the system is considered as a low-bandwidth system; otherwise, it is a high-bandwidth system. The market data for low-bandwidth system is based on the data provided in the FCC filing of Globalstar, which is also a low-bandwidth system. Market projection for high bandwidth satellite service is provided by Pioneer Consulting. The values of A and B for the two types of systems are listed in Table A.4.

It deserves notice that methodologies for doing probabilistic demand modelling are provided by Mathieu Chaize's S.M. thesis at MIT[Cha03].

	A (Million potential subscribers in 2003)	B (Yearly increment of million potential subscribers)
Low-bandwidth system	49.60	2.97
High-bandwidth system	4.92	0.52

Table A.4: Market projections for low-bandwidth and high-bandwidth systems

Earth land area is 148.326 million square kilometers. It is assumed that the potential users are distributed evenly over the land area indiscriminant of developed or developing regions. The reasoning for an even distribution is that in developed regions, although more people can afford the service, a small percentage of these people have an incentive to subscribe to satellite service because the terrestrial system has been in place; in developing or under-developed regions, although fewer people can afford the service, a large percentage of these people have an incentive to purchase the service because terrestrial system has not been in place to provide competitive service. So the number of potential subscribers per square kilometer is

$$N_{PU/km^2} = \frac{GPU_{tot}}{earth\ land\ area} \tag{A.103}$$

The satellite capacity is evenly distributed over the entire earth surface. Earth surface area is $4\pi R_e^2$. So the number of subscribers per square kilometer supportable by the satellites throughout its lifetime is

$$N_{capacity/km^2} = \frac{N_{user} N_{sat} Life_{space}}{earth\ land\ area} \tag{A.104}$$

The number of actual subscribers per square kilometer throughout the satellite lifetime is the smaller of the two

$$N_{subscribers/km^2} = \min(N_{PU/km^2}, N_{capacity/km^2}) \tag{A.105}$$

The total number of subscribers of the system throughout its lifetime is

$$N_{subscribers} = N_{subscribers/km^2} \times (earth\ land\ area) \tag{A.106}$$

The average number of subscribers per year is

$$N_{subscribers/year} = N_{subscribers}/Life_{space} \tag{A.107}$$

If each subscriber is assumed to use the service one hour everyday, 365 days a year, then the total air time throughout the system lifetime (in minutes) is

$$T_{air\ tot} = N_{subscribers}\left(365\frac{\text{year}}{\text{day}}\right)\left(24\frac{\text{hours}}{\text{day}}\right)\left(60\frac{\text{minutes}}{\text{hour}}\right) \tag{A.108}$$

Total data flow throughout the system lifetime (in MB) is

$$R_{tot} = T_{air\ tot}\left(60\frac{\text{seconds}}{\text{minute}}\right)R_{user}/1000 \tag{A.109}$$

This module returns the values of average number of subscribers per year, total air time, and total data flow to SF.

A.10 Output Assignment and Postprocessing

The market module is the last module in the model. After the execution of the market module, we are back in the nested for-loops. The last step in the for-loops is to assign the values of the objectives to the objective vector **J**, the benchmarking parameters to **B**, and requirements to **r**. This concludes the nested for-loop.

The post-processing is carried out at the end of SF. It involves finding the Pareto front and the utopia point of the objective space. These two attributes of the trade space exploration will be introduced in the trade space exploration and optimization section below. Before we explore the trade space, benchmarking should be performed to prove the fidelity of the model.

Appendix B

Inter-Satellite Link Cost and Mass Breakdown

Appendix B gives the breakdown for the cost and mass of RF inter-satellite (ISL) links and optical inter-satellite links. The information is provided by Yoshisada Koyama at Next-Generation LEO System Research Center (NeLS) in Japan.[Koy02]. The Yen-to-Dollar exchange rate during the time of the interview is adopted, when 1 USD = 118 Yens.

When integrating single ISL unit into four ISL units bundle, the four-unit mass is less than four times of the mass of single unit due to sharing of communication, structure, harness wiring, and other common components by the four units. This reduction is expressed as a reduction factor in the following three tables.

	Development Cost (million Yen)	First Unit Cost (million Yen)	Development Cost (million USD)	First Unit Cost (million USD)
30 Mbps RF ISL cost per link	1,600	870	13.56	7.37
300 Mbps RF ISL cost per link	1,700	920	14.41	7.80
Optical ISL cost per link	3,000	2,000	25.42	16.95
30 Mbps RF ISL cost for 4 links	1,600	3,480	13.56	29.49
300 Mbps RF ISL cost for 4 links	1,700	3,680	14.41	31.19
Optical ISL cost for 4 links	3,000	8,000	25.42	67.80

Table B.1: Cost of RF ISL and optical ISL in Japanese and US currencies

	30 Mbps RF ISL per unit (kg)	No. of units	Reduction factor	30 Mbps RF ISL four unit (kg)
Common components	38.00	4	0.80	121.60
Antenna components	37.00	4	1.00	148.00
Structure	50.00	4	0.50	100.00
Wire harness, etc.	20.00	4	0.70	56.00
Total	145.00	4		426.00

Table B.2: Mass breakdown of 30 Mbps RF ISL

	300 Mbps RF ISL per unit (kg)	No. of units	Reduction factor	300 Mbps RF ISL four unit (kg)
Common components	45.00	4	0.80	144.60
Antenna components	45.00	4	1.00	180.00
Structure	50.00	4	0.50	100.00
Wire harness, etc.	20.00	4	0.70	56.00
Total	160.00	4		480.00

Table B.3: Mass breakdown of 300 Mbps RF ISL

	Optical RF ISL per unit (kg)	No. of units	Reduction factor	Optical ISL four unit (kg)
Common components				
Antenna components				
Structure				
Wire harness, etc.				
Total	40.00	4		117.00

Table B.4: Mass breakdown of Optical ISL (The blank cells represent classified information.)

Appendix C

Basic Capacity Calculation Methods and Benchmarking for MF-TDMA and MF-CDMA Communication Satellites (AIAA-2003-2277)

Abstract

This paper introduces basic capacity calculation methods for circuit switched, multiple-beam, low earth orbit (LEO) communication satellites that use MF-TDMA and MF-CDMA schemes. Capacity means the number of simultaneous duplex channels that a satellite can support. This paper integrates the bandwidth limit and the power limit on capacity, and derives the equations by which the capacity of a MF-TDMA or a MF-CDMA system can be calculated using key system parameters. Therefore, these methods enable system designers to quickly estimate the communication system capacity when key system parameters are known. The paper uses the Iridium and Globalstar for benchmarking by comparing the results obtained from the methods with the 1,100 simultaneous channels and 2,500 channels satellite capacity claimed respectively by Iridium and Globalstar.

Nomenclature

α	Expected value of voice activity state
B_g	Guard bandwidth
B_{sat}	Satellite frequency bandwidth
B_T	TDMA carrier bandwidth
f	Transmission frequency or neighboring cell interference factor
F	MF-TDMA framing bits
G_t	Transmitter gain
G_r	Receiver gain
k	Boltzmann's constant
K	Cluster size
L_{tot}	Total loss in link budget
n	Number of bits per time slot in MF-TDMA
N_c	Number of simultaneous channels a satellite supports in a cell
R_b	TDMA carrier data rate in MF-TDMA or channel information data rate in MF-CDMA (b/s)
T	Number of TDMA carriers in MF-TDMA or CDMA carriers in MF-CDMA
T_f	MF-TDMA time frame duration (second)
T_g	MF-TDMA guard time (second)
T_s	System noise temperature
Z	Number of cells in a satellite's footprint

C.1 Introduction

Low earth orbit (LEO) communication systems are generally defined as the communication satellite systems that orbit the Earth at an altitude of 500-1500 km and provide wireless communication between terminals on the ground. The system typically consists of multiple satellites forming a polar or Walker constellation. Some of these systems have inter-satellite links and on-board processing that allow transmission between neighboring satellites in the constellation, while other systems act as "bent pipes" that simply "bounce" the transmission between different

ground users.

User capacity of a LEO communication system is the number of simultaneous duplex channels that the system can support. To maintain multiple simultaneous channels, two physical limits must be overcome: the bandwidth limit and the power limit, of which two the lower one will constrain the capacity. To overcome the bandwidth limit, frequency-division multiple access (FDMA), time-division multiple access (TDMA), or code-division multiple access (CDMA) is implemented. Based on these basic schemes, more sophisticated multiple-frequency time-division multiple access (MF-TDMA) and multiple-frequency code-division multiple access (MF-CDMA) are applied to increase the satellite capacity within a limited frequency bandwidth. To overcome the power limit, higher transmitter power and antennas with higher gain are used, as well as more robust coding scheme.

This paper will first exam both the bandwidth limit and power limit. Then for each of a MF-TDMA and MF-CDMA satellite communication system, it attempts to integrate the two limits into one single equation that gives the capacity of the system. At the end, the results obtained from the equations will be benchmarked against the real Iridium system and Globalstar system.

C.2 Overview of the Bandwidth Limit

This section will exam the MF-TDMA and MF-CDMA schemes. It is partially based on the work by Lutz, Werner, and Jahn[LWJ00].

C.2.1 Frequency Band Utilization

Let R_b denote the bit data rate of a digital signal per channel, and M denote the signal modulation level. The receiver is assumed to use Nyquist filtering to avoid inter-symbol interference (ISI), and β is the filter roll-off factor, normally ranging from 0.2 to 0.5. Then, the channel bandwidth required by the Nyquist-filtered signal is

$$B_{ch} = \frac{(1+\beta)R_b}{\log_2 M} \tag{C.1}$$

where B_{ch} is in Hz and R_b in b/s.

C.2.2 FDMA Capacity

In the U.S., the frequency band for a system is assigned by the Federal Communication Commission (FCC). In FDMA, the assigned frequency band, B_c, is divided into channel bands of width B_{ch}. This division typically happens inside a radio cell and between neighboring radio cells. We will discuss spot beams in the *Capacity When Using Spot Beams* section. These channel bands are separated from each other by guard bands B_g, as illustrated in Figure C-1. The number of FDMA channels that can be supported, N, can be calculated based on Equation C.1 as

$$N = \frac{B_c}{B_{ch} + B_g} = \frac{B_c}{R_b} \cdot \frac{\log_2 M}{1 + \beta + \log_2 M \cdot B_g / R_b} \tag{C.2}$$

where R_b is the data rate per FDMA channel, and B_c, B_{ch}, and B_g are in Hz.

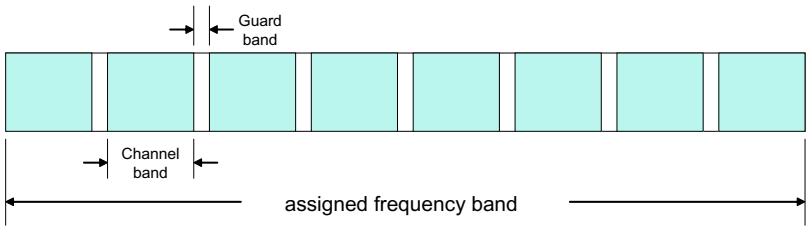

Figure C-1: Frequency division multiple access (FDMA) scheme

C.2.3 TDMA and MF-TDMA Capacity

In TDMA, access time is divided into frames, and frames are again divided into time slots. A basic channel is formed by a particular time slot inside every frame. In the forward link (satellite-to-user downlink) and return link (user-to-satellite uplink), usually the same frame structure is used. In order to avoid simultaneous transmission and reception of a user, the corresponding time slots for the forward and return links are separated in time. The TDMA scheme is illustrated in Figure C-2.

To find the number of TDMA channels, n_f, for a given bandwidth, we first start with the frame duration, T_f, in seconds and the allowed

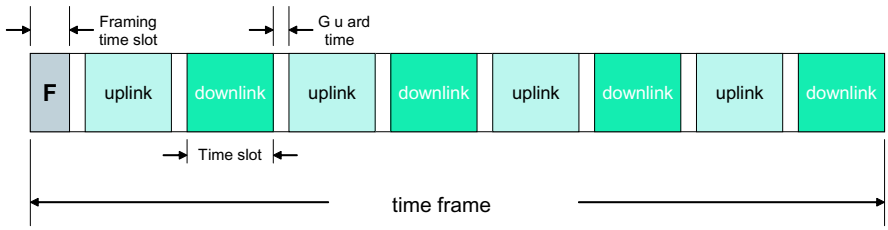

Figure C-2: Time division multiple access (TDMA) scheme

burst rate for each TDMA carrier R_b in b/s, then

$$n_f = R_b T_f \tag{C.3}$$

gives the number of bits within each frame. If the duration of a time slot is T_{slot} in seconds, then n, the number of bits per time slot, is

$$n = R_b T_{slot} \tag{C.4}$$

If each time slot begins with a header of H bits for the purpose of synchronization, and a guard time of T_g seconds is inserted between every two time slots, then the relationship between R_b and the number of half duplex channels per frame N_{hd} is

$$R_b = N_{hd} \frac{H + n}{T_f - N_{hd} T_g} \tag{C.5}$$

where R_b is in b/s.

If we assume that instead of the header, a certain number of framing bits F are added at the beginning of each frame, then Equation C.5 becomes

$$R_b = \frac{F + N_{hd} n}{T_f - N_{hd} T_g} \tag{C.6}$$

To find the number of TDMA channels for a given burst rate, we solve Equation C.5 to get

$$N_{hd} = \frac{R_b T_f}{H + n + R_b T_g} \tag{C.7}$$

If framing bits are used, we solve Equation C.6 to get

$$N_{hd} = \frac{R_b T_f - F}{n + R_b T_g} \tag{C.8}$$

The number of full duplex TDMA channels is

$$N = N_{hd}/2 \tag{C.9}$$

In *MF-TDMA*, multiple TDMA carriers at different frequency channels are used to increase the total number of channels, as illustrated in Figure C-3. In the frequency domain, the bandwidth, B_T, occupied by a TDMA carrier can be obtained from Equation C.1:

$$B_T = \frac{(1+\beta)R_b}{\log_2 M} \tag{C.10}$$

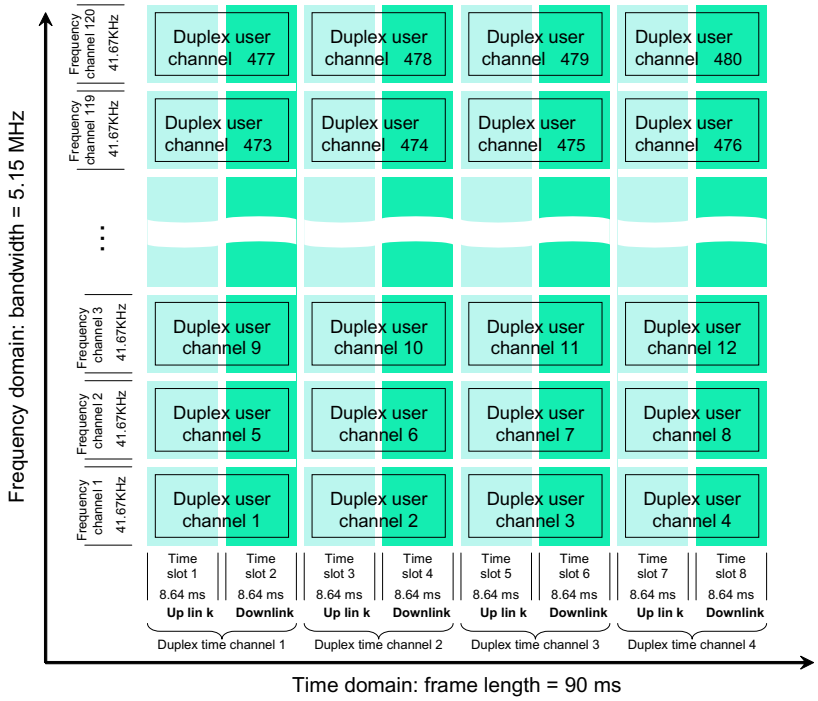

Figure C-3: Multiple frequency-time division multiple access (MF-TDMA) for Iridium

The carriers are separated by guard bands B_g. Therefore, the total bandwidth required to support T TDMA channels is

$$B = T(B_T + B_g) \tag{C.11}$$

The number of active duplex MF-TDMA channels for bandwidth B can be evaluated using Equation C.8, Equation C.10, and Equation C.11

as

$$N_B = T \cdot N = \frac{1}{2} \frac{B}{B_T + B_g} \frac{R_b T_f - F}{n + R_b T_g} \tag{C.12}$$

C.2.4 CDMA and MF-CDMA Capacity

Using a unique pseudorandom noise (PN) code, CDMA transmitting station spreads the signal in a bandwidth wider than actually needed. Each authorized receiving station must have the identical PN code to retrieve the information. Other channels may operate simultaneously within the same frequency spectrum as long as different, orthogonal codes are used. The theory of CDMA technology is illustrated in Figure C-4.

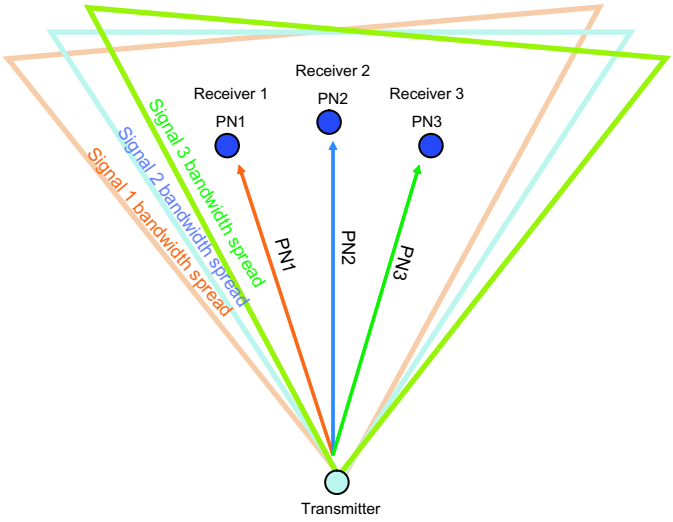

Figure C-4: Code division multiple access (CDMA) scheme

The long PN code is called a *chip*. The chip is modulated by the information data stream. The ratio of the chip rate R_c to the information data rate R_b is called the *processing gain* G.

$$G = \frac{R_c}{R_b} \tag{C.13}$$

Because the CDMA carrier bandwidth $B_T = R_c$, processing gain can also be expressed as

$$G = \frac{B_T}{R_b} \tag{C.14}$$

Then, if E_b is the average bit energy of any channel's signal, the power spectral density of the transmit signal (energy per chip) is

$$E_b R_b / R_c = E_b / G \tag{C.15}$$

By using the PN code, CDMA overcomes the bandwidth limit. But there is still the problem of interference between channels. To find the maximum number of active channels allowed by the system, we do the following derivation.

In typical CDMA technology, when speech pauses, the transmit signal is switched off to save power. The voice activity state of channel n is denoted $a_n \in \{0; 1\}$, and the expected value $E\{a_n\} = a \approx 0.5$. Let's define $\bar{I}_i$ to be the mean value of the power spectral density of the interference noise caused by other channels. Because there are N channels in total, there are $N-1$ channels other than the channel under consideration. Based on Equation C.15,

$$\bar{I}_i = \alpha(N-1)E_b/G \tag{C.16}$$

If N_0 stands for the thermal noise of the system, then the mean total noise power spectral density I_{tot} is the sum of interference noise and thermal noise,

$$I_{tot} = \bar{I}_i + N_0 = \alpha(N-1)E_b/G + N_0 \tag{C.17}$$

We can derive the number of total channels N from Equation C.17 to be

$$N = 1 + \frac{G}{\alpha}\left[\left(\frac{E_b}{I_{tot}}\right)^{-1} - \left(\frac{E_b}{N_0}\right)^{-1}\right] \tag{C.18}$$

If we assume the modulation uses BPSK or QPSK, and the required bit error probability is p_b, we can express the ratio of the bit energy to total noise power spectral density E_b/I_{tot} as

$$\frac{E_b}{I_{tot}} = \left[\mathrm{erfc}^{-1}\left(2p_\mathrm{b}\right)\right]^2 \tag{C.19}$$

In real application, because convolutional coding is used, the actual required value for E_b/I_{tot} is lower than what is given by Equation C.19. This will be covered in the *Convolutional Coding* section. We can

find E_b/N_0 from the link budget equation. This will be covered in the *Overcome the Power Limit* section. Combining Equation C.14 and Equation C.18, we obtain the expression for the number of CDMA channels:

$$N = 1 + \frac{B_T}{R_b}\frac{1}{\alpha}\left[\left(\frac{E_b}{I_{tot}}\right)^{-1} - \left(\frac{E_b}{N_0}\right)^{-1}\right] \tag{C.20}$$

In *MF-CDMA*, multiple CDMA carriers at different frequencies are used to increase the number of channels. In the frequency spectrum, the carriers are separated by guard bands, B_g. If T CDMA carriers are used, the total required bandwidth is

$$B = T(B_T + B_g) = T(GR_b + B_g) \tag{C.21}$$

The total number of channels for bandwidth B will be

$$N_B = T \cdot N \tag{C.22}$$

Combining Equation C.20, Equation C.21, and Equation C.22, we get the following expression that gives the total number of CDMA channels for the given frequency bandwidth B:

$$N_B = T \cdot N = T + \frac{B - TB_g}{R_b}\frac{1}{\alpha}\left[\left(\frac{E_b}{I_{tot}}\right)^{-1} - \left(\frac{E_b}{N_0}\right)^{-1}\right] \tag{C.23}$$

C.2.5 Capacity When Using Spot Beams

A LEO communication satellite typically concentrates its transmission power in multiple spot beams. Each spot beam covers a cell on the ground, and all the cells together form the footprint of the satellite. The spot beam contour is usually defined by a 3-dB decrease of antenna gain relative to the peak gain. The usage of spot beams will offer two advantages: 1. Focusing transmitted power on a much smaller area than the total coverage area of the satellite, spot beams increase the transmitter gain and therefore improve the link budget. 2. The reuse of frequency bands in different cells improves bandwidth efficiency. We will focus on the second advantage in this section and leave the first to be discussed in the *Overcome the Power Limit* section.

The number of frequency bands used in the cells of a satellite is

called *cluster size*, designated by K. For FDMA and TDMA, typical values of the cluster size are $K = 4$ or 7. For CDMA, a cluster size of $K = 1$ can be used because all channels can operate simultaneously within the same frequency band. The Iridium system has totally 48 spot beams with a cluster size of 12, as illustrated in Figure C-5.

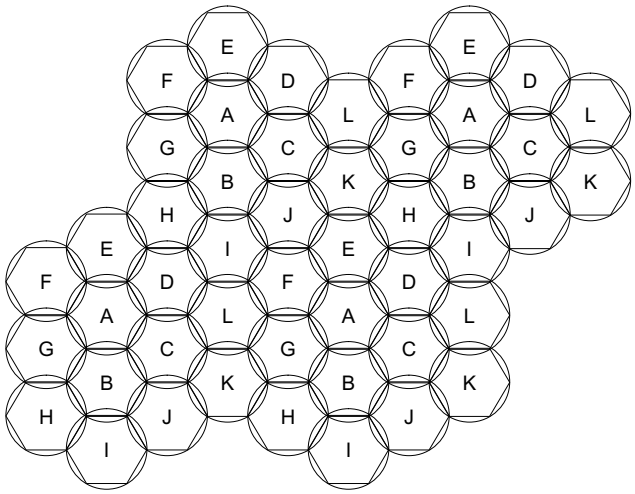

Figure C-5: Footprint pattern of Iridium

Let A_s be the service area, which is equal to the area of the footprint. Let A_c be the cell area, then the number of cells is

$$Z = A_s / A_c \tag{C.24}$$

Next we will look at how the capacities of MF-TDMA and MF-CDMA are affected by the use of spot beams.

1. Capacity of MF-TDMA When Using Spot Beams:

If the bandwidth available for one satellite is B_{sat}, then the cell bandwidth is

$$B_c = B_{sat} / K \tag{C.25}$$

Replacing B in Equation C.12 with the expression for B_c in Equation C.25, we get number of channels per cell to be

$$N_c = T \cdot N = \frac{1}{2K} \frac{B_{sat}}{B_T + B_g} \frac{R_b T_f - F}{n + R_b T_g} \tag{C.26}$$

The number of channels per satellite is

$$N_{sat} = Z \cdot N_c = \frac{Z}{2K} \frac{B_{sat}}{B_T + B_g} \frac{R_b T_f - F}{n + R_b T_g} \tag{C.27}$$

2. Capacity of MF-CDMA When Using Spot Beams:

In CDMA, we set cluster size $K = 1$ because all the cells have an identical frequency band. Therefore $B_c = Bsat$. Based on Equation C.23, the number of channels per cell is

$$N_c = T + \frac{B_{sat} - TB_g}{R_b} \frac{1}{\alpha(1+f)} \cdot \left[\left(\frac{E_b}{I_{tot}} \right)^{-1} - \left(\frac{E_b}{N_0} \right)^{-1} \right] \tag{C.28}$$

And the capacity of the satellite is

$$N_{sat} \;=\; Z \cdot N_c \tag{C.29}$$

where the factor $(1+f)$ represents the increase in interference caused by the users in neighboring cells. A lower bound value for f is 1.36[LWJ00].

C.2.6 Capacity of the Entire Constellation

For a global coverage satellite constellation consisting of S satellites, if the constellation is a Walker constellation, then the total number of channels that can be used at any time is simply

$$N_s = SN_{sat} \tag{C.30}$$

But if the constellation is of polar type, the overlapping cells at the poles will reduce the total capacity to

$$N_s = 0.68SN_{sat} \tag{C.31}$$

C.3 Overcoming the Power Limit

The power limit problem has been worked out in numerous literatures, such as those by Larson and Wertz[LW92] and by Gordon and Morgan[GM93]. The authors takes the pain to reiterate it for a complete and consistent derivation for the final capacity equations.

C.3.1 Link Budget

The link budget is important in estimating the capacity of a LEO communication satellite system. To find physical parameters of the transmission such as data rate or E_b/N_0, a series of factors must be accounted for along the transmission path, including transmitter power, transmitter gain, space loss, atmosphere attenuation, system noise temperature, receiver gain, and other losses. In this section, we will briefly consider each of these factors.

Because the satellite power needs to be divided among all simultaneous channels in the satellite-user forward link, the satellite-user link is generally considered as the bottleneck of the network. Therefore we consider the satellite-user link budget problem. First, the transmitter power of a satellite needs to be divided among all its cells. In the MF-TDMA scheme, the power of each cell is further divided among all the TDMA carriers. In MF-CDMA scheme, the power of each cell is divided among all CDMA channels.

If the transmitter operates at frequency f_{GHz} in GHz, and D is either the diameter in meter of a parabolic antenna transmitter or the side length of a phased-array antenna, then the transmitter half power beamwidth θ in degree can be calculated as

$$\theta = \frac{21}{f_{GHz} D} \tag{C.32}$$

If η_t is the transmitter efficiency, and θ_x and θ_y are the beamwidths of a parabolic antenna on the major and minor axes, or of a phased-array antenna on the long side and short side, then the transmitter gain can be estimated in dB as

$$G_{t\,dB} \approx 46.9 + 10\log(\eta_t) - 10\log(\theta_x \theta_y) \tag{C.33}$$

Let λ be the signal wavelength in m, d be the path length in m, c be the speed of light, and f be the transmission frequency in Hz. Space loss of the transmission L_s is

$$L_s = (\lambda/4\pi d)^2 = (c/4\pi df)^2 \tag{C.34}$$

In dB, $L_{s\,dB}$ is

$$L_{s\,dB} = 147.55 - 20\log d - 20\log f \tag{C.35}$$

Rain and atmosphere attenuation loss, L_a, can be calculated following a complex procedure listed in International Telecommunication Union ITU-R Recommendations[EE00]. Because it is not the purpose of this paper, the procedure is omitted. We will just approximate the atmosphere loss to be -0.2dB.

The gain of the receiver antenna can be obtained in the same way as the gain of the transmitter antenna. But in practice, the antennas of the user terminals of Iridium and Globalstar are of the omni-directional type, with a theoretical gain of 1 (0 dB).

System noise temperatures in satellite communication links in clear weather have been estimated[LW92]. The results are listed in Table 4.2.

Next we consider other possible losses along the link. The line loss between transmitter and antenna in dB is represented by $L_{l\,dB}$, with a typical value of -1 dB. The pointing offset loss of the transmitter in dB is estimated as

$$L_{offset\,dB\,t} = -12(e_t/\theta_t)^2 \tag{C.36}$$

where e_t is the transmitter pointing error, and θ_t is the transmitter antenna beamwidth. For a phased-array antenna utilizing spot beams, the pointing offset loss is negligible.

Polarization mismatch, L_{polar}, adds about -0.3 dB to the link budget, and a loss caused by a radome, L_{rad}, approximates -1 dB. If we also include an implementation loss, $L_{imp\,dB}$, of -1 dB, then the total loss along the path (< 0) is

$$\begin{aligned} L_{tot\,dB} \;=\; & L_{ldB} + L_{offset\,dB} + L_{s\,dB} \\ & + L_{a\,dB} + L_{polar\,dB} \\ & + L_{rad\,dB} + L_{imp\,dB} \end{aligned} \tag{C.37}$$

Besides the losses mentioned above, the signal attenuates due to two additional reasons: shadowing and multipath fading. Shadowing is caused by obstacles in the path that blocks the transmission, for example, terrains, buildings, and natural plantations. Multipath fading is caused by the interference of the echoes that the signal reflects off the

environment. To compensate these losses, some extra budget must be given to the link, and this extra budget is called the *link margin*. For example, the Iridium downlink has a required link margin of 16dB.

After the power, aperture gains, losses, system noise, and margin are defined, the link budget equation becomes a trade-off between the transmission data rate $R_{b\,dB}$ and energy per bit to noise ratio E_b/N_0. The link budget equation, in defining E_b/N_0, is

$$\begin{aligned} E_b/N_{0dB} &= Power_{dB} + G_{t\,dB} + G_{r\,dB} \\ &\quad -k_{dB} - T_{s\,dB} - R_{b\,dB} + L_{tot\,dB} \\ &\quad -margin \end{aligned} \tag{C.38}$$

where $E_b/N_{0\,dB}$ is in dBs^{-1}, $R_{b\,dB}$ in dBb/s, and k, the Boltzmann constant, is $1.38 \cdot 10^{-23} Ws/K = -288.6$ dBWs/K.

C.3.2 Convolutional Coding

Redundancy coded into transmitted information reduces the transmit power required for a specific bit error probability. This reduction process has two important parameters, code rate r and constraint length K. Code rate r is defined by the ratio between the original information bits k and the coded content bits n,

$$R_c = k/n. \tag{C.39}$$

The bit energy to mean total noise power spectral density ratio E_b/I_{tot} corresponding to several bit error probabilities, p_b, for soft-decision Viterbi decoding are listed in Table A.1.

C.4 Combining Bandwidth Limit And Power Limit

With the previous two sections paving the way, in this section we will integrate the power limit and bandwidth limit into one single equation.

C.4.1 MF-TDMA

For MF-TDMA, equation Equation C.38 can also be written as

$$\begin{aligned} R_{b\,dB} &= Power_{dB} + G_{t\,dB} + G_{r\,dB} \\ &\quad -k_{dB} - T_{s\,dB} - E_b/N_{0_{dB}} + L_{tot\,dB} \\ &\quad -margin \end{aligned} \tag{C.40}$$

Notice that if $Power_{dB}$ is the power per TDMA carrier, then $R_{b\,dB}$ is the data rate of each TDMA carrier. Substituting for R_b in Equation C.26 with the $R_{b\,dB}$ in Equation C.40 (after $R_{b\,dB}$ converted to unit in b/s), equation Equation C.26 will give the number of channels per cell. For the same reason, equation Equation C.27 will give the number of channels per satellite, taking into account both the available power and bandwidth.

C.4.2 MF-CDMA

In MF-CDMA, the transmitter power of the satellite is divided among all cells, and the power in a cell is further divided among all CDMA channels in the cell. If $Power_{cell}$ is the transmitter power per cell and N_c is the number of channels per cell, the link budget of a CDMA downlink becomes

$$\begin{aligned} E_b/N_{0_{dB}} &= (Power_{cell}/N_c)_{dB} + G_{t\,dB} \\ &\quad +G_{r\,dB} - k_{dB} - T_{s\,dB} \\ &\quad -R_{b\,dB} + L_{tot\,dB} - margin \end{aligned} \tag{C.41}$$

If we use original units instead of decibel units, equation Equation C.41 can be re-written as

$$E_b/N_0 = \frac{Power_{cell} \cdot G_t \cdot G_r \cdot L_{tot}}{N_c \cdot k \cdot T_s \cdot R_b \cdot margin} \tag{C.42}$$

To find the cell capacity, we substitute Equation C.42 into Equation C.28 and solve for N_c. We get

$$N_c = \left[T + \frac{B_{sat} - TB_g}{R_b}\frac{1}{\alpha(1+f)}\frac{I_{tot}}{E_b}\right] / \left[1 + \frac{B_{sat} - TB_g}{R_b}\frac{1}{\alpha(1+f)}\cdot \frac{k \cdot T_s \cdot R_b \cdot margin}{Power_{cell} \cdot G_t \cdot G_r \cdot L_{tot}}\right] \quad \text{(C.43)}$$

The capacity of the satellite follows as $N_{sat} = Z \cdot N_c$.

C.5 Benchmarking Against Existing Systems

In order to verify predictive accuracies of the capacity equations developed above, we benchmark them against the existing systems of Iridium and Globalstar. To do so, we find public available data on the design parameters of these two systems, and substitute them into the equations. A comparison between the results from these equations and the capacities claimed by the companies will suggest how accurate these equations are.

C.5.1 Benchmarking MF-TDMA against Iridium

Built and launched by Motorola, and now owned and operated by Iridium LLC, Iridium is one of the first generation global LEO systems for telephony. Iridium constellation consists of 66 satellites orbiting at an altitude of 780km. The constellation type is polar, with 6 orbital planes at an inclination of 86.4^o. Iridium is chosen for the benchmarking because it is the most mature LEO communication system that uses MF-TDMA technology. Iridium's key technical specifications are known from various sources. They are listed in Table 1.3. Note that the right column provides more updated information than the left column. The difference is due to the fact that the FCC assigned only half of the requested frequency band to Iridium.

Because the gain of the Iridium antenna in an edge cell is given[Nel99], we will use the edge cells to estimate the channel capacity per cell, and

multiply this cell capacity with the number of cells to get the capacity of a satellite. The beamwidth of the edge cell spot beam is about 13.4^o, estimated based on the transmitter gain in that cell. Using the beamwidth, minimum elevation angle, and orbital altitude, the distance from the satellite to the center of the edge cell is calculated to be 1606.9km. The calculation of the distance, d, is based on basic planar geometry.

According to Equation C.35, the space loss is

$$\begin{aligned} L_{s\,dB} &= 147.55 - 20\log d - 20\log f \\ &= 147.55dB - 20\log(1.6069 \cdot 10^6 m) \\ &\quad -20\log(1.6239 \cdot 10^9 Hz) \\ &= -160.78dB \end{aligned} \tag{C.44}$$

The total loss along the path, as in Equation C.36, is

$$\begin{aligned} L_{tot\,dB} &= L_{ldB} + L_{offset\,dB} + L_{s\,dB} \\ &\quad +L_{a\,dB} + L_{polar\,dB} + L_{rad\,dB} \\ &\quad +L_{imp\,dB} \\ &= -1dB - 0dB - 160.78dB \\ &\quad -0.2dB - 0.3dB - 1dB - 1dB \\ &= -164.28dB \end{aligned} \tag{C.45}$$

As listed in Table 1.3, for the Iridium system the convolutional coding code rate is R_c=3/4, and the constraint length is K=6. In order to achieve a bit error probability of $p_b = 10^{-3}$, E_b/I_{tot} must be 2.6dB-b^{-1} according to Table A.1.

As mentioned above, the gain of Iridium and Globalstar's omnidirectional user terminal antenna is 0dB. The transmitter power is first distributed among 48 cells, and then distributed again among the 10 TDMA carriers in the cell. T_{sdB} = 25.7dBK according to Table 4.2. With all the other variables known, equation Equation C.40 gives the

TDMA carrier data rate as

$$\begin{aligned} R_{b\,dB} &= Power_{dB\,TDMA-carrier} + G_{t\,dB} \\ &\quad +G_{r\,dB} - k_{dB} - T_{s\,dB} \\ &\quad -E_b/N_{0_{dB}} + L_{tot\,dB} - margin \\ &= 10 \cdot \log(400/48/10)W + 24.3dB \\ &\quad +0dB + 228.6dBW(Hz \cdot K) \\ &\quad -25.7dBK - 2.6dB - b^{-1} \\ &\quad -164.28dB - 16dB \\ &= 43.53dB - b/s \end{aligned} \tag{C.46}$$

Then $R_b = 22.542$ kb/s. Substitute this value in Equation C.27,

$$\begin{aligned} N_{sat} &= Z \cdot N_c \\ &= \frac{Z}{2K}\frac{B_{sat}}{B_T + B_g}\frac{R_b T_f - F}{n + R_b T_g} \\ &= \frac{48}{2 \times 12} \cdot \frac{5150kHz}{41.67kHz + 1.236kHz} \cdot \\ &\quad \frac{22542b/s \cdot 90 \times 10^{-3}s \cdot \left(1 - \frac{17.28ms}{90ms}\right)}{414b \cdot \left(1 + \frac{3.5}{90-17.28-3.6}\frac{ms}{ms}\right)} \\ &= 904 \end{aligned} \tag{C.47}$$

The actual Iridium system's number of channels is quoted as being power-limited to 1,100[LWJ00]. The estimated capacity is 196 channels, or about 16.3% lower than the reported capacity.

C.5.2 Benchmarking MF-CDMA against Globalstar

A joint effort of Loral Space Systems, Alcatel, and QUALCOMM, Globalstar is another of the first generation global LEO systems for mobile communications. The system consists of 48 satellites, spread over eight orbital planes with six satellites per plane. The constellation type is a 48/8/1 Walker constellation. The orbits are at an altitude of 1,389km and incline at 52^o. Globalstar is probably the most mature commercial MF-CDMA LEO satellite communication system at present time. Its communication parameters are listed in Table 1.6. The right column has more updated information than the left column as the FCC assigned only a portion of the requested frequency band to Globalstar.

But because the 2,500 reported capacity is based on the original frequency band, for the purpose of benchmarking, we will use the data in the left column for our calculations.

The distance from the satellite to the center of the edge cell is calculated to be 1943.9km. The space loss can be obtained from Equation C.35 as

$$\begin{aligned} L_{s\,dB} &= 147.55 - 20\log d - 20\log f \\ &= 147.55dB - 20\log(1.9439 \cdot 10^6 m) \\ &\quad -20\log(2.4918 \cdot 10^9 Hz) \\ &= -166.15dB \end{aligned} \tag{C.48}$$

The total loss along the path is

$$\begin{aligned} L_{tot\,dB} &= L_{ldB} + L_{offset\,dB} + L_{s\,dB} + L_{a\,dB} \\ &\quad + L_{polar\,dB} + L_{rad\,dB} + L_{imp\,dB} \\ &= -1dB - 0dB - 166.15dB - 0.2dB \\ &\quad -0.3dB - 1dB - 1dB \\ &= -169.65dB \end{aligned} \tag{C.49}$$

After converting from decibel, $L_{tot} = 1.0839 \times 10^{-17}$. The E_b/I_{tot} required can be obtained from the rules of convolutional coding. With $R_c = 1/2$ and $K = 9$, the satellite to user transmission with a bit error rate of 0.01 requires an E_b/I_{tot} of $1.18dB - b^{-1}$, or $1.3122b^{-1}$.

According to the data in Table 1.6, Globalstar's power per cell is

$$Power_{cell} = 380W/16 = 23.75W \tag{C.50}$$

To find some of the other values in Equation C.43, we have

$$\begin{aligned} & \frac{B_{sat} - TB_g}{R_b} \frac{1}{\alpha(1+f)} \\ = & \frac{B_{channel}T}{R_b} \frac{1}{\alpha(1+f)} \\ = & \frac{1.23 \times 10^6 Hz \cdot 13}{2400b/s} \frac{1}{0.5(1+1.36)} \\ = & 5646.19b^{-1} \end{aligned} \tag{C.51}$$

Because the downlink frequency of Globalstar is at about 2.5GHz, the

system noise T_{sdB} is at 27.4 dB-K as shown in Table 4.2, or T_s at 549.54K. The link margin of Globalstar is about 6dB on average, therefore

$$\begin{aligned} & \frac{k \cdot T_s \cdot R_b \cdot margin}{Power_{cell} \cdot G_t \cdot G_r \cdot L_{tot}} \\ = & \frac{1.38 \times 10^{-23} Ws/K \times 549.54K \times 2400b/s \times 10^{0.6}}{23.75W \times 50.12 \times 1 \times 1.0839 \times 10^{-17}} \\ = & 0.005616b \end{aligned} \tag{C.52}$$

Plugging the values into Equation C.43, we obtain

$$\begin{aligned} N_c = & \left[T + \frac{B_{sat} - TB_g}{R_b} \frac{1}{\alpha(1+f)} \frac{I_{tot}}{E_b}\right] / \\ & \left[1 + \frac{B_{sat} - TB_g}{R_b} \frac{1}{\alpha(1+f)} \cdot \right. \\ & \left. \frac{k \cdot T_s \cdot R_b \cdot margin}{Power_{cell} \cdot G_t \cdot G_r \cdot L_{tot}}\right] \\ = & \frac{13 + 5646.19b^{-1}/1.3122b^{-1}}{1 + 5646.19b^{-1} \cdot 0.005616b} \\ = & 131.95 \approx 132 \end{aligned} \tag{C.53}$$

$$N_{sat} = Z \cdot N_c = 16 \times 132 = 2112 \tag{C.54}$$

The Globalstar system claims to have a capacity of 2,500 simultaneous channels at the original design point[LWJ00]. The value estimated here is 388 channels, or 15.52% lower than this claimed value.

C.6 Summary

The method proposed above for capacity estimation of MF-TDMA and MF-CDMA satellite communication systems are accurate within 15-16% of reported actual capacities. The merit of this method lies in its simplicity. With the key design parameters known, both the bandwidth limit and power limit are integrated into a single equation that yields the number of simultaneous channels the system can support. A program coded from the equation can be a useful tool for doing system-level

studies. Typically, this kind of study requires the exploration of a large number of conceptually similar but parametrically different designs. A quick way to estimate the capacity of these designs is necessary, otherwise the effort required would inhibit searching a broad design space in a limited time budget. The method answers this necessity. A LEO satellite communication simulator incorporating this method has been used by the authors at MIT for qualitative assessment of technology infusion in satellite communication constellation architectures.[dWCSM03].

Acknowledgments

The authors are grateful for the accommodation and help that Mr. Suzuki Ryutaro and his colleagues at the Communication Research Laboratory (CRL) and the Next-Generation LEO System Research Center (NeLS) in Japan during the summer of 2002. The research was supported by the Sloan Foundation from Fall 2001 to Fall 2002 . The Sloan grant is administered by Prof. Richard de Neufville and Dr. Joel Cutscher-Gershenfeld of the MIT Engineering Systems Division with Mrs. Ann Tremelling as the fiscal administrator. Dr. Gail Pesyna from the Sloan Foundation is serving as the technical monitor.

Appendix D

Inter-Satellite Link Cost and Mass Breakdown

Appendix D gives the breakdown for the cost of digital beam forming (DBF) and analogue beam forming (ABF). The information is provided by Teruaki Orikasa at Communications Research Laboratory (CRL)in Japan.[Koy02]. The Yen-to-Dollar exchange rate during the time of the interview is adopted, when 1 USD = 118 Yens. Figures D-1 and D-2 show the component diagrams of DBF and ABF. Tables D.1 and D.2 give their cost break down.

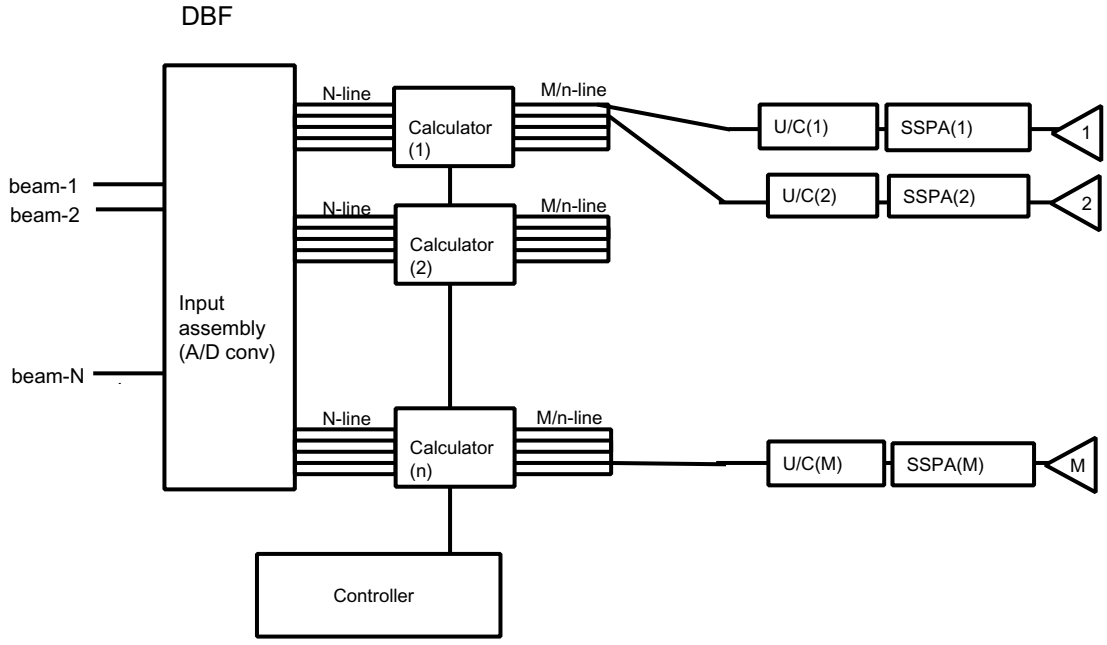

Figure D-1: Component diagram of DBF

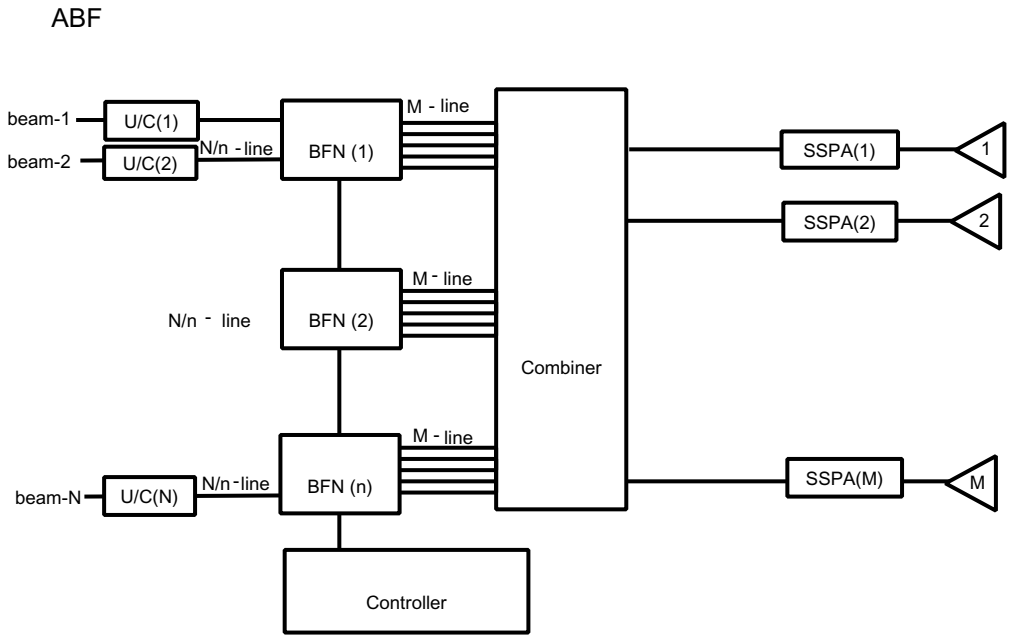

Figure D-2: Component diagram of ABF

	Component	No.	Cost (Yen)	Total Cost (Yen)	Heat Value	Total Heat Value
	UP-converter	100	200,000	20,000,000	1	100
Beam	Calculator	5	50,000,000	250,000,000	40	200
Forming	Controller	1	40,000,000	40,000,000	100	100
Network	Input array	1	40,000,000	40,000,000	50	50
	SSPA	100	200,000	20,000,000	4	400
	Element*	100	100,000	10,000,000	0.1	10
	Heater	10	300,000	3,000,000	5	50
	Integration	1	40,000,000	40,000,000		
	*)0.5dB Loss					
Total				423,000,000		910
Total (in USD)				$3,584,746		

Table D.1: DBF cost breakdown

	Component	No.	Cost (Yen)	Total Cost (Yen)	Heat Value	Total Heat Value
	UP-converter	50	200,000	10,000,000	1	50
Beam Forming Network	Controller	1	40,000,000	40,000,000	100	100
	BFN	5	40,000,000	200,000,000	5	25
	SSPA	100	200,000	20,000,000	4	400
	Element*	100	100,000	10,000,000	0.1	10
	Heater	10	300,000	3,000,000	5	50
	Integration	1	40,000,000	40,000,000		
	*)0.5dB Loss					
Total				323,000,000		635
Total (in USD)				$2,737,288		

Table D.2: ABF cost breakdown

Bibliography

[BC80] L.A. Buss and R.L. Cutts. United states national spectrum management. *Telecommunications Journal*, 47, June 1980.

[CdW03] Darren D. Chang and Olivier L. de Weck. Basic capacity calculation methods and benchmarking for mf-tdma and mf-cdma communication satellites. In *21st AIAA International Communications Satellite System Conference (ICSSC) and Exhibit*, number Paper No. AIAA-2003-2277, 2003. Yokohama, Japan.

[Cha03] Mathieu Chaize. Enhancing the economics of satellite constellations via staged deployment and orbital reconfiguration. Science master, Massachusetts Institute of Technology, 2003.

[dWCSM03] Olivier L. de Weck, Darren D. Chang, Ryutaro Suzuki, and Eihisa Morikawa. Quantitative assessment of technology infusion in communications satellite constellations. In *21st AIAA International Communications Satellite System Conference (ICSSC) and Exhibit*, number Paper No. AIAA-2003-2355, 2003. Yokohama, Japan.

[dWW02a] Olivier L. de Weck and Karen Wilcox. Lecture 11: Solution sensitivity analysis. In *ESD.77 Multidisciplinary System Design Optimizaiton (MSDO)*, April 1 2002. Massachusetts Institute of Technology.

[dWW02b] Olivier L. de Weck and Karen Wilcox. Lecture 13: Multi-objective optimization (i). In *ESD.77 Multidis-*

ciplinary System Design Optimizaiton (MSDO), April 8 2002. Massachusetts Institute of Technology.

[Eco93] The economics of radio frequency allocation. Organization for Economic Co-operation and Development, 1993.

[EE00] Jules E.Kadish and Thomas W.R. East. *Satellite Communications Fundamentals.* Artech House, Boston, 2000.

[Fin] 1963 Space Conference, Final Acts, Resolution 1A, Relating to the Provision and Use of Information Regarding International Satellite Systems.

[Fos98] Carl E. Fossa. An overview of the iridium low earth orbit (LEO) satellite system. *Proceedings of IEEE 1998 National Aerospace and Electronics Conference 1998*, A99-17228(03-01):152–159, 1998.

[GM93] Gary D. Gordon and Walter L. Morgan. *Principles of Communication Satellites.* John Wiley & Sons, New York: Wiley, 1993.

[GS78] Theodore J. Gordon and John G. Stover. Using perceptions and data about the future to improve the simulation of complex systems. *Technological Forcasting & Social Change*, (12), 1978.

[Gum95] Cary Gumbert. Assessing future growth potential of mobile satellite systems using a cost per billable minute metric. Master's thesis, Massachusetts Institute of Technology, Department of Aeronautics and Astronautics, August 1995.

[HC90] Rebecca M. Henderson and Kim B. Clark. Architectural innovation: The reconfiguration of existing product technologies and the failure of established firms. *Administrative Science Quarterly*, 35:9–30, 1990.

[Hom02] Masanori Homma, 2002. ETS-VIII project manager, National Space Development Agency of Japan (NASDA).

[IJH99] Steven J. Isakowitz, Joseph P. Hopkins Jr., and Joshua B. Hopkins. *Reference Guide to Space Launch Systems*. AIAA, Reston, VA, 1999.

[JM02] Cyrus D. Jilla and David W. Miller. A multiobjective, multidisciplinary design optimization methodology for the conceptual design of distributed satellite systems. In *20th AIAA International Communications Satellite Systems Conference*, number Paper No. AIAA-2002-5491, September 4-6 2002. Atlanta, Georgia.

[Kad02] Naoto Kadowaki, 2002. Leader, Broadband Satellite Network Group, Wireless Communication Division, Communications Research Laboratory (CRL). Email: naoto@crl.go.jp.

[Koy02] Yoshisada Koyama, 2002. Senior Researcher, Next-generation LEO System Research Center (NeLS), TAO. Email: koyama@nels.tao.go.jp.

[KSH98] Andjelka Kelic, Graeme B. Shaw, and Daniel E. Hastings. Metric for systems evaluation and design of satellite-based internet links. *Journal of Spacecraft and Rockets*, 35(1):73–81, January-February 1998.

[LA97] Thomas J. Lang and W. S. Adams. Iaf international workshop on mission design and implementation of satellite constellations. In *A Comparison of Satellite Constellations for Continuous Global Coverage*, Nov. 17-19 1997. Toulouse, France.

[LW92] Wiley J. Larson and James R. Wertz, editors. *Space Mission Analysis and Design*. Microcosm, Inc. and Kluwer Academic Publishers, 2 edition, 1992.

[LWJ00] Erich Lutz, Markus Werner, and Axel Jahn. *Satellite Systems for Personal and Broadband Communications*. Springer-Verlag, Berlin, Germany, first edition, 2000.

[MM02] Christopher A. Mattson and Achille Messac. Concept selection in n-dimension using s-pareto frontiers and visualization. In *9th AIAA/ISSMO Symposium on Multidisciplinary Analysis and Optimization*, number Paper No. AIAA-2002-5418, September 4-6 2002. Atlanta, Georgia.

[Nel99] R.A. Nelson. Antennas: the interface with space. Online, September 1999. Available: http://www.aticourses.com/antennas_tutorial.htm.

[oIT03] World Conference on International Telecommunications. Online, November 2003. Available: http://www.itu.int/aboutitu/overview/conferences.html#WCIT.

[oLVTCowEv03] China Academy of Launch Vehicle Technology (CALT) official website English version. Online, August 2003. Available: http://www.calt.com.cn/new/english/.

[Ori02] Teruaki Orikasa, 2002. Research Fellow, Cloud Profiling Radar Group, Applied Research and Standards Division, Communications Research Laboratory (CRL). Email: orikasa@crl.go.jp.

[SdW04] Philip N. Springmann and Olivier L. de Weck. Parametric scaling model for nongeosynchronous communications satellites. *Journal of Spacecraft and Rockets*, 41(4), July-August 2004. (Tentative).

[Sha99] Graeme Shaw. *The Generalized Information Network Analysis Methodology for Distributed Satellite Systems*. PhD dissertation, Massachusetts Institute of Technology, Department of Aeronautics and Astronautics, 1999.

[Sil02] Sam Silverstein. Iridium sets plans for new generation of spacecraft. *Spacenews*, page 3, April 8 2002.

[SNM+02] Ryutaro Suzuki, Iwao Nishiyama, Shigeru Motoyoshi, Eihisa Morikawa, and Yasuhiko Yasuda. Current status of nels project: R&d of global multimedia mobile satellite communications. In *20th AIAA International Communication Satellite Systems Conference and Exhibit*, number AIAA 2002-2038, May 2002. Montréal, Québec, Canada.

[Spa02] Globalstar files for bankruptcy protection. www, February 2002. URL http://www.rand.org/publications/MR/MR864/MR864.apA.pdf - Accessed 5 July 2003.

[SSI+00] Ryutaro Suzuki, Keiichi Sakurai, Shinichi Ishikawa, Iwao Nishiyama, and Yasuhiko Yasuda. A study of next-generation leo system for global multimedia mobile satellite communications. *AIAA*, (AIAA-2000-1102), 2000.

[Suz02] Ryutaro Suzuki, 2002. Leader, Smart Satellite Technology Group, Wireless Communication Division, Communications Research Laboratory (CRL). Email: ryutaro@crl.go.jp.

[Tsc91] Hugo Tschirky. Technology management: An integrated function of general management. In *Portland International Conference on Management of Engineering and Technology*, October 27-31 1991. Portland, Oregon, USA.

[URDM02] Aditya Utturwar, Sriram Rallabhandi, Daneil DeLaurentis, and Dimitri Mavris. A bi-Level optimization approach for technology selection. In *9th AIAA/ISSMO Symposium on Multidisciplinary Analysis and Optimization*, number Paper No. AIAA-2002-5426, September 4-6 2002. Atlanta, Georgia.

[Utt94] James M. Utterback. *Mastering the Dynamics of Innovation*. Harvard Business School Press, Boston, Massachusetts, 1 edition, 1994.

[Vio95] Michael Violet. The development and application of a cost per minute metric for the evaluation of mobile satellite systems in a limited-growth voice communications market. Master's thesis, Massachusetts Institute of Technology, Department of Aeronautics and Astronautics, August 1995.

[vW88] Rias J. van Wyk. Management of technology: New frameworks. *Technovation*, (7):341–351, 1988.

[Web03] Arianespace Official Website. Online, August 2003. Available: http://www.arianespace.com/site/index2.html.

[Wit91] David J. Withers. *Radio Spectrum Management*. Peter Peregrinus Ltd., London, United Kingdom, 1991.